

Dissertation zur Erlangung des Doktorgrades der Fakultät für Chemie und
Pharmazie der Ludwig–Maximilians–Universität München

Structure and functional architecture of the Mediator middle module from budding yeast

Tobias Koschubs



München 2010

Dissertation zur Erlangung des Doktorgrades der Fakultät für Chemie und
Pharmazie der Ludwig–Maximilians–Universität München

**Structure and functional architecture
of the Mediator middle module
from budding yeast**

vorgelegt von
Tobias Koschubs
aus Hannover

München 2010

Erklärung

Diese Dissertation wurde im Sinne von §13 Abs. 3 der Promotionsordnung vom 29. Januar 1998 von Herrn Prof. Dr. Patrick Cramer betreut.

Ehrenwörtliche Versicherung

Diese Dissertation wurde selbstständig und ohne unerlaubte Hilfe erarbeitet.

München, am 26.01.2010

Tobias Koschubs

Dissertation eingereicht am: 27.01.2010

Erstgutachter: Prof. Dr. Patrick Cramer

Zweitgutachter: Prof. Dr. Dietmar Martin

Tag der mündlichen Prüfung: 01.03.2010

*„I am among those who think that science has great beauty.
A scientist in his laboratory is not only a technician: he is also a child placed before natural
phenomena which impress him like a fairy tale. We should not allow it to be believed that all
scientific progress can be reduced to mechanisms, machines, gearings, even though such
machinery has its own beauty.“*

Marie Curie (1933)

Acknowledgement

First of all I would like to thank my supervisor Prof. Dr. Patrick Cramer for giving me the opportunity to work on this challenging and long-standing project. He has guided me in a great manner through my PhD time and taught me how to perceive science always with the enthusiasm it deserves. He has also not only been very motivating, but showed me how to aim, organize and present science, that it can be successful.

I particularly enjoyed the excellent support, discussions and interdisciplinary atmosphere at the Gene Center. Looking back, our laboratory changed a lot. While at the beginning there was only a small crowd of people, especially including the first generation of PhD student who had finished, the lab grew immensely, new people like me and others came in and with that also new equipment. As an indirect consequence, there were always the right people to discuss things with but also the equipment and techniques available, to do things right.

This was probably also a reason why I had so many collaborators whom I would like to thank here. In detail, I would like to start with Sonja Baumli, whose PhD work I continued. She not only gave me a great start on the Mediator middle module by having done a tremendous amount of work before and teaching me how to make these complexes, but also had some great ideas later that significantly contributed to the success of my work. I also appreciated being part of the the "Mediator" team, which has been constituted over the years by many people – so many thanks to Sonja, Sabine, Susanne, Laurent, Erika, Larissa, Christian, Elmar and Martin for the great community, discussions, ideas and your contributions to my publications. Especially I would like to acknowledge Laurent Larivière for teaching me how to process SAD data and creative ideas as well as Martin Seizl for performing *in vitro* transcription assays and discussing microarray data. We also continued during this work a successful external collaboration with Kristina Lorenzen and Albert Heck at Utrecht University. I very much enjoyed working together with them and would like to express my gratitude for their fantastic mass spectrometry work. Additionally, during my thesis I supervised two students – Fabian and Saana. I learned a lot by changing perspective. I hope I did not demand for too much, but finally I was very happy that I could reward their great contributions by offering coauthorships.

Of course I would like to acknowledge all the people in the laboratory in general for the good time and the fun we had together. Especially I would like to mention Elmar, Rieke and Christian from my laboratory bay who constituted also my coffee group and cheered up daily lab-life. I would also like to thank Sebastian with whom I started my PhD work here at the same time for the company. Moreover I would like to thank Stefan Benkert for a lot of Edman sequencing analysis as well as Kerstin Maier for help with microarrays. Dirk and Alan were also very helpful in explaining and processing X-ray data.

I also very much enjoyed learning yeast manipulations and genetics – therefore I would like to thank Dietmar Martin, Heidi Feldmann, Stephan Jellbauer, and Emanuel Clausing for discussions and providing materials for yeast work. Dietmar was also together with Patrick and Daniel Wilson part of PhD advisory committee, which has been very helpful in suggesting on what to actually concentrate work on.

Within the Gene Center, I very much appreciated working together with people from other groups. For instance Achim Tresch from computational biology supported me in learning R/BioConductor or for instance Gregor Witte and other people from the Hopfner laboratory supported me with SAXS analysis. I also used a lot of mass spectrometry service and even tried to establish some new approaches, for which I would like to thank Thomas Fröhlich, Georg Arnold, Axel Imhof and their group members.

Last but not least, I am deeply indebted to my family who always supported me on my way and generously aided in financing my biotechnology studies. Additionally, I am very happy for making new friends here and that my friends from home and from my study times kept the contact through all these years.

Finally, thank you Ronja for the wonderful time together! You are the best that ever happened to me!

Summary

Mediator is a central coactivator complex required for regulated transcription by RNA polymerase (Pol) II in all eukaryotes. Budding yeast Mediator has a size of 1.4 MDa and consists of 25 subunits arranged in the head, middle, tail, and kinase modules. It is thought that Mediator forms an interface between the general RNA polymerase (RNA Pol) II machinery and transcriptional activators leading to promotion of pre-initiation complex (PIC) assembly.

Mediator middle module from budding yeast consists of seven subunits Med1, 4, 7, 9, 10, 21, and 31 and was investigated during this thesis both structurally and functionally. Previously, the structure of a subcomplex comprising the C-terminal region of Med7 (Med7C) and Med21 was solved by X-ray crystallography and protocols for obtaining larger recombinant complexes were established in the laboratory. As structural and functional studies of Mediator are limited by the availability of protocols for the preparation of modules, I pursued these studies and established protocols for obtaining pure endogenous and recombinant complete Mediator middle module.

Another subcomplex of the middle module, comprising the N-terminal part of subunit Med7 (Med7N) and the highly conserved subunit Med31 (Soh1) was successfully crystallized and its structure solved during this work. It is found, that it contains a unique structure and acts also as a functional entity (termed submodule). The Med7N/31 submodule shows a novel fold, with two conserved proline-rich stretches in Med7N wrapping around the right-handed four-helix bundle of Med31. *In vitro*, Med7N/31 is required for activated transcription and can act in *trans* when added exogenously. *In vivo*, Med7N/31 has a predominantly positive function on the expression of a specific subset of genes, including genes involved in methionine metabolism and iron transport. Comparative phenotyping and transcriptome profiling identified specific and overlapping functions of different Mediator submodules.

Crystallization screening of larger middle module (sub-)complexes did not result in crystal formation, even after removal of some flexible regions. Thus alternative methods were applied to characterize the middle module topology. Native mass spectrometry reveals that all subunits are present in equimolar stoichiometry. Ion mobility mass spectrometry, limited proteolysis, light scattering, and small angle X-ray scattering all indicate a high degree of intrinsic flexibility and an elongated shape of the middle module, giving a potential explanation of why crystallization of larger complexes was unsuccessful. Moreover, based on systematic protein-protein interaction analysis, a new model for the subunit-subunit interaction network within the middle module of the Mediator is proposed. In this model, the Med7 and Med4 subunits serve as a binding platform to form the three heterodimeric subcomplexes Med7N/21, Med7C/31, and Med4/9. The subunits Med1 and Med10, which bridge to the Mediator tail module, bind to both Med7 and Med4. Furthermore, first steps in establishing an *in vitro* assay to test endogenous and recombinant middle module functionality have been initiated and will provide the basis for future studies.

Publications

Parts of this work have been published or are in the process of publication:

- Koschubs T., Seizl M., Larivière L., Kurth F., Baumli S., Martin D.E., and Cramer P.
Identification, structure, and functional requirement of the Mediator submodule Med7N/31.
EMBO Journal 2009 Jan 7;28(1):69-80. Epub 2008 Dec 4.
- Koschubs T., Lorenzen K., Baumli S., Sandström S., Heck A.J.R., and Cramer P.
Preparation and topology of the Mediator middle module.
Nucleic Acids Research. Epub 2010 Jan 31.

Contents

Erklärung	I
Ehrenwörtliche Versicherung	I
Acknowledgement	III
Summary	V
Publications	VI
Contents	VII
1 Introduction	1
1.1 Regulation of transcription in eukaryotic cells	1
1.2 RNA polymerase II transcription cycle and the general transcription machinery	2
1.3 Chromatin remodeling	5
1.4 Corepressors	6
1.5 Coactivator complexes	6
1.6 The Mediator complex	7
1.6.1 Discovery and conservation of Mediator	7
1.6.2 Mediator architecture in <i>Saccharomyces cerevisiae</i>	8
1.6.3 Mediator in transcriptional activation and repression	9
1.7 Aims and scope of this thesis	13
2 Materials and Methods	14
2.1 Materials	14
2.1.1 Bacterial strains	14
2.1.2 Yeast strains	14
2.1.3 Plasmids	16
2.1.4 Media and additives	22
2.1.5 Buffers and solutions	22
2.2 General methods	24
2.2.1 Preparation and transformation of competent cells	24
2.2.2 Cloning and mutagenesis	25
2.2.3 Protein expression in <i>E. coli</i> and selenomethionine labeling	26
2.2.4 Tandem affinity purification	26
2.2.5 Protein Analysis	26
2.2.6 Limited proteolysis analyses	27
2.2.7 Crystallization screening with middle module complexes	28
2.2.8 Yeast genetics and assays	28
2.2.9 Bioinformatic tools	29

2.3	Recombinant Med7N/31	29
2.3.1	Preparation of recombinant Med7N/31	29
2.3.2	X-ray structure determination	30
2.3.3	Yeast strains and growth assays	30
2.3.4	<i>In vitro</i> transcription assays	31
2.3.5	Gene expression profiling analysis	31
2.4	Endogenous and recombinant Mediator middle module	32
2.4.1	Purification of endogenous middle module	32
2.4.2	Preparation of recombinant middle module	32
2.4.3	Activity assay trials	33
2.4.4	Coexpression and copurification pull-down assays	34
2.4.5	Native mass spectrometry	34
2.4.6	Static light scattering analysis	34
2.4.7	Small-angle X-ray scattering	35
3	Results	36
3.1	Identification, structure, and functional requirement of the Mediator submodule Med7N/31	36
3.1.1	Identification and crystallization of the Med7N/31 subcomplex	36
3.1.2	The Med7N/31 structure reveals novel folds	39
3.1.3	Possible CTD mimicry by Med7N	39
3.1.4	Med7N/31 is required for normal yeast growth <i>in vivo</i>	41
3.1.5	Med7N/31 is essential for transcription <i>in vitro</i>	41
3.1.6	Med7N/31 is a functional Mediator submodule <i>in vivo</i>	43
3.1.7	Med7N/31 regulates a subset of genes	43
3.1.8	Overlapping and specific functions of Mediator submodules	46
3.1.9	Cooperation of Med7N/31 and TFIIS	48
3.2	Preparation and topology of the Mediator middle module	50
3.2.1	Endogenous Mediator middle module	50
3.2.2	Recombinant Mediator middle module	51
3.2.3	Crystallization trials with middle module complexes	52
3.2.4	Activity assay trials	53
3.2.5	Subunit stoichiometry	54
3.2.6	Module topology	56
3.2.7	Exposed regions in the middle module	56
3.2.8	Intra-module subunit interactions	57
3.2.9	Module shape	60
4	Discussion	63
4.1	The Med7N/31 submodule	63
4.2	Mediator middle module topology	65
5	Conclusion and Outlook	67

6	References	69
7	Abbreviations	86
8	List of figures	88
9	List of tables	89
10	Curriculum Vitae	90

1 Introduction

1.1 Regulation of transcription in eukaryotic cells

Transcription is the fundamental process by which cells convert the DNA-coded information into RNA through RNA polymerase enzymes. This process enables the coded information to be translated into proteins as well as regulation of cellular processes by non-coding RNAs. Regulation of transcription increases the versatility and adaptability of organisms by enabling to adapt protein expression to cellular needs. Thus, responses to external changes are enabled, as well as cellular differentiation and development. To date, four different nuclear RNA Pols have been identified in higher eukaryotes. In contrast, only one RNA Pol is found in prokaryotes and archaea (Thomas and Chiang, 2006). Nevertheless, sequence and structural comparisons reveal the evolutionary conservation of the overall architecture of RNA Pols in the three kingdoms of life (compare Cramer, 2002; Cramer et al., 2008). In eukaryotes, RNA Pol I synthesizes a pre-rRNA, which matures into 28S, 18S and 5.8S rRNAs which form the major RNA sections of the ribosome (Grummt, 1999). RNA Pol III is responsible for synthesis of structural or catalytic RNAs. It transcribes mainly 5S rRNA, tRNAs and U6 snRNA (Dieci et al., 2007; Thomas and Chiang, 2006). RNA Pol II transcribes all protein encoding genes, into mRNA, which serves as the template for protein synthesis (reviewed in Kornberg, 1999). Also most snRNA and microRNA (Sharp, 1988; Lee et al., 2004) are transcribed by RNA Pol II. A major difference compared to the other RNA Pols is the presence of an extended and very flexible carboxy-terminal domain (CTD) on the Rpb1 subunit. It contains multiple repeats of the heptapeptide sequence YSPTSPS. The number of these repeats increases with genomic complexity: 26 in budding yeast, 32 in *Caenorhabditis elegans*, 45 in *Drosophila*, and 52 in mammals (Sims et al., 2004). A fourth RNA polymerase has been identified in plants to facilitate the production of siRNA (reviewed in Thomas and Chiang, 2006). RNA Pols are very large multisubunit enzymes, comprising about 12 to 17 subunits with a total molecular weight of 0.5-0.7 MDa.

Transcription is a highly regulated process, that depends on specific sets of transcription factors and cofactors. While in bacteria σ factors play the key role in regulation (Campbell et al., 2008), the situation in eukaryotes is much more complex. Triggering transcription of genes by RNA Pol II requires not only signal transduction from signaling pathways to gene-specific transcription factors, but also assembly of a many additional factors into large transcription machineries of changing composition. Polymerase-associated factors enable the polymerases to recognize different promoters and to transcribe different classes of genes, to receive different regulatory signals, to direct the co-transcriptional processing of RNA transcripts, and to couple transcription to changes in chromatin structure and modification.

1.2 RNA polymerase II transcription cycle and the general transcription machinery

Transcription can be described as a transcription cycle (Figure 1). This multistep process can be divided in three major stages - initiation, elongation and termination.

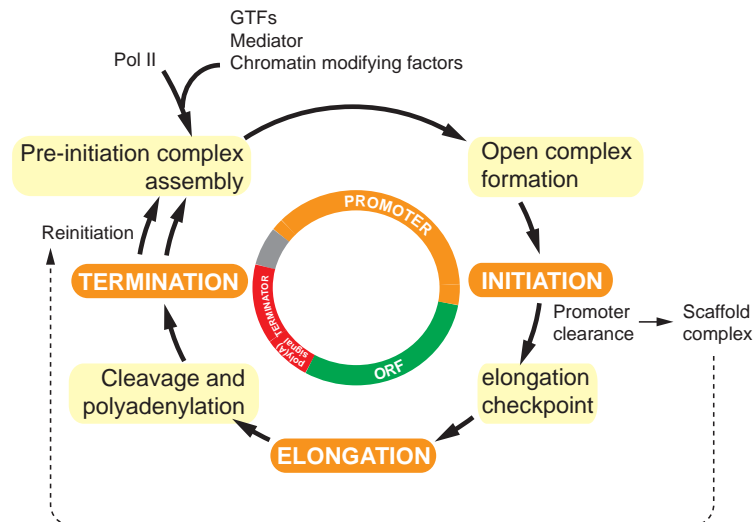


Figure 1: The mRNA transcription cycle.

Main phases of the transcription cycle are colored orange, important events of regulation are colored in yellow. The circle in the middle depicts the occurrence of the events in relation to the gene. ORF = open reading frame. Courtesy of Stefan Dengl, Gene Center Munich.

The prevailing view of transcriptional activation is that many sequence-specific regulators interact with their cognate DNA motifs in response to cellular signals. They recruit transcriptional coactivators (such as SWR1, SWI/SNF, RSC, ISWI, Mediator and SAGA) to alter the local chromatin environment, making it accessible and facilitate assembly of the pre-initiation complex at the promoter. The PIC, or closed complex is composed of core promoter DNA, the general transcription factors (GTFs) and RNA Pol II (Venters and Pugh, 2009; Hahn, 2004). The general transcription factors are TFIIA, TFIIB, TFIID, TFIIIE, TFIIIF, TFIIS, and TFIIF and they mediate promoter recognition and unwinding (Sikorski and Buratowski, 2009; Kim et al., 2007). A detailed listing of the factors involved in PIC assembly is given in Table 1.

The factors and assembly pathways used to form transcriptionally competent PICs can be promoter dependent (Müller et al., 2007; Sikorski and Buratowski, 2009; Huisinga and Pugh, 2007). The classical TATA box is present only in 20% of yeast promoters and several models have been proposed how PICs assemble in its absence. While in metazoans a variety of cis-regulatory elements has been described, yeast seems to exhibit a smaller set of these elements (compare Basehoar et al., 2004; Venters and Pugh, 2009; Sikorski and Buratowski, 2009).

During open complex formation, about 10 bases of the DNA double helix separate, and the single-stranded DNA template strand slips into the active site, which lies in a deep cleft in the polymerase enzyme (Hahn, 2009). Yeast RNA Pol II scans with the help of the

TFIIB reader the DNA for an initiator (Inr) sequence motif that defines the transcription start site (TSS) (Kostrewa et al., 2009) and once found it synthesizes short RNA products (abortive initiation). As soon as a RNA of 7 bases or more is synthesized, the polymerase releases its contacts with the promoter and initiation factors (promoter escape) to enter a processive elongation form termed the elongation complex, which synthesizes full-length RNA transcripts (Kostrewa et al., 2009; Hahn, 2009). The switch to productive transcription in the elongation stage is characterized also by phosphorylation at serine 5 on the CTD repeats of RNA Pol II. Whereas TFIIB and TFIIF dissociate from the promoter, activator, TFIID, TFIIA, TFIIH, TFIIIE and Mediator are left behind in a scaffold complex for the facilitated reinitiation of transcription of the same gene (Hahn, 2004; Yudkovsky et al., 2000).

The polymerase moves along the DNA and links nucleotides into a pre-mRNA transcript, whose sequence is based on the template strand. The efficiency of elongation by RNA Pol II is regulated by a number of additional factors such as TFIIF, TFIIIS, Spt4-Spt5, Spt6, FACT, and Paf (Sims et al., 2004; Kim et al., 2007). RNA Pol II CTD acts as a “landing pad”, binding directly to factors involved in pre-mRNA capping, 3' end processing, transcription elongation, termination, and chromatin modification (Phatnani and Greenleaf, 2006). The change of phosphorylation state of the CTD during transcription has been described as a phosphorylation cycle: Initial phosphorylation of (unphosphorylated) RNA Pol II CTD on serine 5 during PIC formation or before promoter-proximal pausing is achieved by the kinase activity of the Kin28 subunit of TFIIH. Capping enzyme associates with the serine 5-phosphorylated CTD and with Spt5, and the nascent RNA becomes capped during this first stage of elongation. Once proper pre-mRNA capping is ensured, serine 2 residues are phosphorylated by Bur1/2 (yeast homologs of P-TEFb) or Ctk1. Later in elongation, protein phosphatases such as Ssu72 or Fcp1 dephosphorylate the CTD serine residues and recycle RNA Pol II for reinitiation and subsequent rounds of transcription (Sims et al., 2004; Saunders et al., 2006; Egloff and Murphy, 2008; Qiu et al., 2009). Additionally to these prevalent modifications, the CTD can be also be modified by phosphorylation at serine 7, glycosylation, and by cis/trans isomerization of prolines (Egloff et al., 2007; Meinhart et al., 2005).

Termination sites can be located up to 1 kb downstream of the poly(A) site where the nascent transcript is 3'-processed and uncoupled from the transcription machinery by factors that are recruited to the Ser2-phosphorylated CTD of RNA Pol II (Dengl and Cramer, 2009). Introns can be removed by the spliceosome both cotranscriptionally and post-transcriptionally (Bentley, 2002; Proudfoot et al., 2002). Export of mRNAs is extensively coupled to transcription and characterized by assembly into complicated messenger ribonucleoprotein (mRNP) particles that are exported via export factors to the cytoplasm, where they are bound by ribosomes and translated into proteins (Köhler and Hurt, 2007).

Table 1: Complexes involved in *S. cerevisiae* RNA Pol II PIC assembly
(Adapted from Hahn (2004); Thomas and Chiang (2006); Sikorski and Buratowski (2009))

Factor	No. of subunits	Function
RNA Pol II	12	Catalyzes transcription of all mRNAs and a subset of noncoding RNAs including snRNAs and miRNAs; CTD phosphorylation
TFIIA	2	Antirepressor; stabilizes TBP and TFIID-DNA binding; positive and negative gene regulation
TFIIB	1	Binds TBP, RNA Pol II and promoter DNA and thereby stabilizes TBP-TATA complex; start site selection; aids in recruitment of TFIIF/RNA Pol II
TFIID	15	TBP and 14 TBP Associated Factors (TAFs); nucleates PIC assembly either through TBP binding to TATA sequences or TAF binding to other promoter sequences (INR and DPE elements); coactivator activity through direct interaction of TAFs and gene specific activators
TFIIE	2	Helps to recruit TFIIH to promoters; stimulates helicase and kinase activities of TFIIH; binds ssDNA and is essential for promoter melting
TFIIF ^a	3	Tightly associates with RNA Pol II; enhances affinity of RNA Pol II for TBP-TFIIB-promoter complex; necessary for recruitment of TFIIE/TFIIH to the PIC; aids in start site selection and promoter escape; enhances elongation efficiency; involved in RNA Pol II recruitment to PIC and in open complex formation
TFIIS	1	Stimulates intrinsic transcript cleavage activity of RNA Pol II allowing backtracking to resume RNA synthesis after transcription arrest; stimulates PIC assembly at some promoters
TFIIH	10	ATPase/helicase necessary for promoter opening and promoter clearance; helicase activity for transcription coupled DNA repair; kinase activity required for phosphorylation of RNA Pol II CTD; facilitates transition from initiation to elongation
Mediator	25	Bridges interaction between activators and basal factors; stimulates both activator dependent and basal transcription; required for transcription from most RNA Pol II dependent promoters; kinase and acetyltransferase activity; interacts with TBP, TFIIF, TFIIH and TFIIS
SAGA ^b	21	Interacts with activators, histone H3, TBP and TFIIA; histone-acetyltransferase activity; deubiquitinating activity
NC2	2	Binds TBP/DNA complexes and blocks PIC assembly; can have both positive and negative effects on transcription
Mot1	1	Induces dissociation of TBP/DNA complexes in ATP dependent manner; can have both positive and negative effects on transcription
Tup1-Ssn6	2	Represses multiple subsets of genes when recruited to promoters by sequence-specific DNA binding repressors

^a Yeast has one extra nonessential subunit compared with other organisms studied. ^b Yeast also contain SLIK, a closely related complex.

1.3 Chromatin remodeling

Eukaryotic DNA is packed into chromatin with nucleosomes as repeating structural units. DNA is wrapped twice around an octameric complex of histone proteins, which consists of an histone 3-histone 4 (H3–H4) tetramer and two histone 2A–histone 2B (H2A–H2B) dimers. The DNA between the nucleosomes is termed linker DNA. While yeast lacks histone H1, this fifth histone helps to stabilize the formation of more compact, higher-order chromatin structures in higher eukaryotes (Saunders et al., 2006). The regulation of gene transcription involves a dynamic balance between genome packaging into chromatin and allowing transcriptional regulators access regulatory sequences (Cairns, 2009; Clapier and Cairns, 2009). Generally, there are two mechanisms to alter the chromatin structure and thereby enable access to the DNA for regulatory proteins that can activate transcription: through post-translational modification of histones and through alteration of the nucleosome structure.

Histone are predominantly modified at their flexible N-terminal tails (H2A also has a C-terminal tail) that protrude from the core nucleosome, but also some residues within the histone globular domain can be modified (Saunders et al., 2006). These modifications include methylation of arginine (R) residues; methylation, acetylation, ubiquitination, ADP-ribosylation, and sumolation of lysines (K); and phosphorylation of serines and threonines. Histone modifications are reversible, for example histone deacetylases oppose the action of histone acetyltransferases. Modifications that are associated with active transcription, such as acetylation of H3 and H4 or di- or trimethylation (me) of H3K4, are commonly referred to as euchromatin modifications. Modifications that are localized to inactive genes or regions, such as H3 K9me and H3 K27me, are often termed heterochromatin modifications (Li et al., 2007). Typical histone modification patterns can be correlated over the length of active genes (compare in Saunders et al., 2006, Figure 3).

Modifiers such as acetyltransferases, methyltransferases and kinases can promote or deter the targeting or activity of chromatin remodellers on the proper nucleosome (Cairns, 2009). Remodelers use the energy of ATP hydrolysis to change the packaging state of chromatin by moving, exchange for histone variants, ejecting, or restructuring the nucleosomes (Clapier and Cairns, 2009). Chromatin remodeling complexes fall into four families based upon sequence conservation: SWI/SNF (including SWI/SNF and RSC in yeast), INO80 (including INO80 and SWR1 in yeast), ISWI, and CHD (Chd1 is a component of both the SAGA and SLIK complexes). These complexes are often large molecular machines (compare Figure 2) that are apparently most active on promoter nucleosomes (Cairns, 2009; Venters and Pugh, 2009). Recent analysis revealed that two types of promoters exist: open promoters (typical for constitutive genes) that have a depleted proximal nucleosome adjacent to the transcription start site and covered promoters (typical for regulated genes) where the transcription start site is often covered by nucleosomes in its repressed state. Additionally, nucleosome positioning sequence elements determine the position of nucleosomes at these promoters (Cairns, 2009).

1.4 Corepressors

In yeast, three major entities have been found that repress transcription initiation. Two transcription repressors, Mot1 and NC2, act through direct interactions with TBP. Mot1 is a Snf2 family ATPase that removes TBP from promoters. NC2 is a heterodimer that blocks TFIIA and TFIIB from associating with the TBP–TATA complex (Pereira et al., 2003; Auble, 2009; Sikorski and Buratowski, 2009). Both NC2 and Mot1 also have positive roles at many yeast promoters, although the mechanism by which they positively control transcription is still under study (Mohibullah and Hahn, 2008). The Ssn6-Tup1 complex represses more than 180 genes in *Saccharomyces cerevisiae* (*S. cerevisiae*) controlled by different pathways and is thus considered a global corepressor of transcription. Although Ssn6 and Tup1 form a complex, it is largely accepted that Tup1 contributes the bulk of the repression activity and Ssn6 acts as an adapter. Apparently, Tup1 utilizes multiple redundant mechanisms to repress transcription of native genes – for e.g. nucleosome positioning, histone deacetylation, and Mediator interference (Zhang and Reese, 2004; Hallberg et al., 2006).

1.5 Coactivator complexes

Although activators or repressors can interact directly with components associated with the core promoter, they execute their regulation predominantly through coactivators (Fuda et al., 2009). A number of coactivators have been isolated as large multifunctional complexes, and biochemical, genetic, molecular, and cellular strategies have all contributed to uncovering many of their components, activities, and modes of action. Coactivator functions can be broadly divided into two classes: (a) adapters that direct activator recruitment of the transcriptional apparatus, or (b) chromatin-remodeling or -modifying enzymes (compare Figure 2). Strikingly, several distinct coactivator complexes nonetheless share many subunits and appear to be assembled in a modular fashion. Such structural and functional modularity could provide the cell with building blocks from which to construct a versatile array of coactivator complexes according to its needs (Näär et al., 2001).

Aside from the Mediator complex, which will be described in detail below, the SAGA complex and its relatives (SLIK, SALSA) as well as the GTF TFIID appear to be the major complexes in enabling activated transcription as revealed by cross-linking studies (Fishburn et al., 2005; Reeves and Hahn, 2005). In *S. cerevisiae*, the coactivator complexes TFIID and SAGA are critical for TBP recruitment (Mohibullah and Hahn, 2008). It is likely, that coactivators act promoter-specifically, e.g. yeast TFIID tends to regulate promoters of “housekeeping” genes, whereas yeast SAGA typically acts at highly regulated genes that are modulated by stress. SAGA is 1.8 MDa multisubunit complex that is directly recruited to promoters by activators and was originally identified as a histone acetyltransferase (HAT) complex containing the HAT subunit Gcn5 (Mohibullah and Hahn, 2008; Wu et al., 2004). Interestingly, TFIID and SAGA share a common set of TAFs (Huisinga and Pugh, 2004) which may partially explain their overlapping functions.

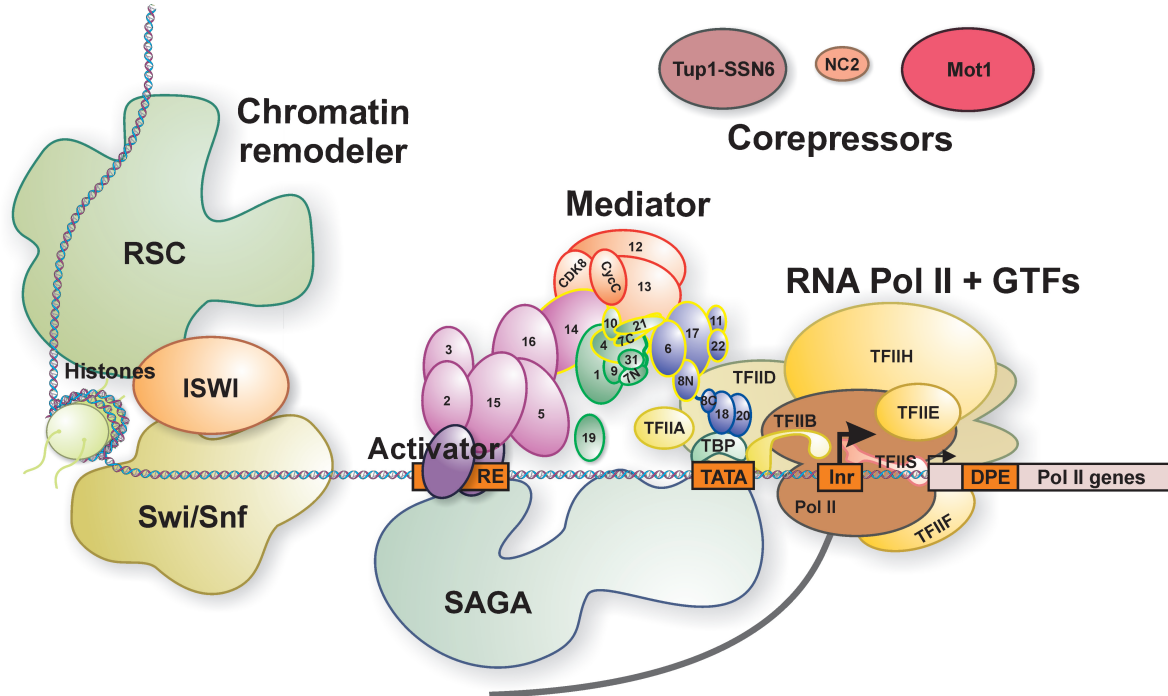


Figure 2: Transcription initiation results from an interplay of several multiprotein complexes. In response to cellular signals, activators bind to their regulatory elements (RE), which are typically located upstream of the promoter sequences. Coactivators are recruited that alter the chromatin environment (Chromatin remodeling and histone modifiers such as RSC, ISWI, Swi/Snf, NuA4, Chd1, INO80, SWR1) and facilitate assembly of the PIC at the promoter (compare Biddick and Young, 2009). The Mediator and SAGA coactivator complexes serve at most genes as adapters that bridge interactions between activators and the basal transcription initiation machinery. Corepressors can antagonize the formation of transcriptionally competent PICs, predominantly by removing TBP from the TATA element. (Proteins and complexes are drawn at relative scale.)

1.6 The Mediator complex

1.6.1 Discovery and conservation of Mediator

The first evidence for an intermediary complex was indirect and came from experiments where one activator interfered (termed as squelched) with another in yeast and mammalian cells *in vivo* (Gill and Ptashne, 1988; Triezenberg et al., 1988). Such interference was attributed to the sequestration of a factor(s), present in a limiting amount, required for activated transcription (Myers and Kornberg, 2000). Independently from these studies, R. A. Young's laboratory identified genes in yeast genetic screens by their ability to suppress the cold-sensitive phenotype of RNA Pol II CTD truncation mutations. These genes encode proteins (termed Suppressor of RNA Pol B (Srb)) which were shown to form a large complex with RNA Pol II and some GTFs together termed RNA Pol II holoenzyme, that could support activated transcription *in vitro* after supplementation with missing GTFs (Nonet and Young, 1989; Thompson et al., 1993; Koleske and Young, 1994; Hengartner et al., 1995; Liao et al., 1995). In parallel, in the laboratory of R. D. Kornberg, attempts to purify the individual components of the RNA Pol II machinery to homogeneity using conventional column chromatography led to the purification of all GTFs and a complex termed as Mediator (Kelleher et al., 1990; Flanagan et al., 1991; Sayre et al., 1992; Svejstrup et al., 1994; Kim et al., 1994).

Mediator turned out to be ubiquitous in eukaryotes and was also purified from human cells (Fondell et al., 1996; Sun et al., 1998; Näär et al., 1999; Rachez et al., 1999; Ryu et al., 1999), mouse (Jiang et al., 1998), fission yeast (Spåhr et al., 2000; Linder et al., 2008), *Drosophila* (Park et al., 2001b) and plant (Bäckström et al., 2007). Biochemical purification of Mediator complexes from different species has identified additional conserved as well as species-specific subunits and a unified nomenclature has been proposed (Bourbon et al., 2004). Moreover, homology analysis in many eukaryotic genomes showed not only its conservation across the eukaryotic kingdom (Boube et al., 2002) but gave also insights into its evolution (Bourbon, 2008). The overall Mediator structure appears to be conserved as most budding yeast subunits have been identified also in the majority of eukaryotes. Differences occur predominantly within the tail and the head modules. The tail module is e.g. smaller in *Schizosaccharomyces pombe* (*S. pombe*) (lacking Med5 and Med16) compared to *S. cerevisiae* but contains additional subunits in mammals (Med23, Med25). Interestingly, the size of individual subunits differs across species, e.g. mammalian Med1 subunit is considerably larger when compared to *S. cerevisiae* (Bourbon, 2008). This reflects likely metazoan diversification as Med1 is apparently responsible for most mammalian activator binding (Blazek et al., 2005).

1.6.2 Mediator architecture in *Saccharomyces cerevisiae*

Budding yeast Mediator has a molecular weight of 1.4 MDa and consists of 25 polypeptide subunits (Table 2). Based on electron microscopy (EM) and biochemical analysis, the subunits have been assigned to four different modules, termed the head, middle, tail, and kinase modules (Asturias et al., 1999; Kang et al., 2001). Later studies refined these assignments and mapped also many subunit interactions (Guglielmi et al., 2004; Béve et al., 2005; Larivière et al., 2006; Takagi et al., 2006). While the head, middle and tail modules form the Mediator core complex, the kinase module appears to be dissociable. Of the 25 subunits, 10 are essential for yeast viability (Myers and Kornberg, 2000). Detailed structural information was obtained by X-ray crystallography for subunit CycC (Hoepfner2005), the subcomplexes Med7C/21 (Baumli et al., 2005), Med18/20, and Med8C/18/20 (Larivière et al., 2006, 2008) (“C” denotes the C-terminal portion of a subunit, “N” denotes the N-terminal portion), and by NMR for the Med15 KIX domain (Yang et al., 2006; Thakur et al., 2008). Electron microscopic studies of Mediator across several species (*S. cerevisiae*, Asturias et al. (1999); Davis et al. (2002); Cai et al. (2009); *S. pombe*, Elmlund et al. (2006); mouse, Asturias et al. (1999); and human, Taatjes et al. (2002, 2004); Knuesel et al. (2009)) show a dynamic arrangement of the modules and hence the exact Mediator architecture is still a matter of debate. For instance in *S. pombe*, the reversibly associated kinase module has been found by cryo-EM at 28 Å resolution located near to the middle module, thereby sterically blocking binding of RNA Pol II if present (Elmlund et al., 2006). In contrast, for human Mediator, a 38 Å reconstruction has been published in which the kinase module was found at the tail module instead (Knuesel et al., 2009). The very low-resolution cryo-EM structure of budding yeast Mediator (Asturias et al., 1999) has recently been replaced by a 28 Å reconstruction suggesting an additional arm domain that was defined on independent mobility comparisons of Mediator portions (Cai et al., 2009).

Table 2: Mediator subunits *S. cerevisiae*.

(Adapted from Myers and Kornberg (2000); Bourbon et al. (2004); Guglielmi et al. (2004); Béve et al. (2005))

Subunit	<i>S. cerevisiae</i> alias	Protein mass (kDa)	Module	Essential for viability	Activity
Med1	Med1	64	Middle	No	
Med2	Med2	48	Tail	No	Activator binding
Med3	Pgd1/Hrs1	43	Tail	No	Activator binding
Med4	Med4	32	Middle	Yes	
Med5	Nut1	129	Tail	No	Histone acetyltransferase
Med6	Med6	33	Head	Yes	
Med7	Med7	26	Middle	Yes	
Med8	Med8	25	Head	Yes	TBP binding
Med9	Cse2	17	Middle	No	
Med10	Nut2	18	Middle	Yes	
Med11	Med11	15	Head	Yes	
Med12	Srb8	167	Kinase	No	
Med13	Srb9/Ssn2	160	Kinase	No	
Med14	Rgr1	123	Middle/Tail	Yes	
Med15	Gal11	120	Tail	No	Activator binding
Med16	Sin4/Ssn4	111	Tail	No	
Med17	Srb4	78	Head	Yes	
Med18	Srb5	34	Head	No	
Med19	Rox3/Nut3/Ssn7	25	(unclear)	No	
Med20	Srb2/Hrs2	23	Head	No	TBP binding
Med21	Srb7	16	Middle	Yes	
Med22	Srb6	14	Head	Yes	
Med31	Soh1	15	Middle	No	
Cdk8	Srb10/Ssn3	63	Kinase	No	Cyclin dependent kinase
CycC	Srb11/Ssn8	38	Kinase	No	Cyclin

1.6.3 Mediator in transcriptional activation and repression

Mediator forms an interface between both the general RNA Pol II machinery and transcriptional activators and thereby promotes PIC assembly (Cantin et al., 2003). Recent data suggest a model in that Mediator plays an active role in transmitting information from activators to the transcriptional machinery and is itself subject to regulation (e.g. phosphorylation) which may explain Mediators' dual ability to act as both a coactivator and a corepressor (Biddick and Young, 2005).

In contrast to mammalian Mediator, where mostly Med1 binds directly to activators, in *S. cerevisiae* and other lower eukaryotes Med15 is the primary subunit for direct activator binding. Med15 is a large subunit located in the tail module (Figure 2 and Table 2) and bears a KIX and presumably also other activator binding domains (Thakur et al., 2008; Jedidi et al., 2010). Recruitment of Mediator to GAL promoters was found to be independent of the RNA Pol II transcription machinery and core promoter elements (Kuras et al., 2003). Similarly, recruitment of the subcomplex Med2/3/15 by Gcn4 in a *med16* Δ strain was independent of the rest of Mediator *in vivo* (Zhang et al., 2004).

Besides activator binding, the tail modules was also found to involved in histone acetylation as the Med5 subunit contains histone–acetyltransferase (HAT) activity (Lorch et al., 2000). Generally, acetylated nucleosomes are associated with a loosening of DNA and consequent increased access of the transcriptional machinery to the promoter (Biddick and Young, 2005). Med5 is not essential like all tail subunits (except for Med14), but this activity may be promoter-specific or redundant with other HATs.

Like TFIID (Stringer et al., 1990) and SAGA (Mohibullah and Hahn, 2008), Mediator can bind directly to TBP. The N-terminal domain of Med8 (Larivière et al., 2006) and also (but more weakly) Med20 (Koleske et al., 1992) bind to TBP *in vitro* and apparently mediate in a bipartite manner the attachment of Mediator. The head module has direct interactions also with TFIID (Esnault et al., 2008) and with a RNA Pol II-TFIID complex (Takagi et al., 2006). TFIID and TFIIE are recruited independently of RNA Pol II in a Mediator-dependent fashion (Esnault et al., 2008). Additionally, binding of TFIIB with Mediator head and middle modules was found using insect cell extracts (Kang et al., 2001), but remains unconfirmed using recombinant complexes (personal communication with S. Baumli; Takagi et al., 2006). However, although evidence for direct binding is unclear, TFIIB recruitment is Mediator-dependent whereas Mediator recruitment is TFIIB-independent (Baek et al., 2006).

The association of Mediator with RNA Pol II, and its function in transcription, depends on the RNA Pol II CTD. Mediator is able to bind an unphosphorylated glutathione S-transferase-CTD fusion protein *in vitro* (Myers et al., 1998) and can be displaced from RNA Pol II using the monoclonal antibody 8WG16, which specifically recognizes the CTD repeat (Kim et al., 1994; Svejstrup et al., 1997). Mediator also interacts with RNA Pol II domains outside of the CTD (Asturias et al., 1999; Davis et al., 2002; Cai et al., 2009). The Mediator kinase module was found to phosphorylate the CTD at serine 5 (Liao et al., 1995; Hengartner et al., 1998; Borggrefe et al., 2002) and to stimulate the kinase activity of TFIID via Kin28, the primary CTD kinase (Kim et al., 1994; Myers et al., 1998). Studies have shown that phosphorylated, elongating RNA Pol II is not associated with Mediator (Svejstrup et al., 1997) and indeed, CTD hyperphosphorylation has been reported to be sufficient to dissociate holo-RNA Pol II (Max et al., 2007). In agreement, inhibition of the kinase activity leads to trapped PICs incapable of transcription elongation (Liu et al., 2004).

In addition to playing a role in activator-dependent transcription, Mediator stimulates also basal transcription *in vitro* (reviewed in Myers and Kornberg, 2000; Biddick and Young, 2005). Biochemical studies have shown a requirement for Med18 and Med20 for basal transcription in a crude extract (Thompson et al., 1993) but no such dependence in a system reconstituted from highly purified transcription proteins (Sayre et al., 1992; Kim et al., 1994). Likewise, it was found that human Mediator is not essential for basal transcription by purified RNA Pol II and GTFs, but is essential for basal transcription in nuclear extracts that contain a more physiological set of factors (Baek et al., 2006). A similar pattern of dependence was also found for RNA Pol II CTD (Li et al., 1994), suggesting that basal transcription is dependent on Mediator to overcome a repressor, and that Mediator acts on the CTD in order to do so (Biddick and Young, 2005). High levels of TFIIB can bypass the Mediator requirement for basal transcription and RNA Pol II recruitment in HeLa nuclear extract,

thus indicating a conditional restriction on TFIIB function and a key role of Mediator in overcoming this restriction. In mammalian cells, Gdown1 was suggested to have this role, but as it is apparently absent in yeast, this may reflect a metazoan-specific regulatory feature (Hu et al., 2006). Additionally, an earlier rate-limiting step involved formation of a TFIID-Mediator-promoter complex in immobilized template assays (Baek et al., 2006). These key roles in basal transcription have led to a debate about whether Mediator should be classified as a GTF (Thompson and Young, 1995; Holstege et al., 1998; Mittler et al., 2001; Wu et al., 2003; Baek et al., 2006; Lewis and Reinberg, 2003; Takagi and Kornberg, 2006). Some genomewide location analyses in *S. cerevisiae* and *S. pombe* found Mediator upstream of almost all active genes and some inactive genes (Andrau et al., 2006; Zhu et al., 2006), but under different growth conditions Mediator did not localize to many active promoters (Fan et al., 2006). Thus, unlike the GTFs and RNA Pol II, the correlation between Mediator presence and transcription activity is less clear and Mediator functions may be promoter-specific (Sikorski and Buratowski, 2009).

Although the majority of findings point to Mediator's role as a coactivator, there is also strong evidence that suggests a negative role for Mediator in transcription as well. Especially the reversibly associated kinase module is mainly involved in transcription repression, notably through phosphorylation of the CTD domain of Rpb1 RNA Pol II subunit (Holstege et al., 1998; Liao et al., 1995), but also through phosphorylation of Ste12, Gcn4 and Msn2 transcription activators (Nelson et al., 2003; Chi et al., 2001). Moreover, cryo-EM studies in *S. pombe* suggested that the kinase module sterically blocks binding of RNA Pol II if present (Elmlund et al., 2006). Mediator mutants can lead also to increased transcription rates at some genes (Sternberg et al., 1987; Jiang and Stillman, 1992; Nishizawa, 2001; van de Peppel et al., 2005), but this effect may be indirect through post-transcriptional modifications, by alteration of expression levels of DNA-binding repressor proteins such as Mig1, Rox1, Ume6 (Biddick and Young, 2005) or by decreased recruitment of a general corepressor like the Ssn6-Tup1 complex (Papamichos-Chronakis et al., 2000). It can be speculated as well, that in some mutants Mediator is locked in an active state for some gene promoters. In general, given the complexity of transcriptional regulation in which Mediator is involved, it seems likely that improper coordination leads to negative regulation.

Even though Mediator may have a key role in coordinating transcription initiation (possibly in a checkpoint model), other coactivators are usually required at promoters *in vivo*. Thus, a number of studies (reviewed in Biddick and Young, 2009) led to the currently prevailing hypothesis that activators are specifically targeted to a gene through a DNA-binding domain and then recruit an array of coactivators via interactions with their activation domains (compare Bhoite et al., 2001; Cosma et al., 2001; Bryant and Ptashne, 2003; Swanson et al., 2003; Yoon et al., 2003; Bhaumik et al., 2004; Cheng et al., 2004; Gao et al., 2004; Lemieux and Gaudreau, 2004; Qiu et al., 2004; Govind et al., 2005; Larschan and Winston, 2005; Qiu et al., 2005; Leroy et al., 2006; Black et al., 2006; Young et al., 2008). Analysis of the recruitment at a variety of promoters showed that the order is promoter-specific. However, even in cases where activators interact with many of the same coactivators, that activator can function in more than one way (Biddick and Young, 2009). More recently, replacement of histone H2A

for the variant H2A.Z at the promoter nucleosomes -1 and +1 came into focus to have a key role in initiation as this was required for proper recruitment of a number of coactivators including Mediator, SAGA and Swi/Snf complexes (Lemieux et al., 2008).

1.7 Aims and scope of this thesis

Mediator complex must convey regulatory signals from transcriptional activators to RNA Pol II and other components of the initiation apparatus. This is possible as the Mediator modules serve various functions (as outlined previously): the tail module binds to activators and repressors (Han et al., 2001; Jeong et al., 2001; Thakur et al., 2008; Zhang et al., 2004), the middle and head modules contact RNA Pol II (Davis et al., 2002) and the general machinery (Baek et al., 2006; Esnault et al., 2008; Kang et al., 2001; Larivière et al., 2006), and the kinase module has inhibitory functions (Elmlund et al., 2006; van de Peppel et al., 2005). Unlike RNA Pol II (Cramer et al., 2008), the precise Mediator architecture and how Mediator functions mechanistically, is not well understood – mainly because atomic structures of Mediator modules or its subcomplexes are lacking. Such information would clarify the relative orientation of Mediator subunits within and between modules. On the functional level, gene expression studies with Mediator deletion mutants have implicated the tail in regulating sporulation genes and genes for oxidative phosphorylation, the tail and middle modules in regulating low-iron response and heat shock genes, the head module in regulating conjugation genes, and the kinase module in regulating genes required during nutrient starvation (Béve et al., 2005; Larivière et al., 2008; Singh et al., 2006; van de Peppel et al., 2005). Additionally, only recently it became clear that the modules may contain structurally and functionally distinct submodules, such as the Med8C/18/20 submodule of the Mediator head (Larivière et al., 2006, 2008).

Thus I aimed at filling this gap and proposed, to obtain structural and functional information on the module level – more precisely on the Mediator middle module from *S. cerevisiae*, a well-suited model organism for studying eukaryotic transcription. The central conserved part of the Mediator termed as middle module is apparently composed of Med1, Med4, Med7, Med9, Med10, Med21, and Med31. Structural studies of this core modules however require its preparation in large quantities and pure form. Thus far, only the head module is available in reconstituted form (Takagi et al., 2006). Previous work in the Cramer laboratory by Sonja Baumli led to a recombinant coexpression and purification strategy for a 6-subunit middle module comprising Med4/7/9/10/21/31. Based on this work, I aimed at crystallizing the module or suitable subcomplexes of it by repetitive limited proteolysis and removal of flexible regions. Obtained crystals would have been used for structure determination by cryo-crystallography with the help of synchrotron radiation and anomalous scattering. As a side goal, this required an in-depth understanding of the middle module intra-molecular interactions. The observed structural interactions should be correlated with their functional roles *in vitro* and *in vivo*. Another side-goal of this work was to optimize and extend the *Escherichia coli* (*E. coli*) coexpression strategy to the complete 7-subunit middle module and establish a functional assay to characterize its activity.

2 Materials and Methods

2.1 Materials

2.1.1 Bacterial strains

Table 3: *E. coli* strains.

Strain	Genotype	Source
XL-1 Blue	<i>rec1A; endA1; gyrA96; thi-1; hsdR17; supE44; relA1; lac[F' proAB lacI^qZΔM15 Tn10(Tet^r)]</i>	Stratagene
BL21-CodonPlus (DE3)RIL	B; F ⁻ ; <i>ompT; hsdS</i> (r _B ⁻ m _B ⁻); <i>dcm</i> ⁺ ; Tet ^r ; <i>gal</i> λ(DE3); <i>endA</i> ; Hte [<i>argU, ileY, leuW, Cam^r</i>]	Stratagene
Rosetta B834 (DE3)	F ⁻ ; <i>ompT; hsdSB</i> (r _B ⁻ m _B ⁻); <i>dcm</i> ⁺ ; <i>metB</i>	Novagen

2.1.2 Yeast strains

Table 4: List of *S. cerevisiae* strains used or generated within this study.

Strain	Genotype	Source
wt	BY4741; <i>MATa; his3Δ1; leu2Δ0; met15Δ0; ura3Δ0</i>	Euroscarf Y00000
wt	BY4742; <i>MATα; his3Δ1; leu2Δ0; lys2Δ0; ura3Δ0</i>	Euroscarf Y10000
wt	BY4743; <i>MATa/MATα; his3Δ1/his3Δ1; leu2Δ0/leu2Δ0; met15Δ0/MET15; LYS2/lys2Δ0; ura3Δ0/ura3Δ0</i>	Euroscarf Y20000
<i>MED7/med7Δ</i>	BY4743; <i>YOL135C::kanMX4/YOL135C</i>	Euroscarf Y26285
<i>MED7</i> shuffle	Y26285 sporulated; <i>MATa</i> or <i>MATα</i> ; <i>YOL135C::KanMX4/p20062</i> (cognate clone plasmid)	this work
<i>med31Δ</i>	BY4741; <i>YGL127C::kanMX4</i>	Euroscarf Y04494
<i>med7NΔ</i>	BY4741; <i>YOL135C::YOL135DN84-ClonNAT</i>	this work
<i>med7N/31Δ</i>	BY4741; <i>YOL135C::YOL135DN84-ClonNAT; YGL127C::kanMX4</i>	this work
wt/ <i>Med18-TAP</i>	BY4741; <i>YGR104C::YGR104C-TAP-URA3</i>	this work
<i>med31Δ/ Med18-TAP</i>	BY4741; <i>YGL127C::kanMX4; YGR104C::YGR104C-TAP-URA3</i>	this work
<i>med7NΔ/ Med18-TAP</i>	BY4741; <i>YOL135C::YOL135DN84-ClonNAT; YGR104C::YGR104C-TAP-URA3</i>	this work

continued on next page

Table 4: List of *S. cerevisiae* strains used or generated within this study.

Strain	Genotype	Source
<i>med7N/31Δ</i> / <i>Med18-TAP</i>	BY4741; <i>YOL135C::YOL135DN84-ClonNAT</i> ; <i>YGL127C::kanMX4</i> ; <i>YGR104C::YGR104C-TAP-URA3</i>	this work
<i>dst1Δ</i>	BY4741; <i>YGL0143W::kanMX4</i>	Euroscarf Y04411
<i>med18Δ</i>	Y24734 sporulated; <i>MATa</i> or <i>MATα</i> ; <i>YGR104C::kanMX4</i>	Larivière et al. (2008)
<i>med8CΔ</i>	Y23333 sporulated; <i>MATa</i> or <i>MATα</i> ; <i>YBR193C::kanMX4</i>	Larivière et al. (2008)
<i>cycCΔ</i>	BY4741; <i>YNL025C::kanMX4</i>	Euroscarf Y05351
<i>med1Δ</i>	BY4741; <i>YPR070W::kanMX4</i>	Euroscarf Y05489
<i>med9Δ</i>	BY4741; <i>YNR010W::kanMX4</i>	Euroscarf Y05385
<i>med2Δ</i>	BY4742; <i>YDL005C::kanMX4</i>	Euroscarf Y13701
<i>med3Δ</i>	BY4741; <i>YGL025C::kanMX4</i>	Euroscarf Y04393
<i>med5Δ</i>	BY4741; <i>YGL151W::kanMX4</i>	Euroscarf Y04518
<i>med14Δ/MED14</i>	BY4743; <i>YLR073C::kanMX4/YLR073C</i>	Euroscarf Y22682
<i>MED14</i> shuffle	BY4743; <i>MATa</i> or <i>MATα</i> ; sporulated; <i>YLR073C::kanMX4/pRS316-MED14</i>	this work
<i>med10Δ/MED10</i>	BY4743; <i>YPR168W::kanMX4/YPR168W</i>	Euroscarf Y25583
<i>MED10</i> shuffle	BY4743; <i>MATa</i> or <i>MATα</i> ; sporulated; <i>YPR168W::kanMX4/pRS316-MED10</i>	this work
<i>med4Δ/MED4</i>	BY4743; <i>YOR174W::kanMX4/YOR174W</i>	Euroscarf Y22430
<i>MED4</i> shuffle	BY4743; <i>MATa</i> or <i>MATα</i> ; sporulated; <i>YPR168W::kanMX4/pRS316-MED4</i>	this work
<i>med19Δ</i>	W303; <i>MATa</i> or <i>MATα</i> ; <i>leu2Δ3</i> ; 112 <i>trp1Δ1</i> ; <i>can1Δ100</i> ; <i>ura3Δ1</i> ; <i>ade2Δ1</i> ; <i>his3Δ11-15</i> ; <i>YBL093C::ClonNAT</i>	S. Jellbauer (Gene Center)
<i>med19Δ</i>	BY4741; <i>YBL093C::clonNAT</i>	S. Jellbauer (Gene Center)
<i>MED19</i> shuffle	BY4741; <i>YBL093C::clonNAT/pUG36-med19</i>	S. Jellbauer (Gene Center)
<i>med19Δ</i> / <i>Med7-TAP</i>	BY4741; <i>YBL093C::clonNAT</i> ; <i>YOL135C::YOL135C-TAP-kanMX4</i>	this work
<i>med19Δ</i> / <i>Med18-TAP</i>	BY4741; <i>YBL093C::clonNAT</i> ; <i>YGR104C::YGR104C-TAP-kanMX4</i>	this work
<i>med19Δ</i> / <i>Med15-TAP</i>	BY4741; <i>YBL093C::clonNAT</i> ; <i>YOL051W::YOL051W-TAP-KanMX4</i>	this work
<i>Med18-3xFlag</i>	BY4741; <i>YGR104C::YGR104C-3xFlag-His3MX</i>	this work
<i>Med18-3xFlag</i> / <i>Med7-TAP</i>	BY4741; <i>YGR104C::YGR104C-3xFlag-His3MX</i> ; <i>YOL135C::YOL135C-TAP-kanMX4</i>	this work
<i>Med15-3xFlag</i>	BY4742; <i>YOL051W::YOL051W-3xFlag-His3MX</i>	this work

continued on next page

Table 4: List of *S. cerevisiae* strains used or generated within this study.

Strain	Genotype	Source
<i>Med15-3xFlag / med19Δ / Med7-TAP</i>	BY4741; <i>YBL093C::clonNAT</i> ; <i>YOL135C::YOL135C-TAP-kanMX4</i> ; <i>YOL051W::YOL051W-3xFlag-His3MX</i>	this work
<i>Med18-3xFlag / med19Δ / Med7-TAP</i>	BY; <i>MATa</i> ; mated; <i>YBL093C::clonNAT</i> ; <i>YOL135C::YOL135C-TAP-kanMX4</i> ; <i>YGR104C::YGR104C-3xFlag-His3MX</i>	this work
<i>Med14-TAP</i>	BY4741; <i>YLR051C::YLR051C-TAP-URA3</i>	this work
<i>med20Δ / Med14-TAP</i>	BY4741; <i>YHR041C::kanMX4</i> ; <i>YLR051C::YLR051C-TAP-URA3</i>	this work
<i>med31Δ / Med14-TAP</i>	BY4741; <i>YGL127C::kanMX4</i> ; <i>YLR051C::YLR051C-TAP-URA3</i>	this work

2.1.3 Plasmids

Table 5: List of vectors for recombinant *S. cerevisiae* Mediator middle module subunits and interaction assays.

Vector	Inserts	Type	Restriction sites	Reference
pSB45	<i>MED7</i> (103-222) <i>MED21-His6</i>	pET21b	Nhe I, EcoR I Sal I, Not I	S. Baumli
pSB48	<i>MED7</i> (103-222) <i>MED21-His6</i>	pET24b	Nhe I, EcoR I Sal I, Not I	S. Baumli
pSB60	<i>MED10</i>	pET21b	Nde I, EcoR I	S. Baumli
pSB77	<i>MED10-His6</i>	pET24b	Nde I, Not I	S. Baumli
pSB91	<i>MED4</i>	pET21b	Nde I, Not I	S. Baumli
pSB102	<i>MED31-His6</i>	pET24d	Nco I, EcoR I	S. Baumli
pSB104	<i>MED10</i> <i>MED7</i> <i>MED21</i>	pET21b	Nhe I, EcoR I Nco I, Sal I Nde I, Xho I	S. Baumli
pSB118	<i>MED9</i> <i>MED4</i>	pET21b	Nde I, BamH I Nde I, Xho I	S. Baumli
pTK01	<i>MED10</i> <i>MED7</i> (1-205) <i>MED21</i>	pET21b	Nhe I, EcoR I EcoR I, Sal I Nde I, Xho I	this work
pTK02	<i>MED10</i> <i>MED7</i> <i>MED21</i> (1-130)	pET21b	Nhe I, EcoR I Nco I, Sal I Sal I, Xho I	this work
pTK03	<i>MED10</i> <i>MED7</i> (1-205) <i>MED21</i> (1-130)	pET21b	Nhe I, EcoR I EcoR I, Sal I Sal I, Xho I	this work
pTK04	<i>MED31-His6</i> <i>MED6-StrepII</i>	pET24d	Nco I, EcoR I Sal I, Not I	this work

continued on next page

Table 5: List of vectors for recombinant *S. cerevisiae* Mediator middle module subunits and interaction assays.

Vector	Inserts	Type	Restriction sites	Reference
pTK06	<i>MED10</i> (8-157)	pET21b	Nhe I, EcoR I	this work
	<i>MED7</i> (1-205)		EcoR I, Sal I	
	<i>MED21</i> (1-130)		Sal I, Xho I	
pTK07	<i>MED10</i> (41-157)	pET21b	Nhe I, EcoR I	this work
	<i>MED7</i> (1-205)		EcoR I, Sal I	
	<i>MED21</i> (1-130)		Sal I, Xho I	
pTK08	<i>MED10</i> (68-157)	pET21b	Nhe I, EcoR I	this work
	<i>MED7</i> (1-205)		EcoR I, Sal I	
	<i>MED21</i> (1-130)		Sal I, Xho I	
pTK09	<i>MED10</i> (8-147)	pET21b	Nhe I, EcoR I	this work
	<i>MED7</i> (1-205)		EcoR I, Sal I	
	<i>MED21</i> (1-130)		Sal I, Xho I	
pTK10	<i>MED10</i> (41-147)	pET21b	Nhe I, EcoR I	this work
	<i>MED7</i> (1-205)		EcoR I, Sal I	
	<i>MED21</i> (1-130)		Sal I, Xho I	
pTK11	<i>MED10</i> (68-147)	pET21b	Nhe I, EcoR I	this work
	<i>MED7</i> (1-205)		EcoR I, Sal I	
	<i>MED21</i> (1-130)		Sal I, Xho I	
pTK12	<i>MED10</i>	pET21b	Nhe I, EcoR I	this work
	<i>MED7</i> (1-211)		EcoR I, Sal I	
	<i>MED21</i>		Sal I, Xho I	
pTK13	<i>MED10</i> (12-157)	pET21b	Nhe I, EcoR I	this work
	<i>MED7</i>		EcoR I, Sal I	
	<i>MED21</i>		Sal I, Xho I	
pTK14	<i>MED10</i> (12-157)	pET21b	Nhe I, EcoR I	this work
	<i>MED7</i> (1-211)		EcoR I, Sal I	
	<i>MED21</i>		Sal I, Xho I	
pTK15	<i>MED9</i>	pET21b	Nde I, BamH I	this work
	<i>MED4</i> (1-250)		Sal I, Xho I	this work
pTK16	<i>MED7</i>	pET21b	Nhe I, EcoR I	this work
	<i>MED21</i>		Sal I, Xho I	this work
pTK17	<i>MED9</i>	pET21b	Nde I, BamH I	this work
	<i>MED4</i> (21-250)		Sal I, Xho I	this work
pTK18	<i>MED10</i> (8-157)	pET21b	Nhe I, EcoR I	this work
	<i>MED7</i>		EcoR I, Sal I	
	<i>MED21</i>		Sal I, Xho I	
pTK19	<i>MED10</i> (41-157)	pET21b	Nhe I, EcoR I	this work
	<i>MED7</i>		EcoR I, Sal I	
	<i>MED21</i>		Sal I, Xho I	
pTK20	<i>MED10</i> (68-157)	pET21b	Nhe I, EcoR I	this work
	<i>MED7</i>		EcoR I, Sal I	
	<i>MED21</i>		Sal I, Xho I	
pTK21	<i>MED10</i> (8-147)	pET21b	Nhe I, EcoR I	this work

continued on next page

Table 5: List of vectors for recombinant *S. cerevisiae* Mediator middle module subunits and interaction assays.

Vector	Inserts	Type	Restriction sites	Reference
	<i>MED7</i>		EcoR I, Sal I	
	<i>MED21</i>		Sal I, Xho I	
pTK22	<i>MED10</i> (41-147)	pET21b	Nhe I, EcoR I	this work
	<i>MED7</i>		EcoR I, Sal I	
	<i>MED21</i>		Sal I, Xho I	
pTK23	<i>MED10</i> (68-147)	pET21b	Nhe I, EcoR I	this work
	<i>MED7</i>		EcoR I, Sal I	
	<i>MED21</i>		Sal I, Xho I	
pTK24	<i>MED31</i> -His ₆	pET24d	Nco I, EcoR I	this work
	<i>MED7</i> (1-101)		Sal I, Not I	
pTK25	<i>MED7</i> (1-101)	pET21b	EcoR I, Sal I	this work
pTK26	His ₆ -thrombin- <i>MED31</i>	pET28b	Nde I, Not I	this work
pTK27	<i>MED7</i> (1-80)	pET21b	EcoR I, Sal I	this work
pTK28	<i>MED7</i> (1-83)	pET21b	EcoR I, Sal I	this work
pTK29	<i>MED7</i> (1-89)	pET21b	EcoR I, Sal I	this work
pTK30	<i>MED7</i> (1-92)	pET21b	EcoR I, Sal I	this work
pTK31	<i>MED31</i> -His ₆	pET24d	Nco I, EcoR I	this work
	<i>MED6</i> (1-199)-StrepII		Sal I, Not I	
pTK32	<i>MED31</i> -His ₆	pET24d	Nco I, EcoR I	this work
	<i>MED6</i> (1-203)-StrepII		Sal I, Not I	
pTK33	<i>MED31</i> -His ₆	pET24d	Nco I, EcoR I	this work
	<i>MED6</i> (1-207)-StrepII		Sal I, Not I	
pTK34	<i>MED31</i> -His ₆	pET24d	Nco I, EcoR I	this work
	<i>MED6</i> (1-189)-StrepII		Sal I, Not I	
pTK35	StrepII- <i>MED1</i>	pET24d	Nco I, Not I	this work
pTK36	<i>MED1</i> -StrepII	pET24d	Nco I, Not I	this work
pTK37	His ₆ - <i>MED14</i>	pET21b	Eco RI, Xho I	this work
pTK38	<i>MED14</i> -His ₆	pET21b	Eco RI, Xho I	this work
pTK39	<i>MED7</i> (1-95)	pET21b	EcoR I, Sal I	this work
pTK40	<i>C. Glabrata MED7</i> (1-95)	pET21b	Nde I, Not I	this work
pTK53	His ₆ -thrombin- <i>ESS1</i>	pET28b	Nde I, Not I	this work
pTK54	<i>SET2</i> -His ₆	pET24d	Nhe I, Xho I	this work
pTK55	<i>SET2</i> WW-His ₆	pET24d	Nco I, Xho I	this work
pTK56	<i>MED31</i> -His ₆	pET21b	Xba I, Eco RI	this work
pTK57	<i>PCF11</i> CID-His ₆	pET21b	Xba I, Not I	H. Kettenberger
pTK60	<i>MED7</i> (19-83)	pET21b	EcoR I, Sal I	this work
pTK61	<i>MED7</i> (22-84)	pET21b	EcoR I, Sal I	this work
pTK62	<i>MED7</i> (1-61)	pET21b	EcoR I, Sal I	this work
pTK63	<i>MED7</i> (1-67)	pET21b	EcoR I, Sal I	this work
pTK64	StrepII- <i>MED7</i> (20-83)	pET21b	NdeI, Sal I	this work
pTK65	StrepII- <i>MED7</i> (23-83)	pET21b	NdeI, Sal I	this work
pTK66	StrepII- <i>MED7</i> (1-61)	pET21b	NdeI, Sal I	this work
pTK67	StrepII- <i>MED7</i> (1-66)	pET21b	NdeI, Sal I	this work

continued on next page

Table 5: List of vectors for recombinant *S. cerevisiae* Mediator middle module subunits and interaction assays.

Vector	Inserts	Type	Restriction sites	Reference
pTK68	StrepII- <i>MED7</i> (1-83)	pET21b	NdeI, Sal I	this work
pTK69	StrepII- <i>MED4</i> (19-250)	pET21b	Sal I, Xho I	this work
pTK70	His ₆ -thrombin- <i>MED9</i>	pET28b	Nde I, Sal I	this work
pTK71	His ₆ -thrombin- <i>MED9</i> (63-149)	pET28b	Nde I, Sal I	this work
pTK72	His ₆ -thrombin- <i>MED9</i> (1-18)	pET28b	Nde I, Sal I	this work
pTK73	His ₆ -thrombin- <i>MED9</i> (1-22)	pET28b	Nde I, Sal I	this work
pTK74	His ₆ -thrombin- <i>MED9</i> Δ(19-63)	pET28b	Nde I, Sal I	this work
pTK75	His ₆ -thrombin- <i>MED9</i> Δ(19-53)	pET28b	Nde I, Sal I	this work
pTK76	His ₆ -thrombin- <i>MED9</i> Δ(23-63)	pET28b	Nde I, Sal I	this work
pTK77	His ₆ -thrombin- <i>MED9</i> Δ(23-53)	pET28b	Nde I, Sal I	this work
pTK78	StrepII- <i>MED31</i>	pET24d	Nco I, Not I	this work
pTK79	<i>MED7</i> (1-83) (12...18 YSPTSPS)	pET21b	EcoR I, Sal I	this work
pTK80	<i>MED7</i> (1-83) (13...19 YSPTSPS)	pET21b	EcoR I, Sal I	this work
pTK81	<i>MED7</i> (1-83) (66...72 YSPTSPS)	pET21b	EcoR I, Sal I	this work
pTK82	<i>MED7</i> (1-83) (65...71 YSPTSPS)	pET21b	EcoR I, Sal I	this work
pTK84	<i>MED7</i> (1-83) (12...18 SPSTPSY)	pET21b	EcoR I, Sal I	this work
pTK86	<i>MED7</i> (1-83) (12...18 YSPTDPS)	pET21b	EcoR I, Sal I	this work
pTK88	<i>MED7</i> (1-83) (12...18 YSPTRPS)	pET21b	EcoR I, Sal I	this work
pTK90	<i>MED7</i> (1-83) (12...18 YDPTSPS)	pET21b	EcoR I, Sal I	this work
pTK92	StrepII- <i>MED7</i> (1-83)	pET24a	Nde I, Sal I	this work
pTK93	<i>MED9</i> (1-63)	pET21b	Nde I, Sal I	this work
pTK94	<i>MED9</i> (1-80)	pET21b	Nde I, Sal I	this work
pTK95	<i>MED9</i> (64-149)	pET21b	Nde I, Sal I	this work
pTK96	<i>MED9</i> (81-149)	pET21b	Nde I, Sal I	this work
pTK97	<i>MED10</i> (1-73)	pET21b	Nde I, EcoR I	this work
pTK98	<i>MED10</i> (74-157)	pET21b	Nde I, EcoR I	this work
pTK99	<i>MED31</i> -His ₆	pET24d	Nco I, EcoR I	this work
	StrepII- <i>MED7</i> (1-83)		Sal I, Not I	
pTK100	<i>MED4</i> -His ₆	pET24a	Nde I, Not I	this work
pTK101	StrepII- <i>MED14</i> (1-259)	pET24d	Nco I, Xho I	this work
pTK102	StrepII- <i>MED14</i> (1-528)	pET24d	EcoRI, Xho I	this work
pTK103	StrepII- <i>MED14</i> (1-745)	pET24d	EcoRI, Xho I	this work
pTK104	StrepII- <i>MED1</i>	pET24d	Nco I, Sal I	this work
	<i>MED14</i> (1-259)		Sal I, Not I	
pTK105	StrepII- <i>MED1</i>	pET24d	Nco I, Sal I I	this work
	<i>MED14</i> (1-528)		Sal I, Not I	
pTK106	StrepII- <i>MED1</i>	pET24d	Nco I, Sal I I	this work
	<i>MED14</i> (1-745)		Sal I, Not I	this work
pTK107	<i>MED1</i>	pET24d	Nco I, Sal I	this work
pTK112	<i>MED31</i> -His ₆	pET24d	Nco I, EcoR I	this work
	<i>MED14</i> (1-259)		Sal I, Not I	
pTK113	<i>MED9</i>	pCDFDuet-1	Asi SI, BamH I (MCS2)	this work
	<i>MED4</i>		Nde I, Xho I (MCS2)	this work

continued on next page

Table 5: List of vectors for recombinant *S. cerevisiae* Mediator middle module subunits and interaction assays.

Vector	Inserts	Type	Restriction sites	Reference
pTK114	StrepII- <i>MED1</i> <i>MED9</i> <i>MED4</i>	pCDFDuet-1	Nco I, Not I (MCS1) Asi SI, BamH I (MCS2) Nde I, Xho I (MCS2)	this work
pTK126	<i>MED10</i> <i>MED7</i> (Q198Stop) <i>MED21</i>	pET21b	Nhe I, EcoR I Nco I, Sal I Nde I, Xho I	this work this work this work
pTK127	<i>MED10</i> <i>MED7</i> <i>MED21</i> (L76P)	pET21b	Nhe I, EcoR I Nco I, Sal I Nde I, Xho I	this work this work this work
pTK128	<i>MED10</i> (S124Stop) <i>MED7</i> <i>MED21</i>	pET21b	Nhe I, EcoR I Nco I, Sal I Nde I, Xho I	this work this work this work
pTK129	<i>MED31</i> <i>MED14</i> (1-259)	pET24d	Nco I, EcoR I Sal I, Not I	this work this work
pTK130	His ₆ - <i>MED9</i> <i>MED4</i>	pCDFDuet-1	Asi SI, BamH I (MCS2) Nde I, Xho I (MCS2)	this work
pTK131	StrepII- <i>MED1</i> His ₆ - <i>MED9</i> <i>MED4</i>	pCDFDuet-1	Nco I, Not I (MCS1) Asi SI, BamH I (MCS2) Nde I, Xho I (MCS2)	this work
pTK133	<i>MED31</i> -His ₆ StrepII- <i>MED7</i> (1-101)	pET24d	Nco I, EcoR I Sal I, Not I	this work
pTK134	<i>MED31</i> -His ₆ <i>MED7</i> (1-83)	pET24d	Nco I, EcoR I Sal I, Not I	this work

Table 6: List of vectors used or generated for *S. cerevisiae* assays and manipulations.

Vector	Inserts	Type	Restriction sites	Reference
p20062	<i>MED7</i>	Cognate clone		Euroscarf
pBS1539	C-TAP-tag / <i>URA3</i>	pBS	PCR-template	Puig et al. (2001)
pFA6a-KanMX4	KanMX4	pFA6a	PCR-template	Wach et al. (1994)
pFA6a-His3MX4	His3MX4	pFA6a	PCR-template	Wach et al. (1997)
pFA6a-natNT2	natNT2	pFA6a	PCR-template	Janke et al. (2004)
pYM13	C-TAP-tag / kanMX4	pYM	PCR-template	Janke et al. (2004)
pZM473	3xFLAG-tag	pZM	PCR-template	Moqtaderi and Struhl (2008)
pTK42	<i>MED7</i> (1-83)	pAL-	Sma I, Xba I	this work
pTK43	<i>MED7</i> (1-89)	pAL-	Sma I, Xba I	this work
pTK44	<i>MED7</i> (1-101)	pAL-	Sma I, Xba I	this work
pTK45	<i>MED7</i> (102-222)	pAL-	Sma I, Xba I	this work
pTK46	<i>MED7</i>	pAL-	Sma I, Xba I	this work
pTK58	natNT2-5'UTR- <i>MED7</i> (84-222)-3'UTR	pBluescript II KS-	Xho I, Xba I	this work
pTK59	natNT2-5'UTR- <i>MED7</i> (84-222)-3'UTR	pRS315	Sal I, Xba I	this work
pTK83	5'UTR- <i>MED7</i> (84-222)-3'UTR-NATNT2	pBluescript II KS-	Xho I, EcoRV	this work
pTK108	5'UTR- <i>MED14</i> -3'UTR	pRS316	Sal I, Not I	this work
pTK109	5'UTR- <i>MED14</i> (1-259)-3'UTR	pRS315	Sal I, Not I	this work
pTK110	5'UTR- <i>MED14</i> (1-528)-3'UTR	pRS315	Sal I, Not I	this work
pTK111	5'UTR- <i>MED14</i> (1-745)-3'UTR	pRS315	Sal I, Not I	this work
pTK115	5'UTR- <i>MED14</i> -3'UTR	pRS315	Sal I, Not I	this work
pTK116	5'UTR- <i>MED10</i> -3'UTR	pRS316	Sal I, Not I	this work
pTK117	5'UTR- <i>MED10</i> -3'UTR	pRS315	Sal I, Not I	this work
pTK118	5'UTR- <i>MED10</i> (1-123)-3'UTR	pRS315	Sal I, Not I	this work
pTK119	5'UTR- <i>MED10</i> (74-157)-3'UTR	pRS315	Sal I, Not I	this work
pTK120	5'UTR- <i>MED10</i> (74-123)-3'UTR	pRS315	Sal I, Not I	this work
pTK132	5'UTR- <i>MED10</i> (S124Stopp)-3'UTR	pRS315	Sal I, Not I	this work
pTK121	5'UTR- <i>MED4</i> -3'UTR	pRS316	Sal I, Not I	this work
pTK122	5'UTR- <i>MED4</i> -3'UTR	pRS315	Sal I, Not I	this work
pTK123	5'UTR- <i>MED4</i> (67-284)-3'UTR	pRS315	Sal I, Not I	this work
pTK124	5'UTR- <i>MED4</i> (67-250)-3'UTR	pRS315	Sal I, Not I	this work
pTK125	5'UTR- <i>MED4</i> (67-193)-3'UTR	pRS315	Sal I, Not I	this work

2.1.4 Media and additives

Table 7: Media for *E. coli* and *S. cerevisiae*.

Media	Application	Description
LB	<i>E. coli</i> culture	1% (w/v) tryptone; 0.5% (w/v) yeast extract; 0.5% (w/v) NaCl
SOB	<i>E. coli</i> transformation	2% (w/v) tryptone; 0.5% (w/v) yeast extract; 8.55 mM NaCl; 2.5 mM KCl; 10 mM MgCl ₂
SOC	<i>E. coli</i> transformation	SOB + 20 mM glucose (before use)
Minimal medium	SeMet labeling	7.5 mM (NH ₄) ₂ SO ₄ ; 8.5 mM NaCl; 55 mM KH ₂ PO ₄ ; 100 mM K ₂ HPO ₄ ; 1mM MgSO ₄ ; 20 mM glucose, 1 µg/l trace elements (Cu ²⁺ , Mn ²⁺ , Zn ²⁺ , Mo ₄ ²⁻), 10 mg/l thiamine; 10 mg/l biotine; 1 mg/l Ca ²⁺ ; 1 mg/l Fe ²⁺ ; 100 mg/l amino acids (A, C, D, E, F, G, H, I, K, L, N, P, Q, R, S, T, V, W, Y); 50 mg/l selenomethionine
YPD	Yeast culture	2% (w/v) peptone; 2% (w/v) glucose; 1% (w/v) yeast extract
Synthetic defined (SD)	Yeast culture	Nitrogen and carbon sources, vitamins, trace elements, minerals according to ForMedium with specific drop outs; only essential amino acids; pH 5.6-6.0
Synthetic complete (SC)	Yeast culture	0.69% (w/v) nitrogen base; 0.6% (w/v) CSM amino acid drop out mix; 2% (w/v) glucose; pH 5.6-6.0
5-FOA plates	Yeast culture	SC (-ura) + 0.01% (w/v) uracil; 0.2% (w/v) 5-FOA
Pre-sporulation plates	Yeast culture	1% (w/v) KCH ₃ COO; 0.1% (w/v) yeast extract; 0.079% (w/v) CSM amino acid complete mix; 0.25% (w/v) glucose; pH 5.6-6.0
Sporulation plates	Yeast culture	1% (w/v) KCH ₃ COO; 0.079% (w/v) CSM amino acid complete mix; pH 5.6-6.0

Table 8: Media additives for *E. coli* and *S. cerevisiae*.

Additive	Description	Stock solution	Applied concentration
IPTG	<i>E. coli</i> induction	1 M in H ₂ O	0.5 mM
Ampicillin	Antibiotic	100 mg/ml in H ₂ O	100 µg/ml for <i>E. coli</i> culture, 50 µg/ml for yeast culture
Kanamycin	Antibiotic	30 mg/ml in H ₂ O	30 µg/ml for <i>E. coli</i> culture
Chloramphenicol	Antibiotic	50 mg/ml in EtOH	50 µg/ml for <i>E. coli</i> culture
Streptomycin	Antibiotic	50 mg/ml in EtOH	50 µg/ml for <i>E. coli</i> culture
Tetracyclin	Antibiotic	12.5 mg/ml in 70% EtOH	12.5 µg/ml for yeast culture
Geneticin (G418)	Antibiotic	200 mg/ml in H ₂ O	200 µg/ml for yeast culture
Nourseothricin (clonNAT)	Antibiotic	100 mg/ml in H ₂ O	100 µg/ml for yeast culture

2.1.5 Buffers and solutions

Standard buffers and solutions were prepared according to Sambrook and Russell (2001).

Table 9: General buffers, dyes and solutions.

Name	Description	Application
4x Stacking gel buffer	0.5 M Tris; 0.4% (w/v) SDS; pH 6.8 at 25°C	SDS-PAGE
4x Separation gel buffer	3 M Tris; 0.4% (w/v) SDS; pH 8.9 at 25°C	SDS-PAGE
Electrophoresis buffer	25 mM Tris; 0.1% (w/v) SDS; 250 mM glycine	SDS-PAGE
5x SDS sample buffer	250 mM Tris/HCl pH 7.0 at 25°C; 50% (v/v); glycerol; 0.5% (w/v) bromophenol blue; 7.5% (w/v) SDS; 12.5% (w/v) β -mercaptoethanol	SDS-PAGE
Gel staining solution	50% (v/v) Ethanol; 7% (v/v) acetic acid; 0.125% (w/v) Coomassie Brilliant Blue R-250	Coomassie staining
Gel destaining solution	5% (v/v) Ethanol; 7% (v/v) acetic acid	Coomassie staining
2x Western transfer buffer	2.4% (w/v) glycine; 0.8% (w/v) Tris; 40% (v/v) methanol	Western blotting
Blotting buffer	10% (v/v) methanol in ddH ₂ O	Edman sequencing
Swelling buffer	200 mM Tris/HCl pH 8.5 at 25°C; 2% (w/v) SDS	Edman sequencing
100x PI	0.028 mg/ml leupeptin; 0.137 mg/ml pepstatin A; 0.017 mg/ml PMSF; 0.33 mg/ml benzamidine; in 100% EtOH p.a.	Protease inhibitor mix
TBE	8.9 mM Tris; 8.9 mM boric acid; 2 mM EDTA (pH 8.0, 25°C)	Agarose gels
6x Loading buffer	10 mM Tris pH 7.6; 0.0015% (w/v) bromophenol blue; 0.0015% (w/v) xylene cyanol; 60% (v/v) glycerol; 100 mM EDTA; 1% SDS	Agarose gels
TFB-1	30 mM KOAc; 50 mM MnCl ₂ ; 100 mM RbCl; 10 mM CaCl ₂ ; 15% (v/v) glycerol; pH 5.8 at 25°C	Chemically competent cells
TFB-2	10 mM MOPS pH 7.0 at 25°C; 10 mM RbCl; 75 mM CaCl ₂ ; 15% (v/v) glycerol	Chemically competent cells
Triple trafo buffer	100 mM CaCl ₂ , 10% (w/v) glycerol	Chemically competent cells
LiAc buffer	1 M Li acetate; pH 7.5 adjusted with acetic acid	Yeast transformation
Buffer A	50 mM Tris pH 8.0; 150 mM NaCl; 10 mM β -mercaptoethanol	Recombinant proteins
Buffer B	50 mM Tris pH 8.0; 100 mM NaCl; 10 mM β -mercaptoethanol	Recombinant proteins
Buffer C	50 mM MES pH 6.5; 150 mM NaCl; 10 mM β -mercaptoethanol	Recombinant proteins
Buffer D	20 mM Tris pH 8.0; 150 mM NaCl; 10 mM β -mercaptoethanol	Recombinant proteins
Buffer E	50 mM Tris pH 8.0; 150 mM NaCl; 10% (v/v) glycerol; 10 mM β -mercaptoethanol	Recombinant proteins
Buffer F	150 mM KCl, 10 mM Hepes pH 7.3, 5 mM DTT	Recombinant proteins
Buffer G	50 mM Hepes pH 7.5; 150 mM NaCl; 10 mM β -mercaptoethanol	Recombinant proteins
Avidin	50 μ mol/l avidin; 50% (w/v) glycerin; 20 mM Tris pH 8.0; 150 mM NaCl; 10 mM β -mercaptoethanol	StrepII-purification
50x d-Desthiobiotin	125 mM d-desthiobiotin; in 500 mM Tris pH 8.0	StrepII-purification
TAP/FLAG buffer I	50mM Tris pH 7.5; 250 mM NaCl; 1.5 mM MgCl ₂ ; 0.1% (v/v) NP40 (Igepal CA-630); 1x PI	TAP- or FLAG-purification
TAP/FLAG buffer II	50mM Tris pH 7.5; 100 mM NaCl; 1.5 mM MgCl ₂ ; 0.1% (v/v) NP40 (Igepal CA-630); 1x PI	TAP- or FLAG-purification
TEV cleavage buffer	TAP buffer II + 1 mM DTT; 0.5 mM EDTA	TAP-purification
Calmodulin buffer	TAP buffer II + 2 mM CaCl ₂ ; 1 mM DTT	TAP-purification
TAP elution buffer	10 mM Tris pH 8.0, 20 mM EGTA	TAP-purification

2.2 General methods

2.2.1 Preparation and transformation of competent cells

Chemically competent *E. coli* cells were prepared from LB overnight pre-cultures. 200 ml LB medium (supplemented with antibiotics if appropriate) were inoculated to a start optical density at 600 nm ($OD_{600\text{ nm}}$) of 0.05, grown at 37°C and chilled on ice for 10 min once $OD_{600\text{ nm}}=0.5$ was reached. Following steps were carried out at 4°C. Cells were centrifuged at 3200g for 10 min, washed with 50 ml TFB-1 buffer, centrifuged again and the pellet resuspended in 4 ml TFB-2 buffer. Aliquots were frozen in liquid nitrogen and cells stored at -80°C. Cells were transformed by heat shock typically using 100 ng (single transformation) or 150 ng (double transformation) vector, or 5-10 μl ligation product. Cells were incubated on ice for 10 min prior to heat shock at 42°C for 1 min in a water bath. Cells were subsequently cooled on ice for 1 min, 250 μl LB medium added and incubated for 1 h at 37°C vigorously shaking in a thermomixer (Qiagen). Cells were plated onto selective plates and incubated over night at 37°C.

For triple transformations, cotransformed cells containing already two vectors were made chemically competent again. One inoculation loop cells were scraped off from selective plates, resuspended in 500 μl Triple trafo buffer and incubated on ice 30 min. Cells were centrifuged for 15 sec at 18000g and 4°C, resuspended again in 50 μl Triple trafo buffer and used directly for heat shock transformation.

Electrocompetent *E. coli* cells were prepared from SOB overnight pre-cultures. Precultures at $OD_{600\text{ nm}}=3.0$ were used to inoculate 1 l (prewarmed) SOB main cultures in 5 l shake flasks to yield a start $OD_{600\text{ nm}}=0.03$. Cells were grown at 37°C and chilled on ice for 15 min once $OD_{600\text{ nm}}=0.5$ was reached. Following steps were carried out at 4°C. Cells were split in 4 portions, centrifuged at 3200g for 10 min and washed with each 100 ml ice-cold, sterile water. Cells were centrifuged again and each pellet washed in 2.5 ml cold, sterile 10% (v/v) glycerol. Cells were pooled, centrifuged again and resuspended in 1.5 ml cold, sterile 10% (v/v) glycerol. Aliquots were frozen in liquid nitrogen and cells stored at -80°C. Cells were electrotransformed typically using 5 μl ligation product using pre-chilled 0.2 cm electroporation cuvettes (Bio-Rad) after 5 min incubation on ice. Cuvettes were pulsed with 2.5 kV (MicroPulser, Bio-Rad) and immediately mixed with 1 ml ice-cold SOC medium. Cells were incubated vigorously shaking in a thermomixer (Qiagen) for 1 h for recovery prior to plating onto selective plates.

Chemical competent yeast cells were prepared from precultures in YPD overnight pre-cultures grown at 30°C. One hundred ml main cultures were inoculated with a start $OD_{600\text{ nm}}$ of 0.2 and grown until $OD_{600\text{ nm}}=0.8$ was reached. Cells were split in two portions, centrifuged at 1250g for 5 min, washed with each 25 ml sterile water and centrifuged again. The pellets were resuspended in 1 ml 1:10 LiAc buffer, centrifuged at 18000g for 15 sec and resuspended to yield 500 μl each. Cells were vortexed, pooled, incubated 10 min to over night and aliquoted to 100 μl portions. After centrifugation, supernatants were discarded and cells used either directly for highest competence or stored at -80°C after addition of 240 μl 50% (w/v) PEG 3350. Following PEG 3350 addition, 36 μl 1 M LiAc, 50 μl pre-heated (10 minutes

at 95°C, then put on ice) salmon sperm DNA (2 mg/ml) and 34 μ l DNA/water mixture was added. Typically, either 1-5 μ g of linear DNA or 200 ng plasmid DNA was used for transformation. Samples were vortexed vigorously for 1 min and incubated 30 min at 30°C. Cells were heat shocked for 25 min at 42°C in a water bath. Samples were centrifuged at 5200g for 15 sec and pellets resuspended in 1 ml YPD without antibiotics. Cells were incubated for at least 1 h up to over night at 30°C rotation for recovery, then centrifuged at 1250g for 5 min, resuspended in 200 μ l 1xTE buffer and plated onto selective plates.

2.2.2 Cloning and mutagenesis

Polymerase Chain Reaction (PCR) primers were typically designed by using the software Primer Designer (now Sci-Ed Software) including an appropriate overhang of several nucleotides at the 5' end (to ease restriction cleavage), followed by the restriction site and at least 20 nt complementary to the sequence of the gene of interest. Purification-tags were introduced either by in-frame cloning into according vectors or by PCR. Additional ribosomal binding sites for multicistronic vectors were introduced as described in Baumli (2005). Sequencing primers were usually around 20 nt long. PCR reactions were carried out with Herculase or Herculase II polymerases (Stratagene), Pwo SuperYield DNA Polymerase (Roche), Phusion High-Fidelity DNA Polymerase (Finnzymes) or Taq polymerase (Fermentas) according to requirements. Reaction were typically performed at 50 μ l scale and contained polymerase specific buffers, 1-30 ng plasmid template or 100-200 ng genomic DNA template, 0.2 mM dNTP-mix, 0.5 μ M forward and reverse primer each, and variable amounts of polymerase (0.5-5U), salt and DMSO. Theoretical annealing temperatures were calculated with the Primer Designer software using the empirical method of Rychlik et al. (1990). Thermocycling programs were adjusted to the specific needs of the individual reactions, especially in terms of annealing temperature and elongation times, and usually contained 30 cycles (Biometra T3000 Thermocycler).

PCR products were purified using PCR-purification kits (Qiagen or Metabion). PCR products and vectors were digested using restriction endonucleases (NEB and Fermentas) as recommended by the vendor and vectors dephosphorylated by addition of 1U FastAP enzyme (Fermentas) following incubation for 10 min at 37°C and heat inactivation for 5 min at 75°C. Samples were separated by agarose gel electrophoresis (typically 1% w/v) in 1xTBE buffer and visualized by ethidiumbromide or SYBR Safe DNA gel stain (1:10 000, Invitrogen). DNA fragments were extracted and purified using the QIAquick Gel Extraction Kit (Qiagen).

PCR products and linearized vectors were ligated using 5U of T4 DNA ligase (Fermentas) in 20 μ l volume in corresponding buffer for 1 h at 20°C or over night at 16-18°C. Variable ratios of vector to PCR product were usually applied (2:15, 2:5, 5:5 v/v) such that the insert was in 5- to 10-fold excess. Ligation products were transformed as described in 2.2.1. Single clones from selective plates were used to inoculate 5 ml overnight cultures. Plasmids were isolated from the *E. coli* clones using Miniprep purification kits (Qiagen or Metabion) and verified by restriction analysis and DNA sequencing (Eurofins MWG).

Site-directed mutagenesis (based on a modified protocol from Mirijam Zeller, Uni Regensburg) was utilized to introduce point mutations into vectors. Usually, 10 ng of template

vector was used in the mutational PCR with Pfu polymerase (Fermentas). Primers typically exhibited 20 complementary nucleotides neighbouring each site of the mutation. PCR reactions were performed with low annealing temperatures (45-50°C) and 2 min/kb extension time. Following, parental vector (containing methylated DNA) was digested by 10U *DpnI* (Fermentas) for 1 h at 37°C and the reaction directly transformed into competent cells.

For the introduction of several point mutations and loop-deletions, the overlap extension method was used. Here, two overlapping PCR-products are produced with primers carrying the desired mutation. In a second PCR reaction these products were used as a template to produce the gene of interest containing the mutation. The resulting PCR product was digested and ligated into the corresponding vector.

2.2.3 Protein expression in *E. coli* and selenomethionine labeling

Recombinant proteins were routinely expressed in *E. coli* BL21-CodonPlus (DE3)RIL cells (Stratagene). Plasmids with desired protein variants were transformed as described as described in 2.2.1. Cells were grown at 37°C in LB medium including antibiotics up to an OD_{600 nm} of 0.5 to 0.8. Cells were cooled on ice for 30 min, induced by addition of 0.5 mM IPTG and grown at 18°C over night. Cells were harvested by centrifugation at 3500g and 4°C for 10 min, resuspended in lysis buffer (see below) and flash frozen in liquid nitrogen. Cell pellets were stored at -80°C.

Selenomethionine labeling was performed using *E. coli* Rosetta B834 (DE3) cells (Novagen) essentially as described (Budisa et al., 1995; Meinhart et al., 2003). Transformed cells were grown in LB medium including antibiotics until an OD_{600 nm} of 0.6 was reached. Cells were harvested, washed and resuspended in minimal medium supplemented with selenomethionine (50 mg/l) and antibiotics. Cells were grown for an additional OD_{600 nm} of 0.2 before induction and overnight expression.

2.2.4 Tandem affinity purification

Tandem affinity purification (TAP) was carried out with tagged strains (see below, 2.2.8) according to the original protocol (Rigaut et al., 1999; Puig et al., 2001) with some modifications (Larivière et al., 2008).

2.2.5 Protein Analysis

Determination of protein concentrations

Total protein concentrations were usually determined by a Bradford assay (Bradford, 1976) at OD_{595 nm} using dye reagent (Bio-Rad) according to the manufacturer's instructions. Reference curves were generated for each new batch of dye reagent using bovine serum albumin (Fraktion V, Roth). Alternatively, protein concentrations were calculated from the absorption rate by OD_{280 nm} measurement using a ND-1000 (NanoDrop) spectrophotometer. Individual molar absorption coefficients for the used proteins were calculated with the help of the ProtParam software (Gasteiger et al., 2005).

SDS-Polyacrylamid gel electrophoresis

Electrophoretic separation of protein was routinely conducted by SDS-PAGE with 15%-19% acrylamide gels (with acrylamide:bisacrylamide = 37.5:1) according to Laemmli (1970) in BioRad gel systems. For protein samples requiring broader or higher resolution separation, pre-casted NuPAGE Novex bis-Tris minigels (Invitrogen) were used according to the manufacturer's instructions. Gels were stained with Coomassie gel staining solution for 20 min and destained over night in gel destaining solution (see Table 9).

Edman sequencing

For N-terminal sequencing, proteins were separated on SDS-PAGE, stained with Coomassie blue and either transferred by Western blotting or by passive adsorption onto PVDF membranes. Western blotting was performed using Western transfer buffer in Mini Trans-Blot Cells (Bio-Rad) according to the manufacturer's instructions. For passive adsorption transfer, bands of interest were excised from the gel, dried in a speed-vac and rehydrated in 20 μ l swelling buffer at room temperature. Next 100 μ l of ddH₂O was added to set up a concentration gradient together with a small piece of pre-wet (ethanol) PVDF membrane (Schleicher & Schuell). Once the solution turned blue, 10 μ l of methanol was added as a catalyst and the sample incubated for 1-4 days until the transfer was complete (clear solution and blue PVDF membrane). The membrane was washed 5 times with 10% methanol by vortexing for 30 sec each time. The protein was N-terminally sequenced from the dry membrane in a PROCISE 491 sequencer (Applied Biosystems).

2.2.6 Limited proteolysis analyses

Limited proteolysis time courses were performed to both identify stable protein fragments and durations suitable for obtaining medium size fragments for further analysis in case of more complex digestion patterns. Time courses were typically performed using chymotrypsin, trypsin or Glu-C proteases at 37°C with individual samples analyzed at 1, 3, 10, 30 and 60 min. Digests were performed using 20 to 50 μ g protein or protein complex with protease (e.g. 0.2 μ g of chymotrypsin, Sigma C3142) in their gel filtration buffer supplemented with 4 M CaCl₂. The reactions were stopped by the addition of SDS sample buffer and were heated immediately to 95°C for 10 min.

For analysis of more complex digestion patterns, purified 3-, 4- and 6-subunit middle module complexes were subjected to limited proteolysis for 10 min using chymotrypsin and after stopping the reaction by addition of a protease inhibitor mixture, loaded onto a Superose 6 gel filtration column (GE Healthcare). For proteolysis, 1 μ g of sample was used for 3- and 4-subunit, and 2 μ g for the 6-subunit middle module. Bands of interest in individual peaks were analyzed on SDS-PAGE after TCA precipitation by mass-spectrometry and Edman-sequencing.

2.2.7 Crystallization screening with middle module complexes

Initial crystallization screening were performed by the sitting-drop (vapor diffusion) method using commercial screens. In-house screens were set up using a Hydra II crystallization robot producing 200 or 500 nl drops in Corning 96-well crystallization plates. Usually a reducing agent, e.g. 5 mM TCEP or 10 mM DTT, was added to the drop or reservoir. Prior to setting up the screen, optimum protein concentrations for crystallization screening were determined. This was achieved by visual control of the behavior of equal volume drops of protein solution and the no. 1 and 6 screening solutions of the Hampton Crystal Screen 1. Plates were incubated at 4 or 20°C and inspected regularly from one day up to 90 days. Crystallization screening for the 7-subunit middle module complex was performed by the Crystallization Facility at the MPI of Biochemistry, Munich. Potential protein crystals were tested by diffraction measurement, by IZIT Crystal Dye (Hampton Research) staining or by the crush test. Promising initial crystals were refined in 24-well hanging drop plates (Easy Xtal Tool, Qiagen) by varying the pH, precipitant and additive concentrations of initial conditions.

2.2.8 Yeast genetics and assays

Gene disruption and epitope-tagging

To disrupt genes or placing purification tags onto proteins of interest, *S. cerevisiae* cells were transformed (see 2.2.1) with linearized DNA or PCR products that allowed for homologous recombination (Baudin et al., 1993). Genomic DNA of potential positive clones was isolated using the DNeasy Blood & Tissue Kit (Qiagen) with a yeast-specific protocol on a QiaCube robot (Qiagen). Genomic manipulations were verified by performing test-PCR reaction with primers upstream and downstream of the mutated site and DNA sequencing after agarose gel separation and isolation of the PCR-product.

Sporulation and tetrad dissection

Diploid BY yeast strains were usually sporulated by streaking them out as a thin layer onto pre-sporulation plates. Cells were incubated at 30°C for 2 days, then restreaked onto sporulation plates and both incubated minimally for 3 days more. In difficult cases, liquid sporulation medium was used alternatively. Sporulation was monitored by light microscopy. For tetrad dissection, a loop of sporulated cells was incubated at 30°C with glucosylase (Perkin Elmer) diluted 1:10 in 100 μ l sterile water to digest the ascus and to release the tetrad. Micromanipulation was performed on a Singer MSM Tetrad Dissection Microscope.

Mating

Mating types were determined by PCR analysis using three primers (oligo 1: agtcacatcaagatcggttatgg, oligo 2: gcacggaatatgggactacttcg, oligo 3: actccactcaagtaagagtttg) simultaneously. Strains were mated from cultures grown until $OD_{600\text{ nm}}=0.2$ in YPD. Cells from one μ l culture each were resuspended in 100 μ l YPD and one strain added to the other. Both strains were allowed to settle and incubated over night at 30°C, shaking in a thermomixer. Cells

were selected on double-selection plates (including restreaking) and potential positive clones analyzed by PCR as described above. In cases where certain genotypes in a haploid strain were desired, strains were sporulated as described above.

Complementation assays

Yeast shuffle strains were generated by transforming a rescue plasmid carrying an *URA3* marker and a gene of interest into diploid strains exhibiting only one intact copy of that gene. Cells were sporulated, tetrads dissected and selected for having both the genomic gene knock-out and the rescue plasmid. These shuffle strains were then transformed with plasmids carrying a *LEU2* marker and mutant variants of the gene of interest. Transformants were dotted onto 5-FOA and YPD plates to test if the mutant variants could complement the loss of the rescue plasmid.

Phenotyping assays

Phenotype analyses of Mediator subunit deletion mutants were performed from cultures grown to stationary phase. Cells were diluted to an OD_{600 nm} of 1.0, washed, and spotted in serial dilution onto plates. Assays were mostly performed as described (Hampsey, 1997). For synthetic defined (SD) (-met) and SD (-SO₄²⁻) and for 6-azauracil plate assays, strains with methionine or uracil auxotrophy were transformed with pRS411 or pRS316 plasmids, respectively. Siderophore uptake assays were performed with SD plates containing 500 mM bathophenanthroline disulphonic acid and 10 mM of siderophores.

2.2.9 Bioinformatic tools

Protein and gene sequences were retrieved from the NCBI or *Saccharomyces cerevisiae* genome databases. Sequence data was visualized and processed using the following software applications: Bioedit (Hall, 2005), VectorNTI (Invitrogen), Serial Cloner (<http://serialbasics.free.fr>) and Staden/GAP4 (<http://staden.sourceforge.net>). Bioinformatic analysis were performed mostly using the Bioinformatics Toolkit (Biegert et al., 2006). Multiple sequence alignments were generated using MUSCLE (Edgar, 2004). Protein secondary structures were predicted by HHpred (Soeding et al., 2005), I-Tasser (Zhang, 2008), PSIPred (Jones, 1999) and CDM (Sen et al., 2006).

2.3 Recombinant Med7N/31

2.3.1 Preparation of recombinant Med7N/31

The gene encoding *S. cerevisiae* Med31 was cloned into a pET-28b vector (Novagen) using the *NdeI/NotI* restriction sites, resulting in a thrombin-cleavable N-terminal hexahistidine tag. DNA encoding Med7 residues 1–83 was cloned into a pET21b vector through the *EcoRI* and *SalI* restriction sites. *E. coli* BL21 (DE3) RIL cells (Stratagene) were cotransformed with the two plasmids and grown in LB medium at 37°C to an optical density at OD_{600 nm} of 0.6. Expression was induced with 0.5 mM IPTG for 16 h at 18°C. Selenomethionine

labelling was carried out as described in 2.2.3. For protein purification, cells were lysed using a highpressure homogenizer (Avestin) in buffer A (see Table 9). After centrifugation, imidazole was added to a final concentration of 20 mM to the supernatant and loaded onto a 3 ml Ni-NTA column (Qiagen) equilibrated with buffer A containing 20 mM imidazole. The column was washed with 20 column volumes (CVs) of buffer A containing 20 mM imidazole and eluted with buffer A containing 200 mM imidazole. Following overnight cleavage with thrombin, proteins were purified by anion exchange chromatography (MonoQ). The column was equilibrated with buffer B, and proteins were eluted with a linear gradient of 20 CVs from 100 mM to 1 M NaCl in buffer B. After concentration, the sample was applied to a Superdex-200 size exclusion column (GE Healthcare) equilibrated with buffer C.

2.3.2 X-ray structure determination

For crystallization, pure Med7N/31 was concentrated to 50 mg/ml, and 5 mM DTT was added. Crystals were grown at 20°C in hanging drops over reservoirs containing 50 mM MES pH 5.6, 1.8 M Li₂SO₄, and 10 mM MgCl₂. Crystals were harvested by gradually adding ethylene glycol to a final concentration of 10% (v/v) and were flash-cooled in liquid nitrogen. Diffraction data were collected at 100 K on a MARCCD 225 and on a PILATUS 6M detector at the Swiss Light Source (SLS), Villigen, Switzerland (native data set and mutant data set, respectively) and on a MARCCD 165 detector at the Berliner Elektronenspeicherring-Gesellschaft für Synchrotronstrahlung m.b.H. BESSY (SAD data set). Diffraction data for selenomethionine-labeled Med7N/31 was processed using XDS and XSCALE (Kabsch, 1993). Program SOLVE (Terwilliger, 2003) identified six selenium sites that were used for phasing. Solvent flattening, two-fold non-crystallographic symmetry averaging, and initial model building was done with RESOLVE (Terwilliger, 2003). The resulting electron density map allowed for manual building of most Med7N and Med31 using COOT (Emsley and Cowtan, 2004). The model was refined using conjugate gradient minimization in the programs CNS (Brünger et al., 1998), REFMAC (Murshudov et al., 1997), and Phenix (Adams et al., 2002). The asymmetric unit contained two Med7N/31 heterodimers that deviate only at the C-termini of the proteins. The mutant structure was solved by molecular replacement using Phaser (McCoy et al., 2007) and processed accordingly. The structures and diffraction data of wild-type Med7N/31 and the mutant complex Med7 (1–83) (12...18 YSPTSPS)/Med31 (mutant 6; Table 12) have been deposited in the Protein Data Bank under accession codes 3FBI and 3FBN, respectively.

2.3.3 Yeast strains and growth assays

The heterozygous *MED7/med7Δ* strain was obtained from Euroscarf (Frankfurt, Germany) and transformed with the cognate gene clone plasmid pYCG_*YOL135C* (containing a *URA3* marker). Diploids were sporulated and tetrads were dissected on YPD plates. To assess functionality, pAL-*med7*_{1–83}, pAL-*med7*_{1–101}, pAL-*med7*_{101–222}, pAL-*med7*_{1–222}, or pRS315-*med7*_{84–222} were transformed into the *MED7* shuffle strain. Transformants were dotted onto 5-FOA and YPD plates. Yeast knockout strains were obtained from Euroscarf. All strains

exhibited a BY background and were, with the exception of *med2* Δ and *med18* Δ , *MATa*. Deletion of the N-terminal region of Med7 (residues 1–83) was obtained by homologous recombination after transforming only the C-terminal part (residues 84–222) fused to a ClonNAT marker into either WT or *med31* Δ strains. Additionally, a C-terminal TAP-tag on Med18 was introduced using an *URA3* marker into wild-type, *med31* Δ , *med7N* Δ , and *med7N/31* Δ strains.

2.3.4 *In vitro* transcription assays

In vitro transcription assays were performed for this work by Martin Seizl as follows: Nuclear extracts were prepared from 3 l of culture as described by the Hahn laboratory (www.fhcr.org/labs/hahn/). Plasmid transcription was performed essentially as described (Ranish and Hahn, 1991). Transcription reactions were carried out in a 25 μ l volume. The reaction mixture contained 100 μ g nuclear extract, 150 ng of pSH515 plasmid, 1x transcription buffer (10 mM HEPES pH 7.6, 50 mM potassium acetate, 0.5 mM EDTA, and 2.5 mM magnesium acetate), 2.5 mM DTT, 192 μ g of phosphocreatine, 0.2 mg of creatine phosphokinase, 10U of RNase inhibitor (GE Healthcare), and 100 μ M nucleoside triphosphates. For activated transcription, 150 ng of Gal4–VP16 or 200 ng of Gal4–Gal4AH was added. The reaction was incubated at room temperature for 40 min and then stopped with 180 μ l of 100 mM sodium acetate, 10 mM EDTA, 0.5% sodium dodecyl sulphate, and 17 μ g of tRNA/ml. Samples were extracted with phenol–chloroform and precipitated with ethanol. Transcripts were analysed by primer extension essentially as described (Ranish and Hahn, 1991). Instead of the ³²P-labeled lacI oligo, 0.125 pmol of a fluorescently labeled 50-FAM-oligo was used. Quantification was performed with a Typhoon 9400 and the ImageQuant Software (GE Healthcare).

2.3.5 Gene expression profiling analysis

All experiments were performed in synthetic complete medium with 2% glucose. For microarray analysis, three independent colonies were used for inoculation, and overnight cultures were diluted in fresh medium to OD_{600 nm}=0.1 (25 ml cultures, 160 r.p.m. shaking incubator 30°C). Cells were harvested by centrifugation (4000 r.p.m., 3 min, 20°C) at OD_{600 nm}=0.8. Total RNA was prepared after cell lysis using a mixer mill (Retsch) and subsequent purification using the RNeasy kit (Qiagen). The total RNA preparation was treated on-column with DNase (Qiagen). All following steps were conducted according to the Affymetrix GeneChip Expression Analysis Technical Manual (P/N 702232 rev. 2). Briefly, one-cycle cDNA synthesis was performed with 1 μ g of total RNA. *In vitro* transcription labelling was carried out for 16 h. The fragmented samples were hybridized for 16 h on Yeast Genome 2.0 expression arrays (Affymetrix), washed and stained using a Fluidics 450 station, and scanned on an Affymetrix GeneArray scanner 3000 7G. Data analysis was performed using R/Bioconductor (Gentleman et al., 2004). *S. pombe* probes were filtered out prior to normalization with the GCRMA algorithm (Wu et al., 2004). Linear model fitting and multiple testing correction using an empirical Bayes approach was performed using the LIMMA package (Smyth, 2004). Differentially expressed genes were defined as having an adjusted P-value smaller than

0.05 and an estimated fold change of at least 2.0 (calculated as the fold change of the average expression in the triplicate measurements). Previously published transcriptome profiles (Larivière et al., 2008) were included in further analyses by matching genes and comparing fold changes. Over-represented biological processes for genes with significant expression changes were determined using the topGO package (Alexa et al., 2006). Clustering was calculated using TIGR MeV application (Saeed et al., 2003). Microarray data were submitted to the ArrayExpress database (<http://www.ebi.ac.uk/microarray>) under accession number E-MEXP-1916.

2.4 Endogenous and recombinant Mediator middle module

2.4.1 Purification of endogenous middle module

The *med19*Δ yeast strain (BY4741; *MATa*, *his3*Δ1, *leu2*Δ0, *met15*Δ0, *ura3*Δ0, *YBL093C*:*clonNAT*) was obtained from Stephan Jellbauer (Gene Center Munich) and C-terminal TAP-tags were introduced on Med7, Med15 or Med18, respectively, using a kanMX4-marker as described in 2.2.8 using vector pYM13 (Janke et al., 2004) as PCR-template. Yeast cultures were cultivated and the protein complexes purified using tandem affinity purification as described in 2.2.4.

2.4.2 Preparation of recombinant middle module

Expression strategy and cloning

Monocistronic vectors were cloned by standard procedures as described in 2.2.2. Bi- or tricistronic vectors were generally created by introducing additional ribosomal binding sites by means of PCR into pET and pCDF-vectors (Novagen) as described (Baumli et al., 2005; Baumli, 2005; Larivière et al., 2006) and illustrated in Figure 12. A detailed listing of all vectors used and created for this study can be found in Table 5. For expression, *E. coli* BL21 (DE3) RIL cells (Stratagene) were transformed with one to three plasmids and grown in LB medium at 37°C to an OD_{600 nm} of 0.6. Expression was induced with 0.5 mM IPTG for 16 h at 18°C. Cells were lysed using a high-pressure homogenizer (Avestin) (large-scale protein purification) or by sonication (Branson) (small-scale purification).

Purification

The quaternary complex Med7/10/21/31-His₆ was expressed from two plasmids encoding Med10, Med7 and Med21 in a tricistronic pET21b vector (pSB104) and Med31-His₆ in a pET24d vector (pSB102). Four liters of *E. coli* culture were harvested and lysed in buffer A (see Table 9) containing protease inhibitors. After centrifugation, imidazole was added to a final concentration of 20 mM to the supernatant and loaded onto a 3 ml Ni-NTA gravity flow column (Qiagen) equilibrated with buffer A containing 20 mM imidazole. The column was washed with 20 column volumes (CVs) of buffer A containing 20 mM imidazole and eluted with buffer A containing 200 mM imidazole. The 4-subunit middle module was further purified by anion exchange and gel filtration chromatography.

The Med4/9 complex was coexpressed from a bicistronic pET21 vector (pSB118) using 2 l of *E. coli* culture. Cells were harvested and lysed in buffer D containing protease inhibitors. Insoluble cell debris were removed by centrifugation and the proteins purified by ammonium sulfate precipitation and anion exchange chromatography. Ammonium sulfate precipitation was achieved by the gradual addition of saturated (20°C) ammonium sulfate solution up to 30% (v/v). After centrifugation the pellet was resuspended and purified on a MonoQ 10/100 column (GE Healthcare) in buffer B using a linear gradient of 20 CVs from 100 mM to 1 M NaCl. A six subunit middle module comprising Med4/7/9/10/21/31 was obtained by assembling the two purified subcomplexes. Assembly was performed at 20°C on a rotating wheel with a 1.3 molar excess of Med4/9. Contaminants, excess Med4/9 and unassembled 4-subunit middle module were separated using anion exchange chromatography (buffer B, 20 CV from 100 mM to 1 M NaCl). Following concentration in a 100 kDa MWCO spin concentrator (Amicon Ultra, Millipore), the 6-subunit middle module was purified to homogeneity by gel filtration chromatography using a Superose 6 size exclusion column (GE Healthcare) with buffer A.

The complete middle module comprising Med1/4/7/9/10/21/31 was expressed from the cotransformed vectors pSB104 (encoding Med10, Med7 and Med21), pTK26 (encoding His₆ Med31) and pTK114 (encoding StrepII-tagged Med1, Med9 and Med4). After cotransformation of two vectors, cells were made competent again in order to transform the third vector. Six liters of *E. coli* culture were harvested and lysed in buffer E containing protease inhibitors. After centrifugation, the complex was purified on 3x 1 ml Strep-Tactin MacroPrep (IBA) gravity flow columns according to the manufacturer's instructions. After elution by d-Desthiobiotin (IBA) addition, the sample was concentrated in a 100 kDa MWCO spin concentrator and subjected to gel filtration using a Superose 6 size exclusion column (GE Healthcare) with buffer A.

2.4.3 Activity assay trials

Nuclear extracts from a *med19Δ/MED7-TAP* yeast strain were generated and *in vitro* transcription assays performed by Martin Seizl as described in 2.3.4. In this assay, addition of either TAP-purified Mediator or recombinant middle module together with recombinant Med19 were tested for activity. In a second approach, middle-less Mediator complex was attempted to be purified. In order to integrate a 3xFLAG-tag (Moqtaderi and Struhl, 2008) onto Med18 in the *med19Δ/MED7-TAP* strain, a *Med18-3xFLAG/Med7-TAP* was generated, both strains mated, then resulting diploid strains tetrad dissected and tested for the desired genotype. In order to generate a *Med15-3xFLAG/med19Δ/MED7-TAP* strain, the 3xFLAG-tag was integrated by homologous recombination. The latter strain was used for further trials to establish middle-less Mediator purification. Cells from 2 to 4 l per experiment were grown to an OD_{600 nm} of 6.0 and harvested by centrifugation. Cells were lysed either with glass beads or following a cryo-lysis protocol with ceramic grinding balls according to Oeffinger et al. (2007) in a planetary bead mill (Fritsch PULVERISETTE 6 classic line). The supernatant of the first purification step of the TAP-purification (see 2.2.4) was purified further with anti-FLAG antibodies. In one series of experiments, 6F7 anti-FLAG antibody (by

courtesy of E. Kremmer, GSF Munich) was coupled to M280 tosylactivated DynaBeads (Invitrogen) and used for the FLAG-purification. In a second approach anti-FLAG M2 agarose (Sigma) was used for purification (according to the manufacturer's instructions). Samples were eluted with FLAG-peptide.

2.4.4 Coexpression and copurification pull-down assays

Coexpression was performed as described in 2.2.3 using 50 ml cultures for StrepII affinity purifications or 7 ml cultures for Ni-NTA purifications. Cell lysates were clarified by centrifugation and copurification pull-down assays performed in batch. StrepII affinity purifications were performed using 25 μ l of Strep-Tactin MacroPrep (IBA). The clarified lysates were incubated with the beads at 4°C on a rotating wheel for 1 h. Beads were washed with 3x1 ml of buffer A and the samples eluted by d-Desthiobiotin. Ni-NTA purifications were performed using 40 μ l of MagneHis beads (Promega). The clarified lysates were incubated with the beads at 4°C on a rotating wheel for 15 min. Beads were washed with 2x1 ml of buffer A and the samples eluted by 400 mM Imidazole in buffer A. Samples were analyzed on SDS-PAGE.

2.4.5 Native mass spectrometry

Native mass spectrometry (MS) analyses for this work were performed by Kristina Lorenzen (Utrecht University) as follows: The buffer exchange for the native MS analysis was performed using 10 kDa cut off membrane spin columns (Millipore, England) by six sequential concentration/dilution cycles against 200 mM ammonium acetate pH 6.8. The concentration for the analysis was 5 μ M (assuming intact protein complexes). Analysis of the intact protein complex, as well as the n-propanol and DMSO measurements were carried out on a LCT mass spectrometer (Waters, UK). Needle voltage was set to 1250 V, cone voltage varied between 100 and 150 V. Tandem mass spectrometry was performed on a modified Q-ToF, here needle voltage was set to 1300 V and cone to 150 V. For further details see Lorenzen et al. (2007) and references within. Ion mobility mass spectrometry (IM-MS) was carried out on a Synapt HDMS (Waters, UK) (Pringle et al., 2007). The source pressure was set to 6.9 mbar, the pressure in the trap was 3.5×10^{-2} mbar, 0.7 mbar in the ion mobility separation (IMS) cell and 2×10^{-6} mbar in the ToF. The wave height in the IMS cell was fixed on 11.3 V and the wave velocity set to 250 m/s. The gas used in the trap was xenon and nitrogen in the IMS cell. Needle voltage was 1200 V and cone voltage 150 V. The bias value was set to 20 V, trap and transfer collision energy to 12 V. Cross section calculations were done as described by Ruotolo et al. (2008). The average volume of global proteins and protein complexes was calculated according to Uetrecht et al. (2008).

2.4.6 Static light scattering analysis

Static light scattering analysis was performed using a Superose 6 gel filtration column (GE Healthcare) combined with a triple detector TDA (Viscotek). Med7C/21 was analyzed in

buffer F at a concentration of 1.8 mg/ml, Med7N/31 and Med4/7/9/10/21/31 was analyzed in buffer A at 1.0 mg/ml. Data analysis was performed with OmniSEC software (Viscotek).

2.4.7 Small-angle X-ray scattering

Small angle X-ray scattering (SAXS) data was collected at the X33-Beamline (EMBL/DESY, Hamburg, Germany). Scattering patterns from 6-subunit Mediator middle module solutions comprising Med4/7/9/10/21/31 were measured in buffer A at 5 mg/ml two times in order to exclude potential radiation damage errors. The ATSAS software package (Konarev et al., 2006) was used for data processing.

3 Results

3.1 Identification, structure, and functional requirement of the Mediator submodule Med7N/31

3.1.1 Identification and crystallization of the Med7N/31 subcomplex

The Mediator middle module contains the subunits Med1, Med4, Med7, Med9 (Cse2), Med10 (Nut1), Med21 (Srb7), and Med31 (Soh1) (Guglielmi et al., 2004; Béve et al., 2005). To work towards the structure and function of the middle module, we purified the trimeric complex Med7/21/31 in recombinant form after bacterial coexpression of the corresponding genes and subjected it to limited proteolysis (Methods 2.2.6). Proteolytic cleavage patterns were consistent with two flexibly linked subcomplexes, the Med7C/21 subcomplex, which we analyzed earlier (Baumli et al., 2005), and a subcomplex of Med31 with the N-terminal region of Med7 (Figure 4A). We therefore coexpressed Med31 with different variants of the Med7 N-terminal region, purified the resulting heterodimeric complexes and screened them for crystal formation (Table 10). A complex that comprised the N-terminal region of Med7 including part of the linker (residues 1–101) was soluble, but did not crystallize, apparently due to flexibility in the proteolytically sensitive linker. Shorter variants resulted in initial crystal hits that could be crystallized, but these crystals diffracted only weakly upon measurement at the synchrotron. A complex that lacked the entire linker and included only Med7 residues 1–83 (Med7N) crystallized at a concentration of 59 mg/ml in condition 1 of Hampton Natrix screen (50 mM MES pH 5.6, 2.0 M Li₂SO₄, and 10 mM MgCl₂). Crystals were reproduced in 24-well plates, refined (Figure 3) and used to solve the X-ray structure of Med7N/31 by selenomethionine labeling and single anomalous diffraction. The structure was refined to a free R-factor of 24.3% at 2.8 Å resolution (Table 11, Methods 2.3.2).

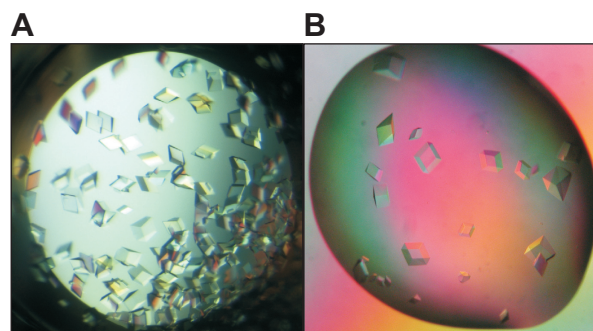


Figure 3: Crystals of Med7N/31 complex. (A) Initial crystals were obtained from a 96-well plate screening in condition 1 (50 mM MES pH 5.6, 2.0 M Li₂SO₄, and 10 mM MgCl₂) of Hampton Natrix screen at 20°C. (B) Refined crystals from 24-well plates (50 mM MES pH 5.6, 1.8 M Li₂SO₄, and 10 mM MgCl₂).

Table 10: Crystallization screening of M7N/31 complex.

Screens were performed at 20°C.

Complex	Concentration	Screen(s) ^a	Buffer
Med7 (1-101)/31-His ₆	10 mg/ml	Classic, Index, JBC I, JBC II, Natrix, PEG/Ion, Anions, Cations, MPD	A + 5 mM DTT
Med7 (1-101)/31-His ₆	23 mg/ml	Classic, Index, JBC I, JBC II, Natrix, PEG/Ion	A + 5 mM DTT
Med7 (1-101)/31-His ₆	47 mg/ml	Classic, Index, JBC I, JBC II, Natrix, PEG/Ion	A + 5 mM DTT
Med7 (1-80)/31-His ₆	57 mg/ml	Classic, Index, JBC I, JBC II, Natrix, PEG/Ion	A + 5 mM DTT
Med7 (1-83)/31-His ₆	65 mg/ml	Classic, Index, JBC I, JBC II, Natrix, PEG/Ion	A + 5 mM DTT
Med7 (1-80)/31-His ₆	43 mg/ml	Classic, Index, JBC I, JBC II, Natrix, PEG/Ion	A + 5 mM DTT
Med7 (1-92)/31-His ₆	50 mg/ml	Classic, Index, JBC I, JBC II, Natrix, PEG/Ion	A + 5 mM DTT
Med7 (1-80)/31-His ₆	85 mg/ml	Classic, Index	A + 5 mM DTT
Med7 (1-92)/31-His ₆	94 mg/ml	Classic, Index, JBC I, JBC II, Natrix, PEG/Ion	A + 5 mM DTT
Med7 (1-92)/31-His ₆	59 mg/ml	Classic	C + 5 mM DTT
Med7 (1-83)/31-His ₆	59 mg/ml	Classic, Index, JBC I, JBC II, Natrix, PEG/Ion	C + 5 mM DTT
Med7 (1-92)/31-His ₆	70 mg/ml	Classic, Index, JBC I, JBC II, Natrix, PEG/Ion	C + 5 mM DTT

^a Commercial screens used for 96-well plate screening were: Index, Natrix, PEG/Ion (all Hampton), Classic screen, pH-clear, anions suite, cations suite, classic suite (all Qiagen), JB Screen Classic HTS I S and JB Screen Classic HTS II S (both Jena Biosciences).

Table 11: Data collection and refinement statistics for Med7N/31.

	Selenomethionine SAD Med7 (1-83)/Med31	Native dataset, mutant construct 6 (Table 12)
Data collection		
Space group	R 32	R 32
Cell parameters		
a, b, c (Å)	174.6, 174.6, 117.8	174.2, 174.2, 115.5
α, β, γ (°)	90, 90, 120	90, 90, 120
Wavelength (Å)	0.98	0.92
Resolution range (Å) ^a	20-2.8 (2.97-2.80)	50-3.0 (3.18-3.00)
Completeness (%)	99.4 (98.0)	99.7 (98.2)
Unique reflections	32,854 (5,275)	13,576 (2,138)
Redundancy	11.3 (9.1)	11.2 (11.0)
R _{sym} (%)	6.0 (61.8)	5.0 (57.4)
$\langle I \rangle / \langle \sigma \rangle$	27.8 (4.1)	32.7 (5.2)
Refinement		
Number of residues	282	278
Number of non-hydrogen atoms	2436	2402
rms bond deviation (Å)	0.007	0.008
rms angle deviation (°)	1.041	1.076
Ramachandran plot (%) (favored/allowed)	95.0/100.0	95.0/100.0
R _{cryst} (%)	19.5	17.8
R _{free} ^b (%)	24.3	23.1

^a Highest resolution shell is shown in parenthesis.

^b 5% of the data were set aside for free R-factor calculation.

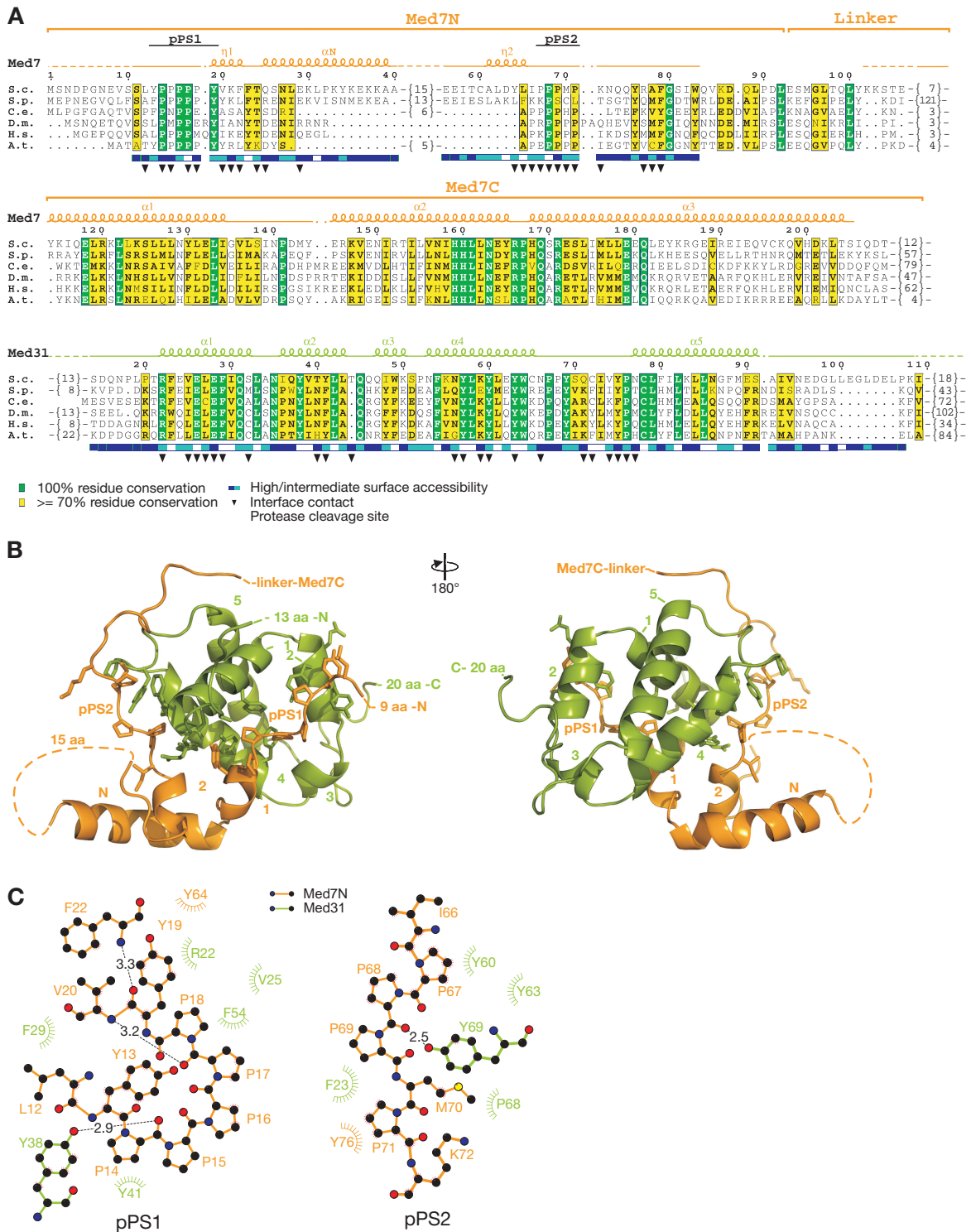


Figure 4: Structure of the Med7N/31 Mediator subcomplex.

(A) Multiple sequence alignment and structural conservation of Med7 and Med31 from *Saccharomyces cerevisiae* (S.c.), *Schizosaccharomyces pombe* (S.p.), *Caenorhabditis elegans* (C.e.), *Drosophila melanogaster* (D.m.), *Homo sapiens* (H.s.) and *Arabidopsis thaliana* (A.t.). Secondary structure elements are indicated above the sequences (spirals, α - and 3_{10} (η)-helices; arrows, β -strands; lines, ordered but without secondary structure; dashed lines, disordered regions). Invariant and conserved residues are highlighted in green and yellow, respectively. Surface accessibility is indicated below the sequences (blue, exposed; white, buried). Cleavage sites revealed by limited proteolysis with trypsin or chymotrypsin are indicated with black arrows. The loop between Med7N helices α_1 and η_2 (residues 41–55) was disordered. Sequence alignments were done with MUSCLE (Edgar, 2004) and figures were prepared with ESPript (Gouet et al., 1999). (B) Ribbon model representation of the Med7N/31 crystal structure. Two views are shown that are related by a 180° rotation around the vertical axis. Med7 is depicted in orange and Med31 in green. Secondary structure elements are labeled according to (A). These and other figures were prepared with PyMol (DeLano, 2002). (C) Ligplot view (Wallace et al., 1995) of the interactions of the Med7N polyproline stretches pPS1 and pPS2 with Med31.

3.1.2 The Med7N/31 structure reveals novel folds

The structure shows that Med31 forms a compact righthanded four-helix bundle, whereas Med7N is extended and wraps around Med31 (Figure 4B). Both folds are novel, as neither DALI nor MSD fold searches (Holm and Park, 2000; Krissinel and Henrick, 2004) produced any hits. The Med7N/31 structure is apparently conserved among eukaryotes, as hydrophobic core residues are identical or similar from yeast to human (Figure 4A), and many residues in the Med7N–Med31 interface are also conserved. The Med7N–Med31 interface is mainly hydrophobic (Figure 4), explaining why isolated recombinant Med7N or Med31 cannot be obtained in soluble form (not shown). The Med7N/31 surface reveals several conserved, non-charged regions (Figure 5A and B) that can account for interactions of Med7N/31 with other subunits of the middle module (Guglielmi et al., 2004) or other potential binding partners.

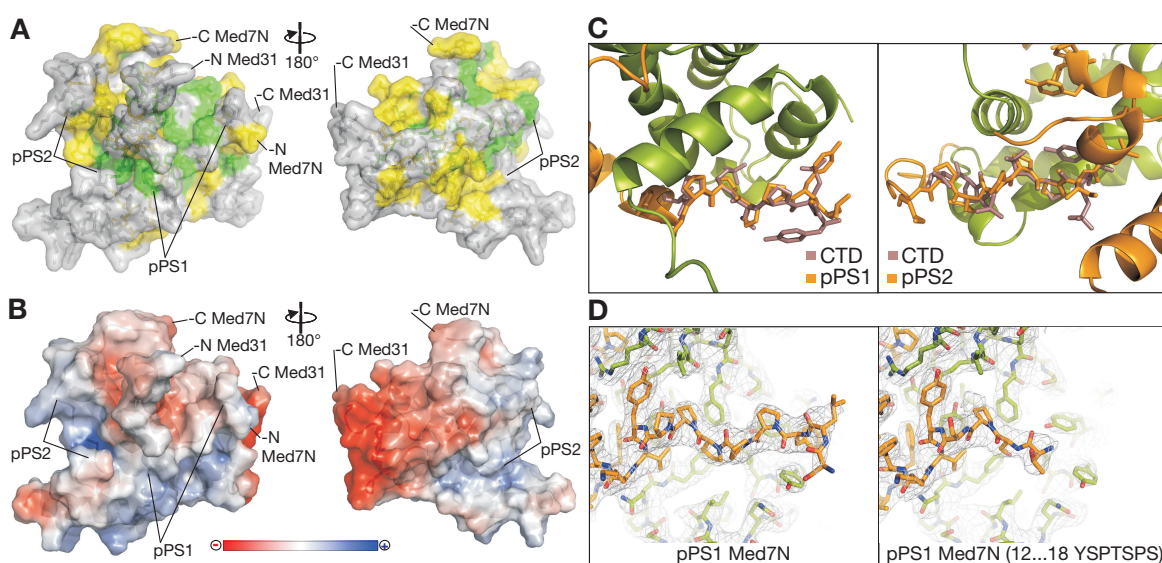


Figure 5: Analysis of the Med7N/31 structure.

(A) Surface conservation of the Med7N/31 subcomplex. Invariant and conserved residues are highlighted in green and yellow, respectively. The surface is semitransparent to show the underlying residues in a stick model. Two views are shown that are related by a 180° rotation around the vertical axis. (B) Surface charge distribution. Red, blue, and white areas indicate negative, positive, and neutral charges, respectively. (C) The Med7N polyproline stretches adopt a CTD-like conformation. Superimposition of Med7N pPS1 and pPS2 (orange) with the Y(SEP)PT(SEP)PS peptide from the human Pin1 structure (1F8A, light purple). (D) Comparison of pPS1 in the crystal structures of Med7N/31 and Med7N/31 with pPS1 mutated to a CTD heptad repeat (mutant 6; Table 12).

3.1.3 Possible CTD mimicry by Med7N

Med7N contacts Med31 mainly through two polyproline stretches (pPS1 and pPS2; Figure 4A–C), which adopt a conformation similar to a left-handed type II polyproline helix (Adzhubei and Sternberg, 1993). A deletion analysis revealed that both pPS1 and pPS2 were required for the formation of a stable complex with Med31 (Table 12; constructs 2–5). pPS2 is tightly packed onto Med31, whereas pPS1 is more accessible (Figure 4C). As the C-terminal repeat domain (CTD) of RNA Pol II is also proline rich, we compared the Med7N stretches with known CTD peptide structures. The conformation of the CTD peptide in complex

with the prolyl isomerase Pin1 (PDB 1F8A; Verdecia et al. (2000)) resembles the structure of Med7N pPS1, and is also distantly related to pPS2 (Figure 5C). The CTD interacts genetically and physically with Mediator (Thompson et al., 1993; Myers et al., 1998; Asturias et al., 1999; Kang et al., 2001). Although *med31* deletion does not suppress the cold-sensitive phenotype caused by CTD truncations (Thompson et al., 1993), it is synthetically lethal with a truncation of the CTD to only 11 intact heptad repeats (Fan et al., 1996). We therefore speculated that the CTD may bind Med31 by replacing pPS1 and/or pPS2 of Med7N under certain conditions. We could however not investigate direct CTD binding to Med31 as isolated Med31 could not be obtained in soluble form. We therefore mutated the Med7N pPS1 and pPS2 stretches such that their sequences correspond to the CTD repeat sequence consensus (Table 12), and tested whether these Med7N mutants formed stable complexes with Med31. The pPS1 mutant, but not the pPS2 mutant, formed a stable complex with Med31 (Table 12). Crystallographic analysis of the pPS1 mutant (mutant 6; Table 12) in complex with Med31 showed that four residues of the CTD heptad repeat (15-TSPS-18) were ordered and bound to Med31, whereas the preceding three residues (12-YSP-14) were flexible (Figure 5D). However, as the Med7N/31 complex also tolerated replacement of pPS1 by the reverse CTD heptad repeat sequence (mutant 10; Table 12), and as the Med7N stretches are present in organisms lacking the canonical CTD repeats (Stiller and Hall, 2002; Bourbon, 2008), a possible CTD mimicry by Med7N and CTD binding by Med31 remains hypothetical.

Table 12: Summary of Med7N mutant constructs of the polyproline stretches 1 and 2.

No.	Med7N construct ^a	Mutation	Replaced sequence	Copurification with Med31
1	Med7 (1-83)	- (crystallized construct)		yes
2	Med7 (20-83)	N-terminus including pPS1 removed		no
3	Med7 (23-83)	N-terminus including pPS1 removed		no
4	Med7 (1-61)	C-terminus including pPS2 removed		no
5	Med7 (1-66)	C-terminus including pPS2 removed		no
6	Med7 (1-83) (12...18 YSPTSPS)	pPS1 replaced by CTD-repeat	LYPPPPP	yes
7	Med7 (1-83) (13...19 YSPTSPS)	pPS1 replaced by CTD-repeat	YPPPPPY	yes
8	Med7 (1-83) (66...72 YSPTSPS)	pPS2 replaced by CTD-repeat	IPPPMPK	no
9	Med7 (1-83) (65...71 YSPTSPS)	pPS2 replaced by CTD-repeat	LIPPPMP	no
10	Med7 (1-83) (12...18 SPSTPSY)	pPS1 replaced by reversed CTD-repeat	LYPPPPP	yes
11	Med7 (1-83) (12...18 YSPTDPS)	pPS1 replaced by mutated CTD-repeat	LYPPPPP	yes
12	Med7 (1-83) (12...18 YSPTRPS)	pPS1 replaced by mutated CTD-repeat	LYPPPPP	yes
13	Med7 (1-83) (12...18 YDPTSPS)	pPS1 replaced by mutated CTD-repeat	LYPPPPP	yes

^a For interaction assays, Med7 (1-83), Med7 (1-61), Med7 (1-66), Med7 (20-83), Med7 (23-83) were cloned into pET21b using *NdeI/SalI*, such that a N-terminal Strep-tag was introduced. With these constructs, copurification was analyzed both via the His-tag on Med31 and via the Strep-tag on the Med7 variants.

3.1.4 Med7N/31 is required for normal yeast growth *in vivo*

Med7 is essential for yeast viability in rich medium (Myers et al., 1998). To investigate which Med7 region is required for viability, we carried out complementation studies in yeast. We generated plasmids expressing full-length Med7, Med7N, and Med7N plus the linker part, which was not present in the Med7C/21 structure (Baumli et al., 2005) or a Med7C variant. Plasmids were introduced into a *med7* Δ strain rescued by a *MED7*-encoding *URA3* plasmid. Complementation was observed with full-length *MED7* or *MED7C*, which allows for loss of the *URA3* plasmid and growth on media containing 5-fluorotic acid (5-FOA; Figure 6A). As the remaining linker residues (102–113) present in the Med7C/21 structure are not conserved, we infer that only Med7C is essential for viability, whereas Med7N and the linker are not. A strain that lacked the region encoding Med7N (*med7N* Δ) exhibited a slowgrowth phenotype, similar to a *med31* Δ strain and a double deletion strain *med7N* Δ /*med31* Δ (*med7N/31* Δ) (Figure 6B; Table 4).

3.1.5 Med7N/31 is essential for transcription *in vitro*

To investigate whether the Med7N/31 subcomplex is required for activated transcription *in vitro*, we used a plasmid-based *in vitro* transcription assay with a *HIS4* core promoter and a single upstream Gal4-binding site (Ranish et al., 1999). A nuclear extract from strain *med7N/31* Δ was defective in basal transcription (not shown) and in transcription activated with the Gal4–VP16 fusion protein or with a fusion protein of the Gal4 DNA-binding domain with the Gal4–Gal4 activation helix (Gal4–Gal4AH) (Figure 6C, lane 1; Figure 7, lane 1). Addition of tandem affinity purification (TAP)-purified Mediator restored transcription (Figure 6C, lane 2), providing a positive control. Transcription could also be restored by the addition of recombinant Med7N/31, demonstrating that the crystallized complex is functionally active and can act *in trans* without being covalently tethered to the Mediator (Figure 6C, lanes 3–5; Figure 7, lane 2). To investigate whether loss of Med7N/31 leads to the dissociation of other subunits from Mediator *in vivo*, we purified Mediator from deletion strains *med7N* Δ , *med31* Δ , and *med7N/31* Δ with the use of a TAP-tag fused to Med18 (Materials and methods 2.2.4). After purification from these deletion strains, the remainder of Mediator stayed intact (Figure 6F). These results show that Med7N/31 forms a peripheral subcomplex on Mediator that is required for activated transcription in our *in vitro* assays.

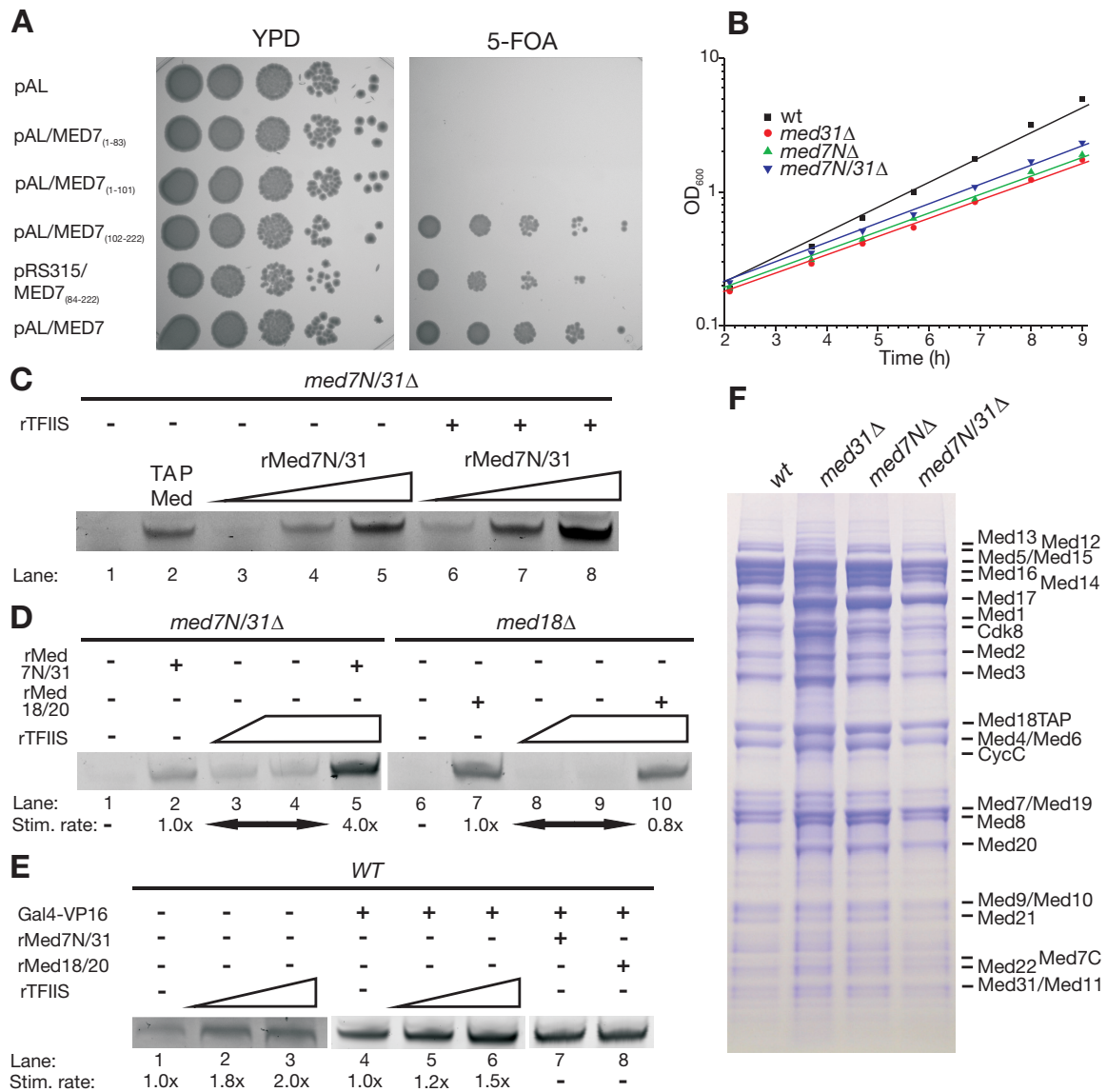


Figure 6: Functional analysis of Med7N/31 in vivo and in vitro.

(A) Yeast complementation assays. Plasmids encoding full-length MED7 or N-terminal truncations of MED7 were cloned into the *SmaI/XbaI* restriction sites of a pAL vector or through *Sall/XbaI* into a pRS315 vector. Individual plasmids were transformed into the *MED7* shuffle strain (Table 4) and streaked onto 5-FOA-containing plates to shuffle out the *MED7* encoding *URA3* plasmid. Yeast cells carrying only *MED7C* (102–222) are viable, whereas the Med7 N-terminal part including part of the linker (residues 1–101) cannot rescue cell growth. (B) Mutant strains exhibit a slow-growth phenotype. Note that growth curves are on a logarithmic scale. (C) Med7N/31 is required for Gal4-VP16-activated transcription *in vitro* (lane 1). Transcription can be rescued by the addition of TAP-purified Mediator (0.2 pmol, lane 2) or recombinant Med7N/31 (rMed7N/31, 2–200 pmol, lanes 3–5). Addition of both rMed7N/31 (2–200 pmol) and recombinant TFIIS (rTFIIS, 20 pmol, lanes 6–8) enhances the signal. (D) A *med7N/31Δ* nuclear extract that was rescued by the addition of recombinant Med7N/31 (lane 2, 200 pmol) was additionally stimulated by the addition of TFIIS (lane 5, 60 pmol). TFIIS alone can partially compensate for loss of Med7N/31 (lanes 3 and 4, 20–60 pmol). This stimulation was not observed with a *med18Δ* nuclear extract that was rescued by the addition of recombinant Med18/20 (rMed18/20, lanes 7–10, 20–60 pmol). (E) TFIIS addition stimulates basal and Gal4-VP16-activated transcription of wild-type (WT) nuclear extracts (lanes 2 and 3, and 5 and 6, respectively, 20–60 pmol). Recombinant Med7/31 or Med18/20 did not stimulate WT nuclear extracts. (F) Deletion of Med7N/31 or its subunits does not lead to loss of additional Mediator subunits. C-terminally TAP-tagged Med18 was purified from *med31Δ*/Med18-TAP, *med7NΔ*/Med18-TAP, and *med7N/31Δ*/Med18-TAP strains as described (Materials and methods 2.2.4). Copurifying proteins were separated on a 12% NuPAGE gel (Invitrogen), and bands were stained with Coomassie blue. The identity of all Mediator subunits was confirmed by mass spectrometry (the Table "Mass spectrometry analysis of Mediator TAP-tag purification" can be viewed online at <http://www.nature.com/emboj/journal/v28/n1/suppinfo/emboj2008254as1.html> in Excel file format). Contaminants such as ribosomal proteins or degradation products of Mediator subunits were especially detected at lower molecular weights and do partially overlap with smaller subunits such as Med7C.

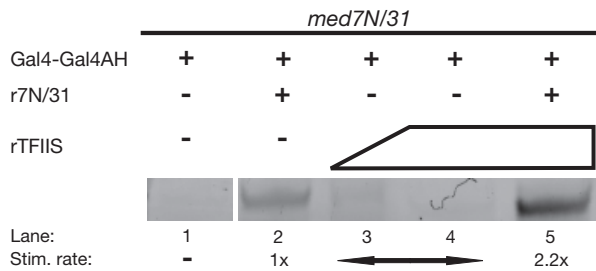


Figure 7: *In vitro* transcription assay using Gal4-Gal4 activation-helix (Gal4-Gal4AH) as activator.

A *med7N/31*Δ nuclear extract was also defective in activated transcription using a Gal4-Gal4AH (Carey et al., 1990) as activator (lane 1) but could be rescued by addition of recombinant Med7N/31 (lane 2, 200 pmol). Similarly as shown in Figure 6D, the reconstituted complex could be further stimulated by addition of recombinant TFIIS (lane 3-5, 20-60 pmol). The assay was performed using 100 μg of nuclear extract.

3.1.6 Med7N/31 is a functional Mediator submodule *in vivo*

To investigate the function of the Med7N/31 subcomplex *in vivo*, we carried out comparative microarray-based gene expression profiling with the yeast deletion strains *med7N*Δ, *med31*Δ, and *med7N/31*Δ. Compared with wild-type cells, the expression profiles of the three deletion strains showed similar overall changes illustrated by high Pearson's correlations (Figure 8A–D; Table 13; Table 14). A majority of changes in mRNA levels that are induced by deletion of both Med7N and Med31 are already observed when either Med7N or Med31 is lacking from cells. This shows that Med7N/31 serves as a functional submodule of the Mediator *in vivo* at a majority of affected genes. Some differences between profiles for the *med7N*Δ, *med31*Δ, and *med7N/31*Δ strains at selected genes (Figure 8C) indicate subunit-specific functions that may result from additional protein interactions (unpublished data). As the majority of affected genes is downregulated (Figure 8D), the Med7N/31 submodule has a predominantly positive function, consistent with previous expression data on a *med31*Δ strain (van de Peppel et al., 2005).

3.1.7 Med7N/31 regulates a subset of genes

Gene ontology (GO) analysis of genes with significantly changed mRNA levels revealed an over-representation of genes involved in sulphate/methionine metabolism, iron homeostasis, and transport functions (Table 13; Table 14B). A group of genes involved in telomere maintenance was also over-represented, consistent with the observation that a *med31*Δ strain exhibits shortened telomers (Askree et al., 2004). The differential expression profiles for Med7N/31 were largely distinct from the previously published profiles (Larivière et al., 2008) of the tail subunit deletion strains *med2*Δ and *med3*Δ, and correlated only moderately with those of strains *med8C*Δ, *med18*Δ, and *med20*Δ, which lack parts of the head submodule Med8C/18/20 (Figure 8A and B). However, both the Med7N/31 and the Med8C/18/20 submodules regulate genes responsible for siderophore transport and conjugation. Thus, the Med7N/31 submodule is required not only for the regulation of a specific subset of genes but also those genes that depend on other parts of the Mediator.

To identify transcription factors that regulate the differentially expressed genes, we used the transcription factor to gene promoter mapping matrix from the YEASTRACT website (Teixeira et al., 2006), and performed Fisher's exact test with the R/Bioconductor software (Gentleman et al., 2004) (Table 14F). This analysis revealed that the differentially expressed genes contained over-represented target genes for certain transcription factors, including Cst6,

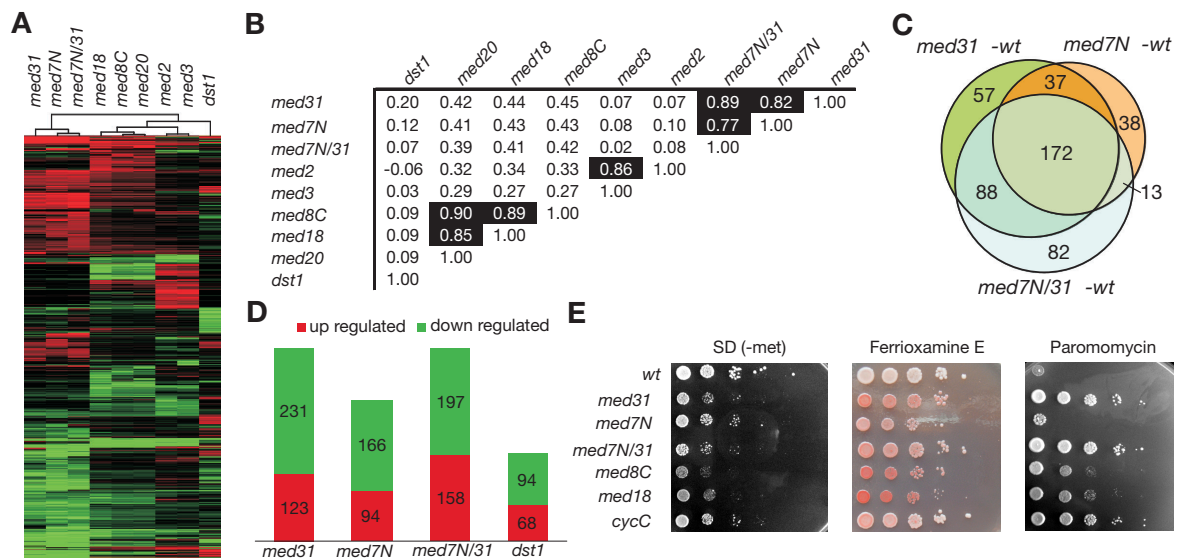


Figure 8: Transcriptome profiling analysis and phenotypic correlation.

(A) Cluster diagram (Euclidean distance) of genes exhibiting significantly altered mRNA levels (at least 1.7-fold, vertical axis) for different Mediator subunit deletion strains and TFIIIS (horizontal axis). Changes in mRNA levels compared with the wild-type strain are depicted in red (up), green (down), or black (no change). (B) Pearson's correlation matrix for expression profiles of the Mediator middle subunit deletion strains *med7N* Δ , *med31* Δ , *med7N/31* Δ , the head subunit *med8C* Δ , *med18* Δ , *med20* Δ , the tail subunit deletion strains *med2* Δ , *med3* Δ , and the deletion profile of the general transcription factor *dst1* Δ strain. (C) Venn diagram showing the overlap between the investigated *med31* Δ , *med7N* Δ , and *med7N/31* Δ strains. While these three strains exhibit a very high overlap, the overlap with the *dst1* Δ strain was not regarded as statistically significant. (D) Number of significantly altered genes of all four investigated deletion strains, split into up- and downregulated genes. (E) Selected phenotyping analysis results. Using 10-fold serial dilutions of yeast strains spotted onto selective agar plates, we screened for phenotypes, occurring under certain growth conditions. All assays were compared with a control plate on YPD, synthetic complete (SC), or SD media plates. As typical examples, the results from the growth inhibition assay on SD (-met) plates, the siderophore uptake assay (detected using bathophenanthroline disulphonic acid (BPDS)), and the growth inhibition on paramomycin assay are depicted.

Aft1, Msn2, Msn4, Yap family factors, Met28, Met31, Met32, Hsf1, and Pdr1. Consistent with the GO analysis, Msn2, Msn4, and Yap family members are involved in stress response, Cst6 regulates genes involved in telomere maintenance, and Aft1 is required for activating the low iron response regulon through Mediator (van de Peppel et al., 2005). The mRNA levels for these factors were unaltered in the investigated strains, except for Met28 and Msn4. Met28 was downregulated for Med7N/31 deletions and upregulated for Med2/Med3 deletions (Table 14G), explaining corresponding negative and positive responses, respectively, of target genes involved in methionine and cysteine biosynthesis (Table 14D).

Table 13: Summary of common biological terms overrepresented in GO analysis of the differentially expressed genes in *med31Δ*, *med7NΔ* and *med7N/31Δ* strains.

GO term (Biological process) ^a	Description	<i>med7N/31Δ</i> submodule			
		Annotated	Up-regulated	Down-regulated	Expected
GO:0015891	siderophore transport	9	7		0.3
GO:0000097	sulfur amino acid biosynthetic process	35		8	1.0
GO:0006555	methionine metabolic process	38		8	1.1
GO:0000103	sulfate assimilation	10		4	0.3
GO:0015698	inorganic anion transport				
- GO:0008272	- sulfate transport	5		3	0.2
GO:0043419	urea catabolic process	2	2		0.1
GO:0000749	response to pheromone during conjugation				
- GO:0000750	- pheromone-dependent signal transduction	28	1	4	0.8
GO:0015846	polyamine transport	11	2	1	0.3
GO:0007050	cell cycle arrest	12	1	2	0.4
GO:0000723	telomere maintenance				
- GO:0007004	- telomere maintenance via telomerase	17	1	2	0.5
- GO:0016233	- telomere capping	5	1	1	0.2
GO:0001403	invasive growth (sensu <i>Saccharomyces</i>)	45	1	4	1.3
GO:0032147	activation of protein kinase activity	6	2		0.2
GO:0001402	signal transduction during filamentous growth	7	1	1	0.2
GO:0008645	hexose transport	20		3	0.6

^a GO terms are ranked according to the topGO weight algorithm (Alexa et al., 2006) exhibiting a score smaller than 0.02. Lower level GO terms (marked with a "-") are listed below of the hierarchically higher GO terms. For the complete analysis including the associated genes and the analysis for the *dst1Δ* strain see also Tables 14B and C.

Table 14: The Table "Analysis of transcriptome profiling" could not be included here due to its huge size but the Excel file can be viewed in online at <http://www.nature.com/emboj/journal/v28/n1/suppinfo/emboj2008254as1.html>.

(A) List of up- and down-regulated genes in the yeast deletion strains *med31Δ*, *med7NΔ*, *med7N/31Δ* and *dst1Δ*. (B) Overrepresented biological processes and associated genes detected in the GO analysis of *med31Δ*, *med7NΔ*, *med7N/31Δ* and *dst1Δ* profiles. (C) GO analysis for the *med7N/31Δ*, *med8C/18/20Δ* and *med2/3Δ* submodule profiles. (D) GO-comparison table and visualization of the three submodule deletion profiles. The data was split into up- and down regulated genes (red and green bars, respectively). (E) Complete list of expression values of the yeast deletion strains *med31Δ*, *med7NΔ*, *med7N/31Δ* and *dst1Δ*. (F) Ranking of transcription factors based on Fisher's exact test which are potentially regulating the differentially expressed genes in *med31Δ*, *med7NΔ*, *med7N/31Δ* and *dst1Δ* strains. (G) Ranking of transcription factors based on Fisher's exact test which are potentially regulating the differentially expressed genes in *Med7N/31*, *Med8C/18/20* and *Med2/3* submodule deletion strains.

3.1.8 Overlapping and specific functions of Mediator submodules

To investigate the deregulation of genes induced by disruption of Med7N/31, we analyzed the growth of several yeast strains with deletions in Mediator genes (Table 4) on various selective agar plates (Table 15). The phenotypes of Med7N/31 deletions correlated well with results from transcription profiling. In the absence of methionine, these deletion strains grew poorly (Figure 8E), consistent with the observed downregulation of genes involved in methionine/sulphate metabolism. In the presence of siderophores, several deletion strains took up more complexed iron, as indicated by a red color (Figure 8E), consistent with higher expression of siderophore transport genes (some likely regulated by Aft1). Sensitivities of the deletion strains towards osmotic and cell wall stress were consistent with reported impaired cell wall metabolism of Mediator subunit deletion strains of *Schizosaccharomyces pombe* (Linder et al., 2008). A decreased sensitivity of the *med31* Δ and *med7N/31* Δ strains for the translation inhibitor paramomycin can also be explained by impaired cellular uptake or transport (Figure 8E). Most deletion strains were further impaired in their response to temperature, oxidative, and DNA repair stresses (Table 15). Also observed were inositol⁻ phenotypes that are often indicative of defects in the general transcriptional apparatus (Hampsey, 1997).

This comparative phenotyping of Mediator deletion strains showed that the *med8C* Δ and *med18* Δ strains exhibited the most severe growth defects (Table 15), possibly reflecting an important function of these subunits in the initiation complex assembly (Ranish et al., 1999). Deletion of subunits Med1, Med5, or Med9 was less detrimental. In agreement with earlier studies (van de Peppel et al., 2005), Cdk8 behaves partially contrasting with the phenotyping assays. On the transcriptome level, analyses of Med7N/31 and Med8C/18/20 submodule deletion profiles with *med2* Δ and *med3* Δ profiles (Table 14C and D) reveal different overlaps in enriched GO terms. Some GO terms are exclusively enriched for specific Mediator submodules (e.g. telomere capping for Med7N/31), whereas other GO terms are affected for two different submodules (e.g. siderophore transport for Med7/31 and Med8C/18/20 or serine family amino-acid catabolism with Med8C/18/20 and Med2/3), and other GO term groups are affected by all investigated mutations (e.g. response to pheromone). Such overlap in the phenotyping assays (Table 15) and the GO analysis (Table 13; Table 14C and D) shows that the characterized non-essential parts of Mediator are generally required for regulating metabolic sensing, stress response, and amino-acid biosynthesis pathways.

Table 15: Comparative phenotyping of Mediator deletion strains.

	Sensitivity test ^a	wt	Middle					Head		Tail			Kinase
			<i>med31</i> Δ	<i>med7N</i> Δ	<i>med7N/31</i> Δ	<i>med1</i> Δ	<i>med9</i> Δ	<i>med8C</i> Δ	<i>med18</i> Δ	<i>med2</i> Δ	<i>med3</i> Δ	<i>med5</i> Δ	<i>cycC</i> Δ
Siderophore-uptake	SD + ferrichrome	+	+++	++	++	+	+	+++	+++	++	++	-	++
	SD + ferrioxamine E	+	+++	++	++	+	+	+++	+++	++	++	-	++
Lack of amino acids	SD (-met)	-	++	+	++	-	-	+++	++	++	++	-	+
Growth on S-Sources	SD (-SO ₄ ²⁻)	+	++	+	++	-	-	++	++	+	+	-	+++
Growth on C-Sources	YP Na-acetate	-	++	+	+	-	-	+	+++	+++	+++	+	+++
Growth on N-Sources	SD urea	-	-	+	-	-	-	++	++	++	+	-	+
Temperature	YPD 16°C	-	+	+	+	+	+	++	++	++	++	-	+
	YPD 37°C	-	++	+	+	+	++	+++	+++	++	++	-	+++
Salt stress	YPD NaCl (1 M)	-	++	+	+	+	+	+++	++	-	-	+	++
	YPD KCl (1 M)	-	++	+	++	-	+	+++	+	+	+	-	+
	YPD LiCl (0.4 M)	+	+	+	+	+	++	+++	+++	-	-	+	++
Cell wall stress	YPD SDS (0.01 %)	-	+	+	+	-	-	+++	+++	+	+	-	++
Osmotic stress	YPD glycerol (2 M)	-	++	++	++	+	-	+++	+++	+	+	-	+
Oxidative stress	YPD Menadione (20 mM)	-	-	++	+	-	-	-	++	+	+	-	-
DNA repair	YPD MMS (0.05 %)	-	++	++	++	++	++	++	++	+	+	+	-
	YPD HU (100 mM)	+	++	++	++	+	+	+++	+++	++	++	+	+++
Transcription	SC (-inositol)	-	++	++	++	-	-	+++	+++	++	++	-	+
Transcription elongation	SC (-ura) 6-AU (100 mg/ml)	++	+	-	-	-	-	-	+	++	+	+	-
Translation	YPD cycloheximide (0.1 mg/ml)	-	+++	+++	+++	-	+	++	+++	+++	+++	+	+
	YPD paromomycin (2.5 mg/ml)	+++	-	+++	-	-	-	++	++	-	-	-	-
Miscellaneous	YPD caffeine (8 mM)	+	++	+	+	+	+	++	+++	++	++	-	++
Starvation	YP media 6 days, 30°C, then resported on YPD	-	++	+	+	ND	ND	+++	+++	ND	ND	ND	+

^a All measurements are growth inhibition, except for the siderophore assay, where cellular iron content was measured. Growth inhibition (with the exception of the siderophore uptake assays) is indicated by relative estimates (+, moderate hypersensitivity; ++, high hypersensitivity; +++, very high hypersensitivity; -, no hypersensitivity; ND, not determined).

3.1.9 Cooperation of Med7N/31 and TFIIS

As Med31 interacts genetically with the elongation factor TFIIS (Krogan et al., 2003; Malagon et al., 2004; Collins et al., 2007; Guglielmi et al., 2007), we tested whether Med7N/31 cooperates with TFIIS during activated transcription *in vitro*. Indeed, transcription in a *med7N/31*Δ nuclear extract that was rescued by recombinant Med7N/31 could be enhanced four-fold by the addition of recombinant TFIIS using Gal4–VP16 as an activator (Figure 6D). A stimulatory effect of TFIIS, although only about two-fold, was also seen for basal and activated transcription in wild-type (WT) extracts (Figure 6E). Addition of TFIIS to a *med7N/31*Δ extract resulted in a signal even in the absence of recombinant Med7N/31, although TFIIS was not limiting in the extracts, as a three-fold higher concentration did not further increase transcription (Figure 6D, lanes 3 and 4). TFIIS also stimulated transcription activated with the alternative activator Gal4–Gal4AH, although only about two-fold (Figure 7). In contrast, transcription in a *med18*Δ extract was not enhanced at all by TFIIS addition (Figure 6D, lanes 8 and 9) and a *med18*Δ extract that was rescued by the addition of recombinant Med18/20 was not further stimulated by the addition of TFIIS (Figure 6D, lane 10). These results show that TFIIS can partially compensate for the loss of Med7N/31, and that highest transcript levels required the addition of both TFIIS and Med7N/31. These observations were specific for the *med7N/31*Δ extract, as this effect was not obtained in corresponding experiments with a *med18*Δ extract. The results are further consistent with an important role for TFIIS during initiation (Guglielmi et al., 2007; Kim et al., 2007).

To investigate whether TFIIS and Med7N/31 cooperate at specific genes *in vivo*, we determined the gene expression profile for a yeast strain that lacks the gene for TFIIS, *dst1* (Table 14A, B, E and F). Only 162 mRNA levels were significantly altered (at a two-fold expression change cutoff and a false discovery rate of $P < 0.05$; Table 14A), consistent with a lack of a phenotype of the *dst1*Δ strain in rich medium (Clark et al., 1991). Pearson's correlation and GO analysis did not reveal any significant overlap between *dst1*Δ and *med7N/31*Δ profiles (Figure 8B; Table 14). Consistently, we could not detect a direct physical interaction between TFIIS and recombinant Med7N/31 (not shown). Instead, analysis of synthetic lethality partners suggests that Med31 and TFIIS are functionally connected through the SWR1 complex that is involved in exchange of histone H2A by the variant H2A.Z (Figure 9A). Similar correlations were also found for the Mediator subunits Med1, Med9, and Med20 (not shown). Additionally, the Mediator kinase module is a highly significant phenotypic suppressor of core Mediator subunits and TFIIS (Figure 9B). Taken together, the functional cooperation of Med7N/31 and TFIIS is apparently not gene specific *in vivo*, but may generally occur during initiation, and could further be linked to Swr1-dependent histone variant exchange near transcription start sites (Santisteban et al., 2000; Zanton and Pugh, 2006; Zlatanova and Thakar, 2008).

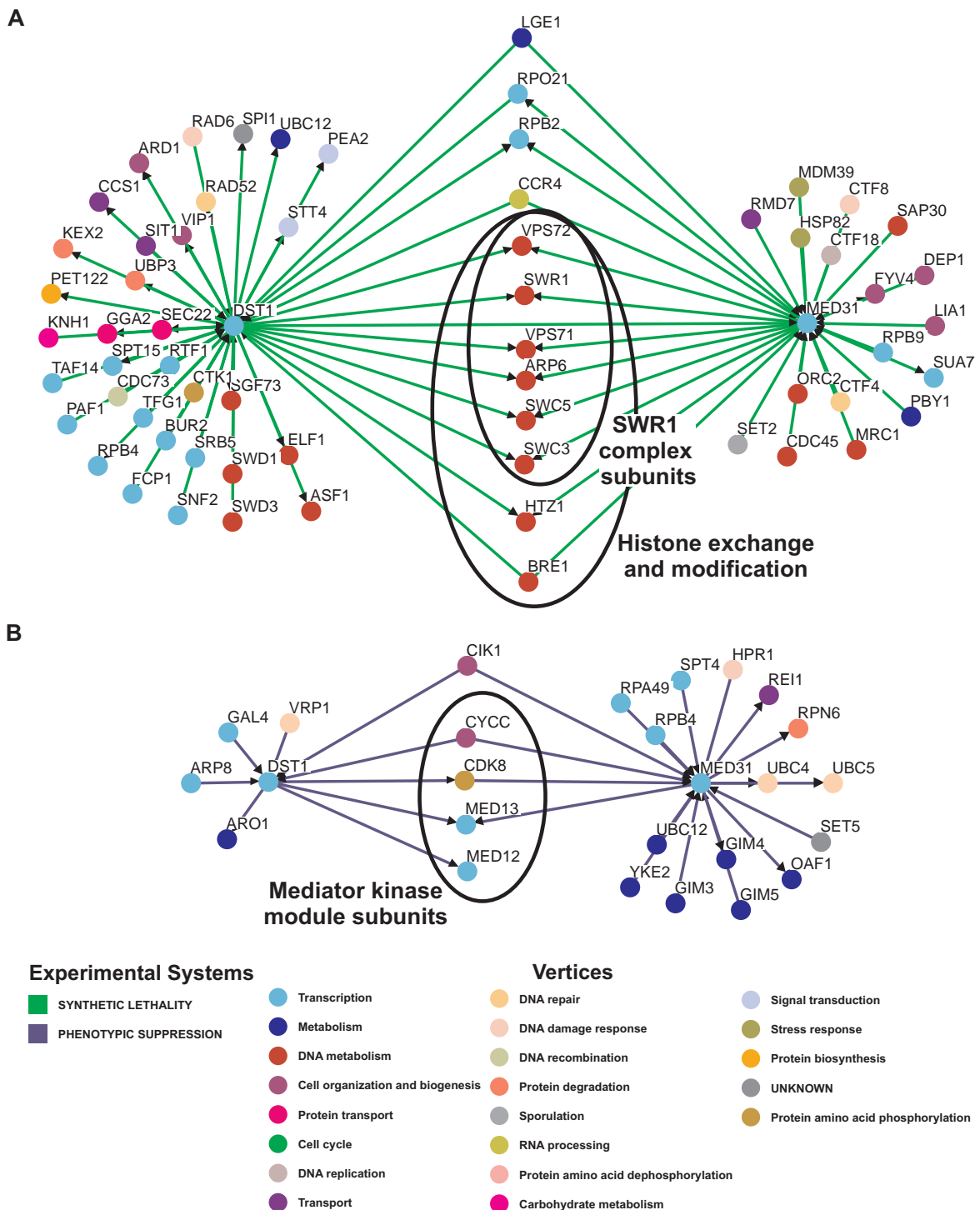


Figure 9: Analysis of published genetic interactions of Med31 and TFIIS.

(A) Common and disparate synthetic lethality partners of Med31 and TFIIS are depicted as nodes. (B) Common and disparate phenotypic suppression partners of Med31 and TFIIS. Figures were prepared using the Osprey software (Breitkreutz et al., 2003) with interaction data downloaded from BioGrid database (Stark et al., 2006). Interaction data references are available online at <http://www.nature.com/emboj/journal/v28/n1/supinfo/emboj2008254as1.html>

3.2 Preparation and topology of the Mediator middle module

3.2.1 Endogenous Mediator middle module

It was previously reported that the middle module is lost from Mediator that is purified from a *med19* Δ strain under stringent conditions (Baidoobonso et al., 2007). To purify middle module from a *med19* Δ strain, we introduced a C-terminal tandem affinity purification (TAP) tag on the middle module subunit Med7. TAP purification resulted in pure middle module without the need for the previously used urea dissociation (Baidoobonso et al., 2007), indicating that the tag further destabilizes the Mediator. Fusing a TAP-tag with Med15 or Med18 did not lead to purification of individual parts of Mediator (Figure 11). The high yield and purity of our preparation from the *med19* Δ /*MED7*-TAP strain (Figure 10C) enabled us to determine unambiguously by mass spectrometry (Methods) that the endogenous yeast Mediator middle module comprises the subunits Med1, Med4, Med7, Med9 (Cse2), Med10 (Nut2), Med21 (Srb7) and Med31 (Soh1), consistent with previous description (Guglielmi et al., 2004; Béve et al., 2005; Bourbon, 2008; Linder et al., 2006).

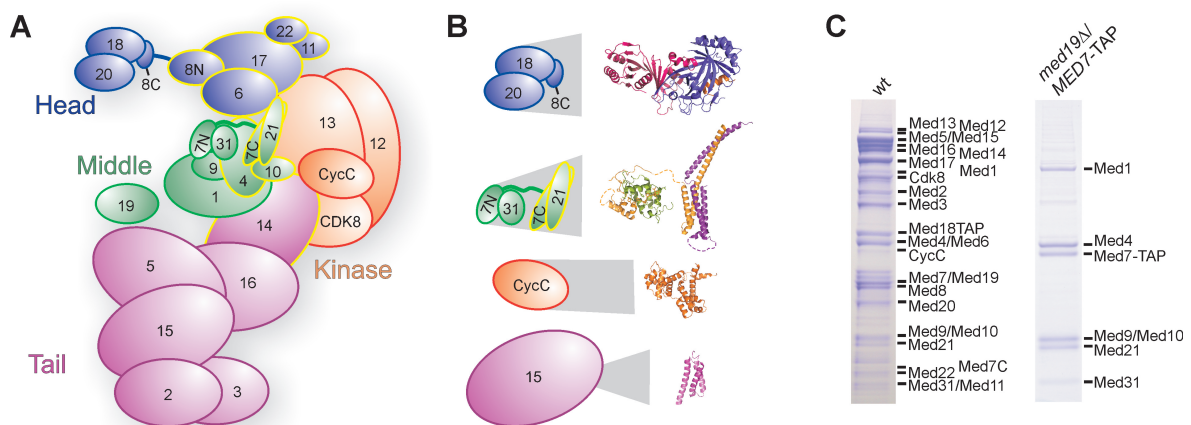


Figure 10: Endogenous Mediator and its middle module.

(A) Schematic view of Mediator subunit arrangement and modular structure, taking into account known and found (see below) subunit interactions. Subunits that are essential for yeast viability are outlined in yellow. (B) Available detailed structural information on subunits and subcomplexes of Mediator (Baumli et al., 2005; Hoepfner et al., 2005; Larivière et al., 2006; Thakur et al., 2008, this work, see 3.1). Structures are enlarged in proportion to the full subcomplex or subunit sizes. (C) SDS-PAGE analysis of endogenous Mediator and 7-subunit Mediator middle module purified from wild-type (left) and *med19* Δ yeast strains containing a C-terminal TAP-tag on the Med7-subunit. Copurifying proteins from 4 l yeast cells were separated on a 12% NuPAGE gel (Invitrogen), and bands were stained with Coomassie blue. The identity of all Mediator subunits except Med31 could be confirmed by mass spectrometry (not shown).

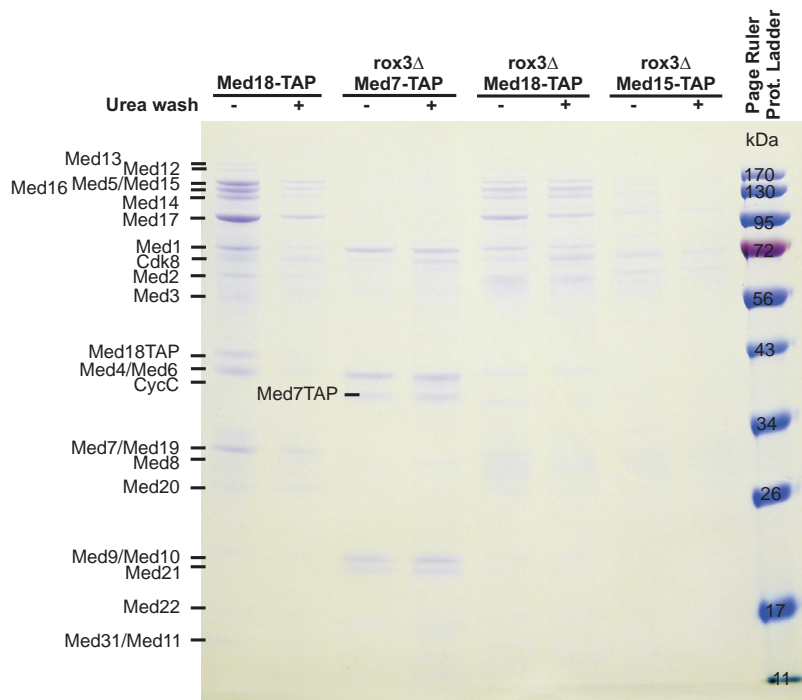


Figure 11: Destabilization of the Mediator complex.

Mediator has been purified in *med19Δ* background strains via a C-terminal TAP-tag on Med7 from the middle module, Med18 from the head module and Med15 from the tail module. Copurifying proteins were separated on a 12% NuPAGE gel (Invitrogen), and bands were stained with Coomassie blue. Using our strain background, we did not observe loss of the middle module for *Med18-TAP/med19Δ* or *Med15-TAP/med19Δ* strains even after 1 M urea washing during purification (using 2 l yeast culture per lane). However, in a *Med7-TAP/med19Δ* strain, the remaining modules are lost during purification even without urea treatment and exclusively the middle module is purified.

3.2.2 Recombinant Mediator middle module

We previously used heterologous coexpression of physically associated Mediator subunits in *E. coli* to obtain milligram quantities of Mediator subcomplexes of up to three subunits (Baumli et al., 2005; Larivière et al., 2006, this work, see 3.1). Here, based on commercial pET- and Duet-vectors (Novagen), we created poly-cistronic expression constructs with additional ribosomal binding sites between middle module subunit open reading frames (Figure 12). For expression of a 4-subunit complex comprising Med7, 10, 21, and 31, we constructed a tricistronic pET21b vector encoding Med10, 7 and 21 (Figure 12B) and a pET24d vector encoding C-terminally hexahistidine-tagged Med31. These vectors were cotransformed into *E. coli* BL21(DE3) RIL cells (Stratagene) and after coexpression, the 4-subunit complex could be purified (Figure 12B, Methods 2.4.2). To obtain a 6-subunit complex that comprised also subunits Med4 and Med9, these two subunits were coexpressed separately using a bicistronic pET21b vector. A partially purified Med4/9 heterodimer was assembled with the pure 4-subunit complex and the resulting 6-subunit complex was purified to homogeneity. To obtain complete 7-subunit middle module, three vectors were cotransformed into *E. coli* BL21(DE3) RIL cells, the tricistronic vector encoding Med10, 7 and 21, a vector encoding N-terminally hexahistidine-tagged Med31, and a vector encoding Med4, Med9, and N-terminally StrepII-tagged Med1 (Figure 12C, Methods 2.4.2). After coexpression of

the seven proteins from these three vectors, the 7-subunit module was purified in two steps, including a StrepII affinity step (Figure 12C, Methods 2.4.2).

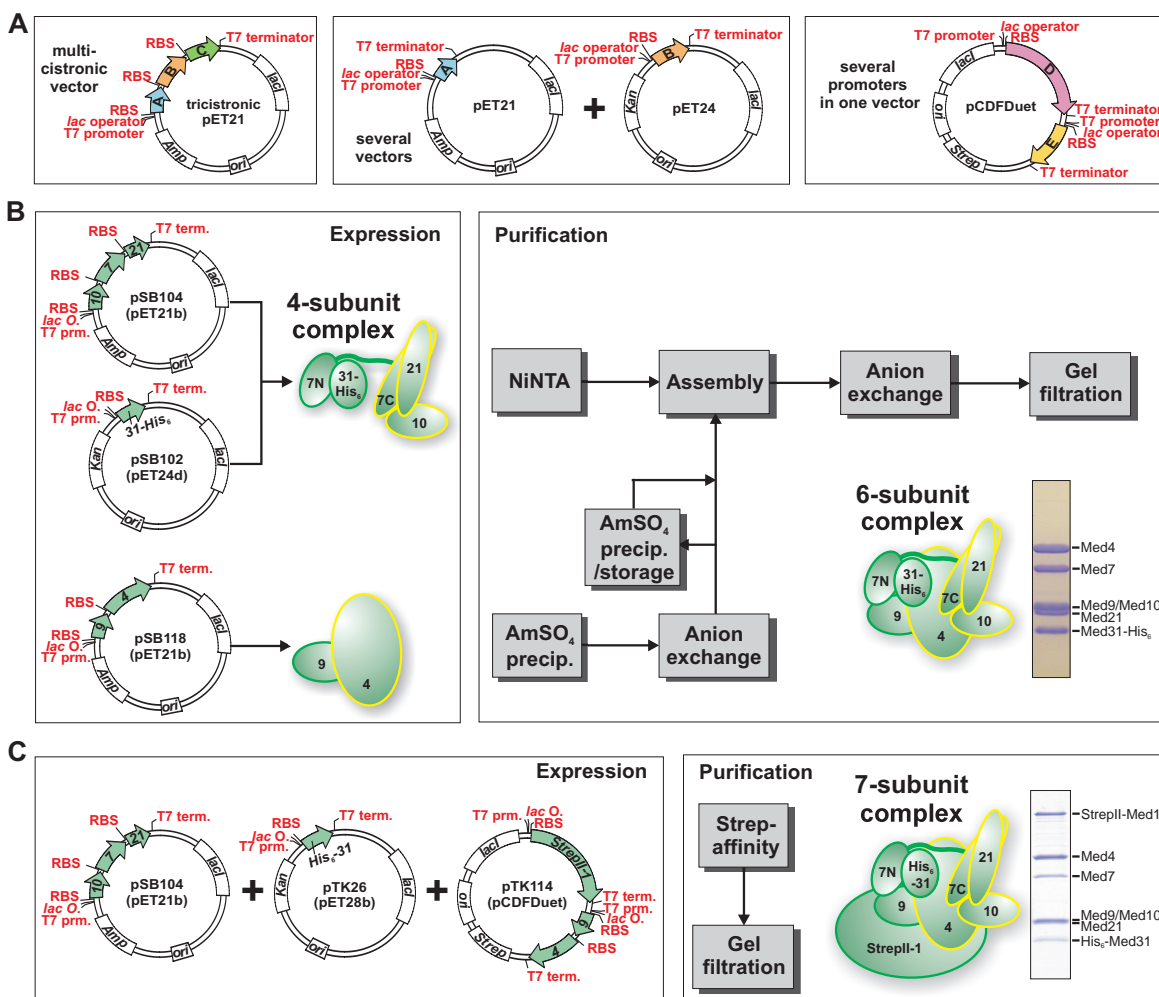


Figure 12: Recombinant Mediator middle module.

(A) Recombinant coexpression of multisubunit protein complexes in *E. coli* is possible by using multicistronic expression vectors, several compatible vectors cotransformed into *E. coli*, vectors with several promoters, and combinations of these. (B) Coexpression of 4-subunit Mediator middle complex containing Med7/10/21/31 is accomplished using a tricistronic pET21 and a monocistronic pET24 vector. The dimeric Med4/9 complex is coexpressed using a bicistronic pET21 vector. After cell-disruption and prepurification, both complexes are assembled into the 6-subunit middle complex containing Med4/7/9/10/21/31 and purified further to homogeneity. (C) Recombinant 7-subunit middle module consisting of Med1/4/7/9/10/21/31 is obtained by coexpression using a tricistronic vector encoding for Med7/10/21, a monocistronic vector encoding for His₆-Med31 and a pCDFDuet vector with StrepII-tagged Med1 from MCS I and Med4/9 bicistronically expressed from MCS II. Purification after cell disruption is performed by StrepII-affinity purification and subsequent gel filtration.

3.2.3 Crystallization trials with middle module complexes

Recombinant middle module complexes and subcomplexes were tested in crystallization screenings (Methods 2.2.7) when crystallization grade complexes could be purified (evaluated by purity, stability and stoichiometry). Truncated variants – based on crystal structure (Baumli et al., 2005), secondary structure prediction and limited proteolysis – were generated to remove potential flexible regions and these complexes were screened for crystallization

Table 16: Crystallization screening of recombinant Mediator middle module and its subparts. All screens were performed at 20°C.

Complex	Concentration	Screen(s) ^a	Buffer
Med7/21/31-His ₆	5 mg/ml	Classic, Index, JBC I, JBC II, Natrix, PEG/Ion, pH-clear	A + 5 mM DTT
Med7/10/21/31-His ₆	10 mg/ml	Classic, Index, JBC I, Anions, Cations	G + 5 mM DTT
Med7/10/21/31-His ₆	8, 7, 6 and 4 mg/ml	JBC I	G + 5 mM DTT
Med7/10/21/31-His ₆	3 and 6 mg/ml	JBC I	A + 5 mM DTT
Med7/10/21 (1-130)/31-His ₆	8 mg/ml	Classic, Index, JBC I, Natrix, PEG/Ion	A + 5 mM DTT
Med7 (1-205)/10 (8-157)/21 (1-130)/31-His ₆	4 mg/ml	Classic, Index, JBC I, Natrix, PEG/Ion	A + 5 mM DTT
Med7 (1-205)/10 (41-157)/21 (1-130)/31-His ₆	4 mg/ml	Classic, Index, JBC I, Natrix, PEG/Ion	A + 5 mM DTT
Med7 (1-205)/10 (68-157)/21 (1-130)/31-His ₆	4 mg/ml	Classic, Index, JBC I, Natrix, PEG/Ion	A + 5 mM DTT
Med4/9	8 mg/ml	Classic, Index, JBC I, Anions, Cations, Natrix, PEG/Ion	G + 5 mM DTT
Med4 (21-284)/9	10 mg/ml	Classic, Index, JBC I, JBC II, Natrix, PEG/Ion	A + 5 mM DTT
Med4 (1-250)/9	10 mg/ml	Classic, Index, JBC I, JBC II, Natrix, PEG/Ion	A + 5 mM DTT
Med4 (21-250)/9	10 mg/ml	Classic, Index, JBC I, JBC II, Natrix, PEG/Ion, pH-clear	A + 5 mM DTT
Med4 (21-250)/9 Δ(19-63)	4 and 8 mg/ml	Classic, Index, JBC I, JBC II, Natrix, PEG/Ion	A + 5 mM TCEP
Med4/7/9/10/21/31-His ₆	5 mg/ml	Classic, Index, JBC I, Natrix, PEG/Ion, Anions, Cations, MPD	G + 5 mM DTT
StrepII-Med1/4/7/9/10/21/31-His ₆	5 mg/ml	Magic 1, Magic 2, Classic, Index	A + 5 mM DTT

^a Commercial screens used for 96-well plate screening were: Index, Natrix, PEG/Ion (all Hampton), Classic screen, pH-clear, anions suite, cations suite, classic suite (all Qiagen), JB Screen Classic HTS I S and JB Screen Classic HTS II S (both Jena Biosciences).

as well. Unfortunately, except for the Med7N/31 complex (see 3.1.1), no protein crystals were obtained that could be confirmed and reproduced (Table 16). Notably, protein complex yield of variants including Med7 (1-205) were considerably lower compared to variants including Med7 (1-211).

3.2.4 Activity assay trials

We were interested in testing functionality of native and recombinant middle modules by an activity assay. As an assay has not been described yet, we followed two approaches to establish such an assay *in vitro*. We speculated that in a *med19Δ/MED7-TAP* strain some middle module complexes might be spontaneously lost and prepared a nuclear extract from that strain. However, addition of recombinant Med19 restored the majority of the transcription activity but addition of neither native nor recombinant middle module increased transcription levels in an *in vitro* transcription assay (not shown). We concluded that the middle module is apparently not spontaneously lost in the nuclear extract but only during TAP-purification. Thus, in a second approach, we tried to establish purification of a middle-less Mediator similar as described by Baidoobonso et al. (2007). We intended to reconstitute a complete Mediator complex by assembly with recombinant middle module plus Med19

and test functionality in an *in vitro* transcription assay using a Mediator-depleted WT nuclear extract. A *Med18-3xFLAG/med19Δ/Med7-TAP* yeast strain was generated (similar to Baidoobonso et al. (2007) but with an additional TAP-tag on Med7 C-terminus), but liquid cultures did not reach sufficient cell densities due to a severe flocculation phenotype. A *Med15-3xFLAG/med19Δ/Med7-TAP* yeast strain exhibited only a weak flocculation phenotype and was used for experiments to establish middle-less Mediator purification. In brief, the supernatant of the Protein A purification step from TAP purification was purified further by Anti-FLAG antibodies. These experiments (not shown) led to purification of FLAG-tag purified Mediator as shown by mass spectrometry, but complex purity was neither sufficient for the intended assay nor to judge if the middle module was indeed lacking. As purification from a *Med15-3xFLAG* strain yielded a very similar band pattern in SDS-PAGE analysis, FLAG purification according to standard parameters (Methods 2.4.3) is apparently not sufficient to be used in the intended assays.

3.2.5 Subunit stoichiometry

To investigate the subunit stoichiometry in the recombinant middle module and its subcomplexes, we used native MS that allows determination of molecular weights of entire protein complexes (Heck, 2008; Sharon and Robinson, 2007). The detected masses were $191,650 \pm 60$ Da for the complete 7-subunit middle module (191,335 Da expected), $124,760 \pm 50$ Da for the 6-subunit complex (124,471 Da expected) and $75,840 \pm 30$ Da for the 4-subunit complex (75,620 Da expected) (Figure 13 and 14A). We calculated expected masses taking into account that the N-terminal methionines of Med4, 7, 10, 21 and 31 were lacking (Edman sequencing data, not shown). The slightly higher experimental masses can be explained by incomplete desolvation of the complexes (McKay et al., 2006). The MS analysis also revealed that the 4- and 6-subunit complexes tend to dimerize. This is likely due to exposed hydrophobic surfaces, since addition of DMSO eliminated the dimers from the recorded MS spectra (Figure 14B). These results reveal that only a single copy of each subunit is present in the complexes and establish the equimolar subunit stoichiometry of the middle module.

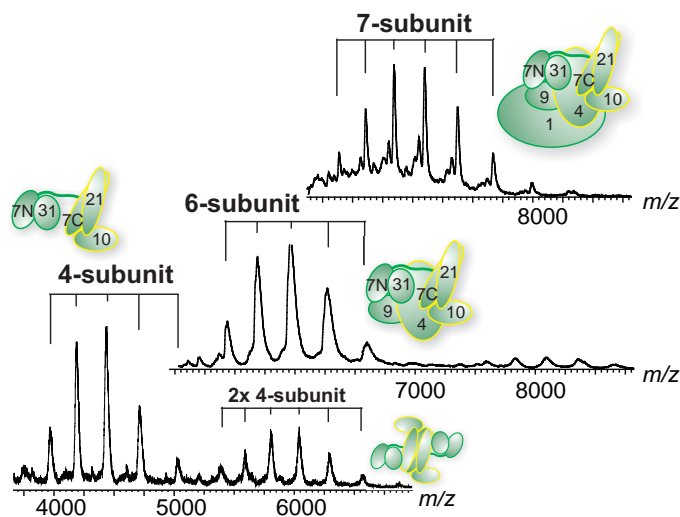


Figure 13: Native mass spectrometry analyses of Mediator middle module. Shown are from top to bottom spectra of the 7-, 6-, and 4-subunit middle module complexes. All individual subunits are present in equimolar stoichiometry. The distributions are labeled accordingly to the corresponding schematics.

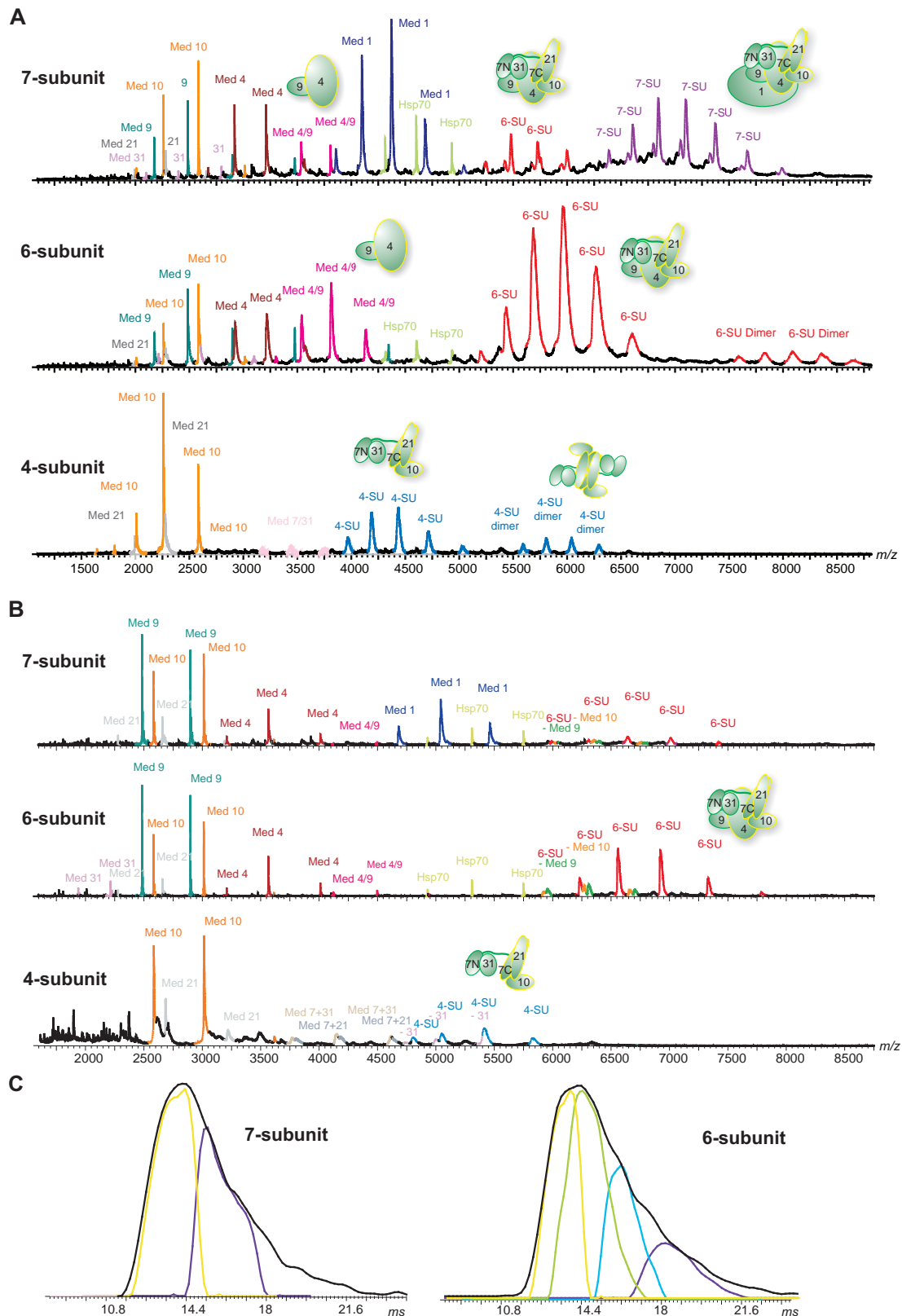


Figure 14: Mass spectrometry analyses of Mediator middle modules.

(A) Native mass spectrometry analyses of Mediator middle modules. Shown are spectra of 4-, 6-, and 7-subunit (SU) middle subcomplexes, respectively and of their subcomponents. All subunits are present in monomeric stoichiometry. The composition of each complex and subcomplex has been confirmed by tandem MS. Hsp70 (DnaK) is a common contaminant in purifications, it has been confirmed by proteomics experiments that the protein with the mass of 69 kDa is DnaK. (B) DMSO Spectra of the Mediator middle modules. Shown are spectra of 4-, 6-, and 7-subunit middle subcomplexes, respectively and of their subcomponents. The marked complexes and subcomplexes have been confirmed by Tandem MS experiments. (C) Drift time plots for 7- and 6-subunit middle modules (charge state 27^+ and 20^+ , respectively) analogous to Figure 18D.

3.2.6 Module topology

We next investigated the topology of the middle module by MS analysis. We observed spontaneous dissociation of subunits and subcomplexes in the buffer used for the native MS experiments. This effect could be enhanced by addition of DMSO or n-propanol (Figure 14). Dissociation of the 7-subunit module revealed that Med1 could detach from the module separately, to result in the 6-subunit complex. Dissociation of the 6-subunit complex revealed a dimer of Med4/9, confirming the interaction between those two subunits. Dissociation of the 4-subunit complex resulted in the trimers Med7/10/31 and Med7/21/31, and in the dimers Med7/31 and Med7/21. Overall, Med7 never dissociated from the middle module, showing it is an architectural subunit, whereas Med9 and Med10 were least stably attached. To further analyze the module topology, we investigated fragmentation of the 4-, 6- and 7-subunit complexes by tandem mass spectrometry. Generally consistent with solution dissociation experiments, Med9 and Med10 readily dissociated from the complexes, whereas Med7 never did, except to a low extent when the complete middle module was used. Taken together, the dissociation and fragmentation experiments are consistent with earlier structural and interaction analysis of the middle module and the existence of heterodimers Med7N/31, Med7C/21, and Med4/9 within intact middle module (Baumli et al., 2005; Guglielmi et al., 2004, this work, see 3.1).

3.2.7 Exposed regions in the middle module

To detect exposed and flexible protein regions, middle module complexes were subjected to limited proteolysis using chymotrypsin (Methods 2.2.6). In an attempt to separate stable fragments, we stopped proteolysis by addition of protease inhibitor at certain time points, and subjected the samples to gel filtration. Peak fractions were TCA-precipitated and analyzed by SDS-PAGE and Edman sequencing (Figure 13). This approach could identify stable subcomplexes suitable for crystallization, like Med7N/31 and Med7C/21, which result from proteolysis of a Med7/21/31 trimer (Figure 16A) (Baumli et al., 2005, this work, see 3.1).

Limited proteolysis of the 4-subunit complex revealed protease cleavage within regions predicted to form flexible loops, but also cleavage in some helical regions of Med21 (known structure) and Med10 (predicted) (Figure 16B, and C). Two subcomplexes were detected based on Med7N/31 and Med7C/21 that both contain N-terminally truncated Med10 (Figure 16C). Proteolysis of the 6-subunit complex also revealed Med7C/21 and Med7N/31 in different gel filtration fractions, but now associated with different truncated variants of Med10 (Figure 16D). Consistently, native MS analysis of an early 7-subunit complex preparation revealed an intact middle module with a truncated form of Med10 that lacked 66 N-terminal residues (not shown). Med9 showed only one chymotrypsin cleavage site and was detected either as full-length subunit (star in Figure 16D) or as an N-terminally shortened variant (star and triangle peak in Figure 16D). Med4 was cleaved at multiple sites, but preferentially from the C-terminus.

This analysis supports a submodular architecture of the middle module based on the Med7N/31 and Med7C/21 core subcomplexes connected via a flexible Med7 linker. Med4,

9, and 10 are associated with both core subcomplexes, but their proteolytic fragments were not sufficient to hold these subcomplexes together. The C-terminal region of Med4, the N-terminal region of Med9, and the N-terminal region of Med10 are not stably bound to the core subcomplexes and may be involved in contacts with other Mediator modules or external factors. Consistently, yeast complementation assays revealed that the flexible Med4 C-terminal residues 194-250 are required for viability, whereas the N-terminal residues 1-66 are not (Figure 15).

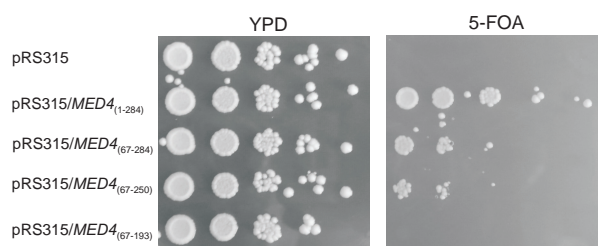


Figure 15: Yeast complementation assay for *MED4*

Plasmids encoding full-length *MED4* or N- and C-terminal truncations of *MED4* were cloned into the *SalI/NotI* restriction sites of a pRS315 vector. Individual plasmids were transformed into a *MED4* shuffle strain (EuroScarf Y22430 sporulated; *MATa* or *MATα*; YOR174W::kanMX4/ pRS316-*MED4*) and streaked onto 5-FOA-containing plates to shuffle out the *MED4* encoding *URA3* plasmid. Yeast cells carrying only *MED4* (67-250) are viable, whereas the Med4 C-terminal part including residues 193-250 was required to rescue cell growth.

3.2.8 Intra-module subunit interactions

To further elucidate the subunit interactions within the middle module, we used coexpression pull-down experiments (Figure 17A and Table 17). Our biochemical analysis generally confirmed previous subunit interactions based on yeast two hybrid (Y2H) assays and immunoprecipitation (Guglielmi et al., 2004), but additionally allowed us to distinguish weak and strong subunit interactions, and to detect interaction domain boundaries (Figure 17B, C). Important findings from this analysis were the following. First, Med7N/31 neither bound Med7C/21 nor Med4/9. For interaction of Med4/9 to any Med7-containing complex, the Med7 linker between Med7N and Med7C was required. Second, the Med4/9 heterodimer binds to Med1. Med4/9 heterodimer formation neither required the 18 N-terminal residues of Med4 nor the predicted loop in Med9 comprising residues 19-63, consistent with the prior observation that Med9 contains two domains (compare Takahashi et al., 2009). Third, Med10 and Med4 interacted weakly and Med21 stabilized this interaction. The C-terminal part of Med10 was sufficient for binding the Med7C/21 subcomplex. Med10 was also found to stably bind to Med14, confirming previous data (Guglielmi et al., 2004) and showing that Med14 (1-259) is sufficient to establish a connection of middle module towards Mediator tail module. Finally, reported Y2H interactions between Med21 and Med31 were not confirmed. Stable expression of Med9 always required coexpression with Med4, but was not possible with Med1 or Med7, suggesting that Med9 has no direct interaction with these. Together with published data, this analysis establishes the middle module subunit interaction network (Figure 17C).

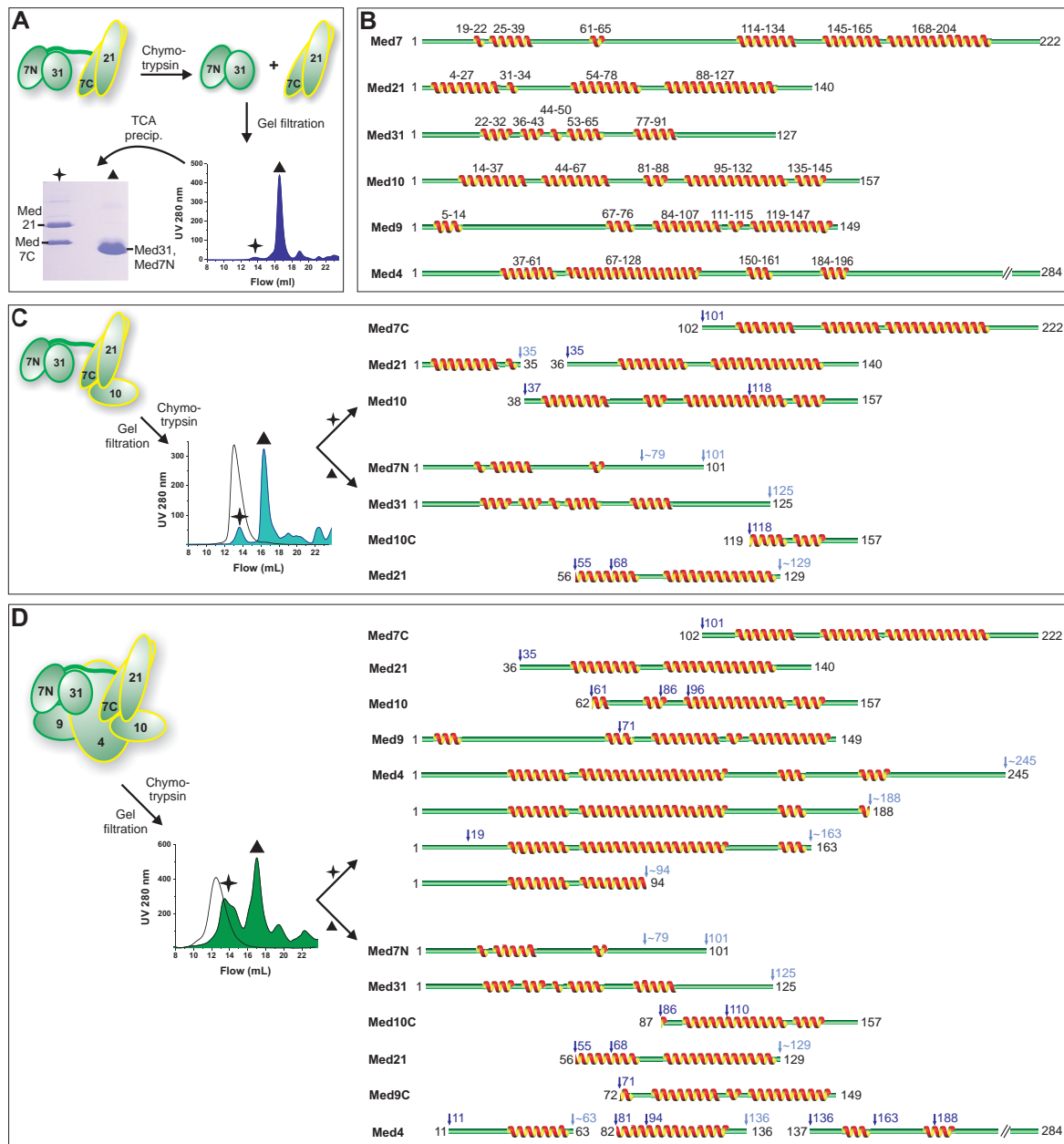


Figure 16: Limited proteolysis analysis of Mediator middle module.

(A) Recombinant complexes were subjected to limited proteolysis by chymotrypsin after identifying suitable digestion durations using time courses. The samples were subjected to gel filtration, the eluting peaks precipitated by TCA, fractions separated on SDS-PAGE and subjected to Edman sequencing. (B) Secondary structures and secondary structure predictions for yeast middle module subunits. Multiple sequence alignments were used whenever possible. Given are consensus predictions by HHpred (Soeding et al., 2005), I-Tasser (Zhang, 2008), PSIPred (Jones, 1999) and CDM (Sen et al., 2006). (C) Schematic diagram of limited proteolysis of Med7/10/21/31 using chymotrypsin, analogous to (A). The chromatogram of undigested complex is indicated by the black curve. Proteolytic cleavage sites are indicated above the protein cleavage schemes in dark blue (sequenced) and light blue (estimated from SDS-PAGE). Ambiguous C-terminal sites are marked with a tilde. In cases in which more than one N-terminus was sequenced, the alternative N-terminal cleavage sites are marked additionally. (D) Schematic diagram of limited proteolysis results for the Med4/7/9/10/21/31 complex using chymotrypsin, analogous to (C).

Table 17: Mediator middle module interaction assays^a.

Subunit 1	Subunit 2	Subunit 3	Subunit 4	Technique	Reference
Med7 (101-222)	Med21 fl ^b	–	–	Structure	Baumli et al. (2005)
Med4 fl	Med21-His ₆ fl	–	–	Gel filtration	Baumli et al. (2005)
Med10 fl	Med21-His ₆ fl	–	–	Gel filtration	Baumli et al. (2005)
Med4-His ₆ fl	Med21 fl	Med7	–	Gel filtration	Baumli et al. (2005)
Med7 (1-83)	Med31 fl	–	–	Structure	This work
StrepII -Med7 (1-101)	Med31-His ₆	Med4 fl	Med9 fl	Coexpr. & pull-down	This work
StrepII -Med7 (1-84)	Med31-His ₆	Med4 fl	Med9 fl	Coexpr. & pull-down	This work
StrepII -Med7 (1-84)	Med31 fl	Med7	Med21 fl	Coexpr. & pull-down	This work
StrepII -Med14 (1-259)	Med10 fl	–	–	Coexpr. & pull-down	This work
StrepII -Med14 (1-259)	Med4 fl	Med9 fl	–	Coexpr. & pull-down	This work
Med21- His₆ fl	Med7 (104-222)	Med10 (74-157)	–	Coexpr. & pull-down	This work
Med10- His₆	Med4*	–	–	Coexpr. & pull-down	This work
Med10- His₆	Med4 fl*	Med9 fl*	–	Coexpr. & pull-down	This work
StrepII -Med1 fl	Med4 fl	Med9 fl	–	Coexpr. & pull-down	This work
StrepII -Med1 fl	Med14 (1-259)*	–	–	Coexpr. & pull-down	This work
StrepII -Med1 fl	Med14 (1-259)*	Med10 fl*	–	Coexpr. & pull-down	This work
StrepII -Med1 fl	Med14 (1-259)	Med10 (1-73)	–	Coexpr. & pull-down	This work
StrepII -Med1 fl	Med14 (1-259)	Med10 (74-157)	–	Coexpr. & pull-down	This work
Med31- His₆	Med7 (1-84)	Med10 fl	–	Coexpr. & pull-down	This work
His₆ -Med9 fl	Med4 (19-250)	–	–	Coexpr. & pull-down	This work
His₆ -Med9 Δ(19-63)	Med4 fl	–	–	Coexpr. & pull-down	This work

^a Bold letter indicated the protein purification tags which have been used in the assay. Red subunits were not detected in pull-down experiments. Weak interactions are indicated by a star. ^b full-length

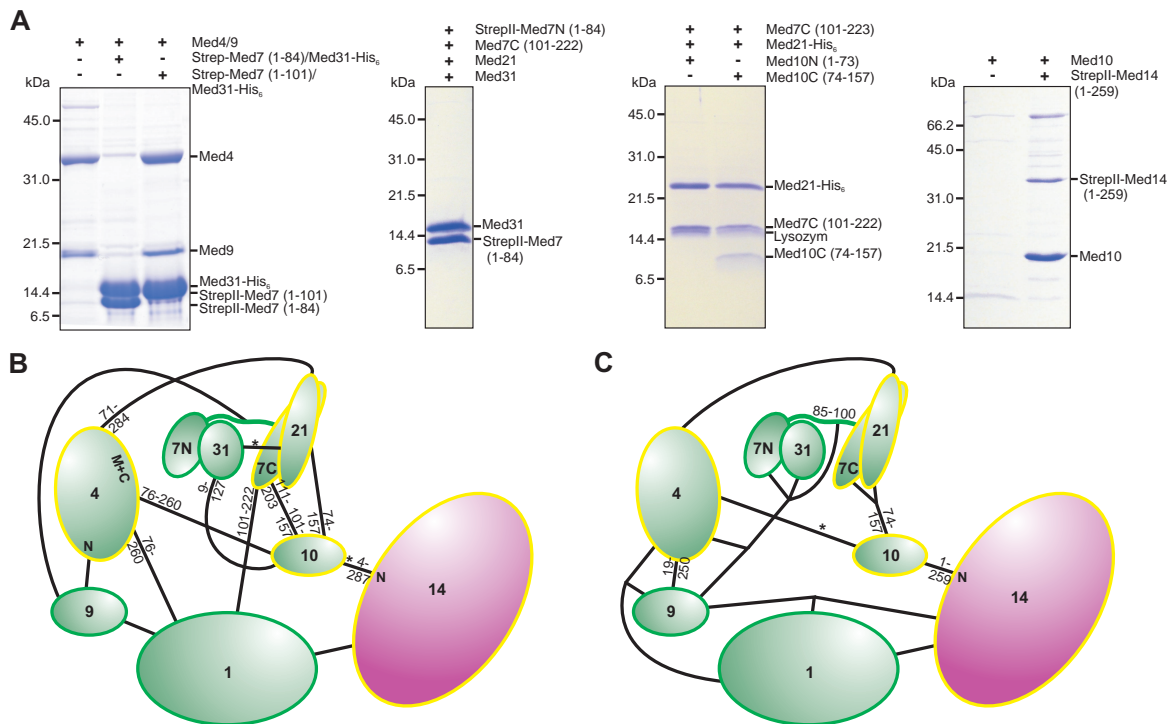


Figure 17: Intramolecular interactions within the middle module.

(A) Middle module subunits and subcomplexes were tested for interaction with other middle module subunits or subcomplexes by coexpression and subsequent copurification pull-down assays. (B) Mediator middle module interaction map based on previously published (Guglielmi et al., 2004) yeast-two-hybrid (Y2H) assays and structural data (Baumli et al., 2005, this work, see 3.1). The length of truncated subunit variants that gave interactions with its partner, are indicated closely to the molecules. Interactions based only on single Y2H clones are indicated by a star. (C) Mediator middle module interaction map based on coexpression and copurifications. The map integrates published data (Baumli et al., 2005, this work, see 3.1) with the findings depicted in Figure 12B, C, 17A and Table 17. As coexpression and copurification was required to obtain stable complexes, connections to more than one partner are indicated for some proteins. Weak interactions are indicated by a star.

3.2.9 Module shape

To investigate the overall shape of the middle module in solution we used light scattering and SAXS. Static light scattering analysis of the 6-subunit complex revealed a hydrodynamic radius of 66 Å, 34% larger than that of Med7C/21, which exists as a heterotetramer in solution (compare Table 18). SAXS analysis showed that the 6-subunit middle module was partially aggregated at the high concentrations required for the analysis (Figure 18A and Table 18). Thus we could not reliably determine the radius of gyration and could not calculate low-resolution structural models. Nevertheless, the scattering curve shows clearly that the middle module exhibits an elongated shape (compare Volkov and Svergun, 2003, Figure 1, e.g. model body 10). The Kratky-plot further indicates that the protein complex is folded and consists of a few globular areas (Figure 18B). Unfortunately, analysis of the 7-subunit middle module by SAXS was hampered by susceptibility of the Med1 subunit to degradation and difficulties in complex concentration.

To add support to the results obtained in solution, we used ion mobility (IM) MS analysis. IM-MS can provide the collisional cross section (CCS), which corresponds to an averaged

Table 18: Static light scattering (SLS) and Small-angle X-ray scattering (SAXS) measurements.

Technique	Sample	R_H^a (nm)	R_G^b (nm)	Dim. ^c (nm)	MW_D^d (kDa)	MW_T^e (kDa)	Oligomeric state	Conc. (mg/ml)
SLS	Med7C/21	4.9	-	11.1 x 3.0 x 3.0	60	32	Hetero- tetramer	1.8
SLS	Med7N/31	2.6	-	4.0 x 4.5	30	27	Hetero- dimer	1
SLS	Med4/7/9/ 10/21/31	6.6	-	-	130	125	Hetero- hexamer	1
SAXS	Med4/7/9/ 10/21/31	-	6.6	-	(607)	125	-	5

^a Hydrodynamic radius ^b Radius of gyration ^c Dimensions from X-ray structure
^d Determined molecular weight ^e Theoretical molecular weight

lateral cut through the protein (Utrecht et al., 2008). We applied IM-MS to the three recombinant Mediator middle module complexes (Figure 18C). Calculation of calibrated CCS revealed conformational flexibility in all complexes, consistent with our inability to crystallize any of these complexes and published *in silico* analysis data (Tóth-Petróczy et al., 2008). This becomes more clear even when looking at an averaged drift time analysis (Figure 18D and Figure 14C). Compared to standard proteins of similar mass (Konarev et al., 2006), the most abundant conformations for the 4- and 6-subunit complexes represented extended structures. The conformation of the complete 7-subunit middle module was, however, more compact (Figure 18C). The average calculated densities for the 4-, 6- and 7-subunit complexes were 0.48, 0.50 and 0.56 g/cm³ respectively. Thus, three different experimental methods are consistent with an elongated shape of the middle module, which is further consistent with published cryo-electron microscopic data (Cai et al., 2009; Elmlund et al., 2006; Knuesel et al., 2009).

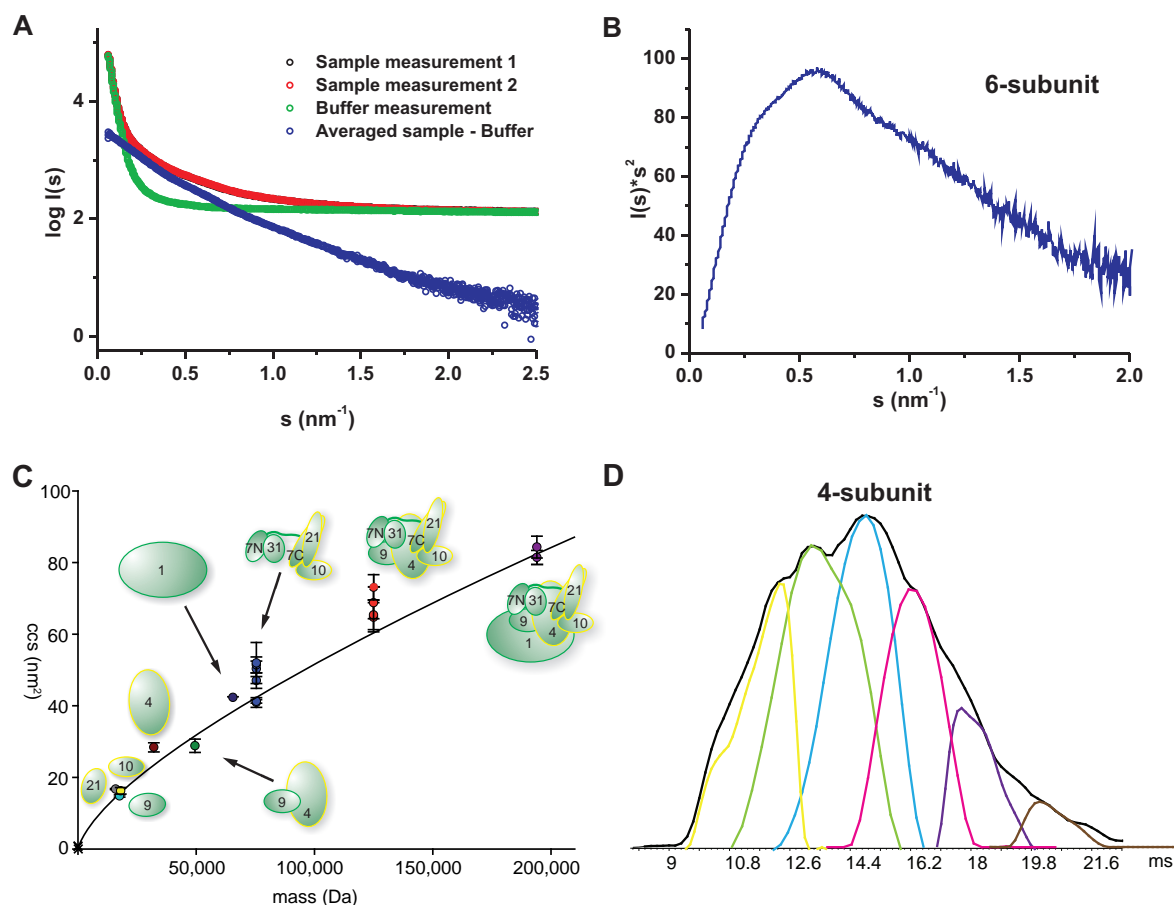


Figure 18: Shape of the middle module.

(A) The experimental SAXS curve of 6-subunit Mediator middle module indicates an elongated protein complex. I_0 signal intensity in comparison with the BSA standard measurement suggested a molecular weight of the complex far above the theoretical weight. Therefore, the Guinier radius could not be reliably determined and useful models could not be calculated. (B) The corresponding Kratky-plot shows no classical bell-shape, but is stretched towards higher scattering angles. The complex is nevertheless folded and the plot indicates a multidomain architecture with flexible linkers. (C) Ion mobility MS experiments. Plotted are the calibrated collision cross sections (CCS) of the single subunits and (sub-)complexes. The graph indicates a general trend of CCS versus mass for globular proteins (determined both experimentally (Utrecht et al., 2008) and derived from globular structures deposited in the PDB <http://www.rcsb.org>). The graph extends up to a mass of 801 kDa and a CCS of 229 nm^2 . Only the section relevant for the Mediator complexes is shown. The color coding is: grey – Med21, cyan – Med9, orange – Med10, brown – Med4, dark green – Med4/7, dark blue – Med1, blue – 4-subunit middle, red – 6-subunit middle, purple – 7-subunit middle. (D) Flexibility of the Mediator middle module. From IM-MS measurements, we generated the averaged drift time plot (in ms) for the 4-subunit Mediator middle (charge 16^+) (shown in black). Using the Drift Scope software (Waters, UK), we extracted the different conformations that contribute to the averaged drift time plot. We can detect up to six conformations that make up this charge state of the 4-subunit Mediator middle in the gas phase, thereby reflecting the flexibility of the Mediator middle module.

4 Discussion

Understanding the mechanisms that eukaryotes use to regulate gene transcription through Mediator on a molecular level requires a detailed analysis of its four multisubunit modules, for which only a few partial substructures are available. Previous work in the laboratory by Sonja Baumli focusing on the Mediator middle module from *Saccharomyces cerevisiae* was continued and both structural and functional information on this module and its subparts obtained. Structural investigations require large and very pure amounts of protein, which can only be achieved by recombinant expression, or by recombinant coexpression which is generally advantageous or even required for protein complexes. Recombinant expression and purification of the Mediator middle module enabled here the detailed investigation of the middle module topology and its functional substructures. The established coexpression strategies may also be valuable for the preparation of other large and flexible multiprotein complexes by coexpression in *E. coli*.

4.1 The Med7N/31 submodule

First, our limited proteolysis experiments of the trimeric Med7/21/31 subcomplex led to the identification and characterization of a functional substructure of the middle module – the Med7N/31 submodule. Med31 was initially called Soh1 as it was found in a *S. cerevisiae* screen for suppressors of a hyper-recombination phenotype caused by Hpr1 deletion (Fan and Klein, 1994), and was later described as a Mediator subunit (Gu et al., 1999; Boube et al., 2000; Park et al., 2001a; Gu et al., 2002; Guglielmi et al., 2004; Linder and Gustafsson, 2004); Park et al, 2001). Med31 is one of the best conserved Mediator subunits and shows 28% sequence identity between yeast and human, but is not essential for yeast viability (Fan and Klein, 1994). Med31 is required for telomere maintenance (Askree et al., 2004), DNA repair (Fan and Klein, 1994), meiotic DNA processing (Jordan et al., 2007) and transposition (Nyswaner et al., 2008). The Med31 orthologue in *Drosophila* is a maternal-effect gene for segment specification during early *Drosophila* embryogenesis (Bosveld et al., 2008).

Here, we describe the Med31 atomic structure, its interaction with the Med7N domain, and the functional analysis *in vitro* and *in vivo* on the transcriptome level of the highly conserved Med7N/31 subcomplex. The Med7N/31 structure exhibits a novel fold, and together with the previously determined Med7C/21 structure unravels the highly unusual overall structure of Med7 (Figure 19). Med7N forms a non-essential tether for the compact peripheral Med31 subunit and is flexibly linked to Med7C, which forms an extended essential heterodimer with Med21 (Figure 19). Other Mediator subunits may also show such an extended, modular, and astonishing architecture. Intriguing features of the Med7N/31 structure are the two con-

served proline-rich stretches of Med7N that bind Med31. The similarity of these stretches to the proline-rich CTD of RNA Pol II suggests that the CTD may dynamically replace one or both stretches and bind Med31. The Med7N stretches may also detach from Med31 and bind factors that comprise a domain that recognizes polyproline peptides, such as WW, SH3, and GYF domains (Macias et al., 2002; Hesselberth et al., 2006; Kofler and Freund, 2006), or a proline isomerase. pPS1 contains the PPxY motif that can be bound by certain WW domains (Espanel and Sudol, 2001). Finally, proline-rich activators could replace one or both Med7N stretches and bind to Med31. However, individual insolubility of recombinant Med31 and Med7N hampered a biochemical investigation of these models. The high conservation of Med31 may reflect the putative CTD interaction, but may also stem from an alternative interaction with the polymerase or other factors. A subsequent structure-based functional analysis investigated the cooperation of Med7N/31 with TFIIS during activated transcription, and established the subcomplex as a predominantly positive gene-regulatory submodule at the periphery of the essential middle module of Mediator. A combination of transcriptome analysis and phenotyping assays revealed the processes that are affected by a lack of intact Med7N/31, including methionine metabolism and siderophore transporter synthesis. Med7N/31 also has a role in the regulation of conjugation genes, similar to the head submodule Med8C/18/20, and in contrast to the Mediator tail subunits Med2 and Med3. Distinct phenotypes and mRNA levels were observed for mutants that do not contain an intact Med7N/31 submodule, consistent with the idea that there are gene-specific and overlapping functions associated with different Mediator submodules. The observed overlaps in phenotyping assays and in the GO analysis of differential transcriptome data show that metabolic sensing, stress response, and certain amino-acid biosynthesis pathways are generally affected by deletion of different Mediator submodules. At present it remains difficult to decipher the *cis*-elements and *trans*-acting factors that underlie the observed changes in gene expression. However, we provide evidence that Met28 and Msn4 are important transcription factors involved in Med7N/31-mediated gene regulation. Msn4 is downregulated upon Med7N/31 deletion (this study) and functions in stress response (Gasch et al., 2000; Causton et al., 2001). Met28 is downregulated upon Med7N/31 deletion but upregulated upon Med2/3 deletion, explaining the observed down- and upregulations in methionine and cysteine metabolism, respectively, as a secondary effect. Differently expressed genes were also often found to contain binding sites for Yap family transcription factors that regulate stress response (Fernandes et al., 1997). In the future, factors may be identified that use Med7N/31 as a target for gene regulation.

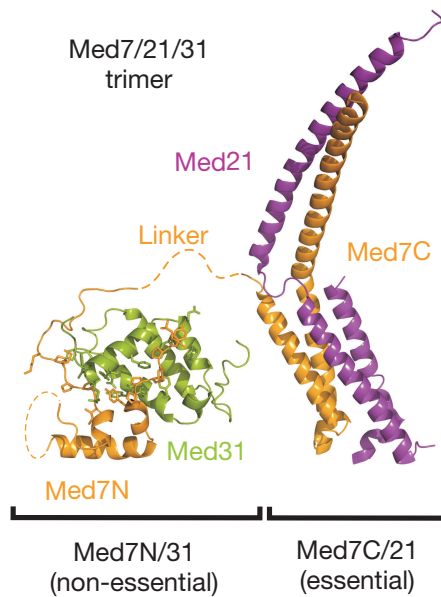


Figure 19: Structural overview of the trimeric Med7/21/31 complex architecture.

Structures of the non-essential Med7N/31 submodule (this work) and the previously described essential Med7C/21 subcomplex are drawn to scale.

4.2 Mediator middle module topology

We developed and describe protocols for obtaining pure endogenous and recombinant complete Mediator middle module from *Saccharomyces cerevisiae* consisting of seven subunits, Med1, 4, 7, 9, 10, 21, and 31. We confirmed the subunit composition of the complete endogenous *S. cerevisiae* middle module, after its purification from a *med19Δ* yeast strain. We have used the defined middle complex preparations and its 4- and 6-subunit subcomplexes in various biophysical assays to determine the subunit stoichiometry, subunit interactions, and the elongated shape of the complex. Crystallization of other or larger middle module complexes than the Med7N/31 or Med7C/21 was not successful, but likely explanations for this observation became evident from our studies of the middle module topology. We found by native MS analysis, that in our preparations all subunits are present as single copies, excluding over- or understoichiometry. Light and X-ray scattering as well as IM-MS suggest that the 6-subunit middle module has an elongated shape. Similarly, as shown for the Med7C/21 subcomplex, this indicated an increased flexibility which is generally known to interfere with crystallization. Interestingly, our later analysis found that the complete 7-subunit middle module is more compact. A third feature known to interfere with crystallization are exposed, flexible regions. Such regions were identified within the middle module (except for the Med1 subunit) and truncated middle module variants tested in crystallization screening, especially for the 4-subunit middle module. However, detailed analysis of the subunit-subunit interaction network within the middle module revealed that Med7 and Med4 subunits interact via the linker between Med7N and Med7C. Our interaction data validate most subunit contacts mapped by yeast-two hybrid analysis (Guglielmi et al., 2004) but also identify a few false positives and reveal new details about subunit interactions. Our proteolysis, interaction experiments, and MS data all suggest that Med7 and Med4 serve as a binding platform to form three stable heterodimers, Med7N/31, Med7C/21 and Med4/9. Thus, crystallization of a 4-subunit middle module complex comprising only Med7/10/21/31 seems improbable. The Med4/9 subcomplex was obtained in large and pure quantities. Flexible regions at the Med4

C-terminus and a large loop within the Med9 N-terminal part were removed, but even after these truncations no crystals were obtained. Interestingly, Med1 and Med10 both bridge between the heterodimers Med7C/21 and Med4/9, suggesting that the 6-subunit or 7-subunit middle module preparation could be more suitable for crystallization. This would also reduce exposed hydrophobic surfaces compared to only partial middle module complexes. However, as we did not obtain any crystals of these complexes either, we believe that intrinsic flexibilities have thus far impeded crystallization of the middle module. Nevertheless, as the 7-subunit middle module is generally more compact, future crystallization trials could focus on this complex.

In order to understand how Mediator integrates regulatory signals and how it enables activated transcription, we aimed at establishing an assay by which the activity of the essential Mediator middle module and its parts could be elucidated. Despite extensive efforts, we were however unable to test the functionality of the middle module *in vitro*. Although initial steps have been taken, establishing such an *in vitro* assay for middle module-dependent activated transcription will thus remain a future goal. Analysis of mutations *in vivo* using yeast complementation assays turned out to be fruitful in general as shown for Med7 and Med4. However, such complementation studies with Med14 and Med10 showed that this assay is not universally suited. In this respect Med14 (1-745) could not complement in a *med14* shuffle strain with a BY strain background although equivalent to the *med14* Δ 2 strain which is viable and in which the complete Mediator tail module is lost (Li et al., 1995). Similarly, Med10 (1-123) did not complement in a *med10* BY background shuffle strain, which was equivalent of the *EWE5* strain (*nut2-1002*) (Singh et al., 2006). It is possible, that the domain boundaries for viability need to be refined for the BY background. Additionally, the frame-shift mutation in the *med14* Δ 2 strain may have some stabilizing effect. On the other hand, we sporulated the *med10* shuffle strain, which had been transformed with a Med10 (1-123) encoding plasmid and dissected tetrads. Viability statistics of the resulting spores showed that Med10 (1-123) could complement in this assay, indicating that the previous assay observation more likely resulted from too harsh conditions through 5-FOA selection. Thus, future work will be required to further elucidate the activity of the essential Mediator middle module and its parts both *in vitro* and *in vivo*.

5 Conclusion and Outlook

During this thesis protocols were established for obtaining pure endogenous and recombinant complete Mediator middle module from *Saccharomyces cerevisiae*. Extension of previous structural and functional analyses of Mediator subcomplexes (Baumli et al., 2005; Hoepfner et al., 2005; Larivière et al., 2006, 2008) led to the identification, structure, and *in vitro* and *in vivo* functional analyses of the highly conserved Med7N/31 subcomplex which is formed by the N-terminal region of Med7 (Med7N) and Med31. A combination of biochemistry, X-ray crystallography, yeast phenotyping, and transcriptome analysis established Med7N/31 as a structurally and functionally distinct submodule that is required for activated transcription. Furthermore, the middle module topology was investigated in detail revealing many physical properties including stoichiometry, subunit-subunit interactions and molecular shape. By applying a number of experimental techniques such as mass spectroscopy, limited proteolysis, coexpression & pull-down assays, light scattering and small angle X-ray scattering analyses, a new model for the middle module topology was put forward and its high intrinsic flexibility revealed experimentally for the first time.

Future goals include the following:

1. Crystallization and structure solution of larger middle module complexes.
Crystallization trials could focus on the complete 7-subunit middle module as it was found to be more compact than for example 4- or 6-subunit middle module complexes. A drawback with this complex, however, is the stability of Med1. Exposed regions in this subunit could be identified as well using approaches described in this work and stability be increased upon removal of these regions. The results obtained by the topology investigation could then guide further experiments and crystallization may become feasible. However, it may be required to first obtain additional lower resolution structural information of the middle module. While cryo-EM microscopy was not possible mainly due to the limited size of the middle module, small-angle scattering analysis should be highly informative if the described obstacles can be overcome. Especially, comparison of the different recombinant middle module complexes may give interesting insights.
2. Extension of the complete middle module towards larger recombinant assemblies.
Extension of the recombinant middle module towards the tail module seems possible as it was found that the Med10 N-terminus is flexible and exposed, but likely involved in binding Med14. Apparently due to its large size, recombinant expression of Med14 in *E. coli* was only possible with a shortened variant comprising residues 1 to 259. It has been suggested that Med14 could be bipartite middle and tail subunit that bridges the tail, middle and head modules (Baidoobonso et al., 2007). Therefore future investiga-

tion could focus on this subunit, possibly after recombinant expression using another expression system like Baculovirus. Strikingly, we did not yet succeed in assembling recombinant middle and head module complexes, which might also enable cryo-EM analysis of recombinant complexes.

3. Establishing an *in vitro*, middle module-dependent, activated transcription assay to evaluate functionality of the middle module or variants.

Establishing such an assay was mainly hampered by difficulties in obtaining pure, middle-less Mediator complex. To overcome this problem, the purification strategy must be improved. For instance high-salt washing steps could be suited as Mediator complex is known to tolerate even some urea washing (Kang et al., 2001; Baidoobonso et al., 2007). Alternatively, additional purification steps using other principles such as ion exchange or heparin affinity purification may be required. Once this assay is successfully established for the complete middle module, partial assemblies as well as mutants such as the EWE mutations (Singh et al., 2006) could be tested in transcription activation.

4. Analysis of interactions of the middle module with activators, cofactors and the general transcription machinery.

A number of interactions of the middle module with external factors has been suggested (compare BioGrid database), but in most cases it needs to be still proven that these interactions are direct. For instance we did not find a direct interaction of the middle module with Gal4-VP16 by bandshift analysis or with TFIIS by pull-down assays (this study) or with TFIIB by bandshift analysis (Baumli (2005)), nor stable assembly with RNA Pol II. In the latter case, triggering CTD binding, possibly as suggested via our model with Med31, might be a prerequisite, but interactions required for PIC assembly may be cooperative in nature and therefore difficult to detect. Immobilized template assays combined with both nuclear extracts and purified factors may resolve these issues and clarify the order of events.

5. Identification of regulatory factors that govern gene regulation through Mediator submodules and modeling of regulatory networks.

To reveal the underlying regulatory networks of gene regulation and how information is transmitted through the Mediator complex will remain a long term goal. On the submodule level, our analyses revealed already both specific and overlapping functional requirements. Gene expression information about the function of essential Mediator subunits or submodules can be achieved through analysis of point mutation strains such as the EWE strains. *In silico* correlation allows in general identification of regulatory factors as shown for the Med7N/31 submodule here. But to dissect direct and indirect regulations as well as reveal the hierarchy of the regulatory factors, is a challenge, and may only be overcome by extensive analysis of those regulatory factors and its targets both on single promoter level and at the genome-wide scale.

Bibliography

- P. D. Adams, R. W. Grosse-Kunstleve, L. W. Hung, T. R. Ioerger, A. J. McCoy, N. W. Moriarty, R. J. Read, J. C. Sacchettini, N. K. Sauter, and T. C. Terwilliger. PHENIX: building new software for automated crystallographic structure determination. *Acta Crystallogr D Biol Crystallogr*, 58(Pt 11):1948–1954, Nov 2002.
- A. A. Adzhubei and M. J. Sternberg. Left-handed polyproline II helices commonly occur in globular proteins. *J Mol Biol*, 229(2):472–93, 1993.
- A. Alexa, J. Rahnenfuhrer, and T. Lengauer. Improved scoring of functional groups from gene expression data by decorrelating GO graph structure. *Bioinformatics*, 22(13):1600–7, 2006.
- J.-C. Andrau, L. van de Pasch, P. Lijnzaad, T. Bijma, M. G. Koerkamp, J. van de Peppel, M. Werner, and F. C. P. Holstege. Genome-wide location of the coactivator mediator: Binding without activation and transient Cdk8 interaction on DNA. *Mol Cell*, 22(2):179–192, Apr 2006.
- S. H. Askree, T. Yehuda, S. Smolikov, R. Gurevich, J. Hawk, C. Coker, A. Krauskopf, M. Kupiec, and M. J. McEachern. A genome-wide screen for *Saccharomyces cerevisiae* deletion mutants that affect telomere length. *Proc Natl Acad Sci U S A*, 101(23):8658–8663, Jun 2004.
- F. J. Asturias, Y. W. Jiang, L. C. Myers, C. M. Gustafsson, and R. D. Kornberg. Conserved structures of mediator and RNA polymerase II holoenzyme. *Science*, 283(5404):985–987, Feb 1999.
- D. T. Auble. The dynamic personality of TATA-binding protein. *Trends Biochem Sci*, 34(2):49–52, Feb 2009.
- H. J. Baek, Y. K. Kang, and R. G. Roeder. Human Mediator enhances basal transcription by facilitating recruitment of transcription factor IIB during preinitiation complex assembly. *J Biol Chem*, 281(22):15172–15181, Jun 2006.
- S. M. Baidoobonso, B. W. Guidi, and L. C. Myers. Med19(Rox3) regulates Intermodule interactions in the *Saccharomyces cerevisiae* mediator complex. *J Biol Chem*, 282(8):5551–5559, Feb 2007.
- A. D. Basehoar, S. J. Zanton, and B. F. Pugh. Identification and distinct regulation of yeast TATA box-containing genes. *Cell*, 116(5):699–709, Mar 2004.
- A. Baudin, O. Ozier-Kalogeropoulos, A. Denouel, F. Lacroute, and C. Cullin. A simple and efficient method for direct gene deletion in *Saccharomyces cerevisiae*. *Nucleic Acids Res*, 21(14):3329–3330, Jul 1993.

-
- S. Baumli. *Structure of the MED7/MED21 heterodimer and reconstitution of a recombinant Mediator middle module complex*. PhD thesis, University of Munich, 2005.
- S. Baumli, S. Hoepfner, and P. Cramer. A conserved mediator hinge revealed in the structure of the MED7.MED21 (Med7.Srb7) heterodimer. *J Biol Chem*, 280(18):18171–18178, May 2005.
- S. Bäckström, N. Elfving, R. Nilsson, G. Wingsle, and S. Björklund. Purification of a Plant Mediator from *Arabidopsis thaliana* Identifies PFT1 as the Med25 Subunit. *Mol Cell*, 26(5):717–729, Jun 2007.
- D. Bentley. The mRNA assembly line: transcription and processing machines in the same factory. *Curr Opin Cell Biol*, 14(3):336–342, Jun 2002.
- S. R. Bhaumik, T. Raha, D. P. Aiello, and M. R. Green. In vivo target of a transcriptional activator revealed by fluorescence resonance energy transfer. *Genes Dev*, 18(3):333–343, Feb 2004.
- L. T. Bhoite, Y. Yu, and D. J. Stillman. The Swi5 activator recruits the Mediator complex to the HO promoter without RNA polymerase II. *Genes Dev*, 15(18):2457–2469, Sep 2001.
- R. Biddick and E. T. Young. Yeast mediator and its role in transcriptional regulation. *C R Biol*, 328(9):773–782, Sep 2005.
- R. Biddick and E. T. Young. The disorderly study of ordered recruitment. *Yeast*, 26(4):205–220, Apr 2009.
- A. Biegert, C. Mayer, M. Remmert, J. Söding, and A. N. Lupas. The MPI Bioinformatics Toolkit for protein sequence analysis. *Nucleic Acids Res*, 34(Web Server issue):W335–W339, Jul 2006. URL <http://toolkit.lmb.uni-muenchen.de/>.
- J. C. Black, J. E. Choi, S. R. Lombardo, and M. Carey. A mechanism for coordinating chromatin modification and preinitiation complex assembly. *Mol Cell*, 23(6):809–818, Sep 2006.
- E. Blazek, G. Mittler, and M. Meisterernst. The mediator of RNA polymerase II. *Chromosoma*, 113(8):399–408, Mar 2005.
- T. Borggreffe, R. Davis, H. Erdjument-Bromage, P. Tempst, and R. D. Kornberg. A complex of the Srb8, -9, -10, and -11 transcriptional regulatory proteins from yeast. *J Biol Chem*, 277(46):44202–44207, Nov 2002.
- F. Bosveld, S. van Hoek, and O. C. M. Sibon. Establishment of cell fate during early *Drosophila* embryogenesis requires transcriptional Mediator subunit dMED31. *Dev Biol*, 313(2):802–813, Jan 2008.
- M. Boube, C. Faucher, L. Joulia, D. L. Cribbs, and H. M. Bourbon. *Drosophila* homologs of transcriptional mediator complex subunits are required for adult cell and segment identity specification. *Genes Dev*, 14(22):2906–2917, Nov 2000.
- M. Boube, L. Joulia, D. L. Cribbs, and H.-M. Bourbon. Evidence for a mediator of RNA polymerase II transcriptional regulation conserved from yeast to man. *Cell*, 110(2):143–151, Jul 2002.
-

- H.-M. Bourbon. Comparative genomics supports a deep evolutionary origin for the large, four-module transcriptional mediator complex. *Nucleic Acids Res*, 36(12):3993–4008, Jul 2008.
- H.-M. Bourbon, A. Aguilera, A. Z. Ansari, F. J. Asturias, A. J. Berk, S. Bjorklund, T. K. Blackwell, T. Borggreffe, M. Carey, M. Carlson, J. W. Conaway, R. C. Conaway, S. W. Emmons, J. D. Fondell, L. P. Freedman, T. Fukasawa, C. M. Gustafsson, M. Han, X. He, P. K. Herman, A. G. Hinnebusch, S. Holmberg, F. C. Holstege, J. A. Jaehning, Y.-J. Kim, L. Kuras, A. Leutz, J. T. Lis, M. Meisterernest, A. M. Naar, K. Nasmyth, J. D. Parvin, M. Ptashne, D. Reinberg, H. Ronne, I. Sadowski, H. Sakurai, M. Sipiczki, P. W. Sternberg, D. J. Stillman, R. Strich, K. Struhl, J. Q. Svejstrup, S. Tuck, F. Winston, R. G. Roeder, and R. D. Kornberg. A unified nomenclature for protein subunits of mediator complexes linking transcriptional regulators to RNA polymerase II. *Mol Cell*, 14(5):553–557, Jun 2004.
- M. M. Bradford. A rapid and sensitive method for the quantitation of microgram quantities of protein utilizing the principle of protein-dye binding. *Anal Biochem*, 72:248–254, May 1976.
- B. J. Breitkreutz, C. Stark, and M. Tyers. Osprey: a network visualization system. *Genome Biol*, 4(3):R22, 2003.
- A. T. Brünger, P. D. Adams, G. M. Clore, W. L. DeLano, P. Gros, R. W. Grosse-Kunstleve, J. S. Jiang, J. Kuszewski, M. Nilges, N. S. Pannu, R. J. Read, L. M. Rice, T. Simonson, and G. L. Warren. Crystallography & NMR system: A new software suite for macromolecular structure determination. *Acta Crystallogr D Biol Crystallogr*, 54(Pt 5):905–921, Sep 1998.
- G. O. Bryant and M. Ptashne. Independent recruitment in vivo by Gal4 of two complexes required for transcription. *Mol Cell*, 11(5):1301–1309, May 2003.
- N. Budisa, B. Steipe, P. Demange, C. Eckerskorn, J. Kellermann, and R. Huber. High-level biosynthetic substitution of methionine in proteins by its analogs 2-aminohexanoic acid, selenomethionine, telluromethionine and ethionine in *Escherichia coli*. *Eur J Biochem*, 230(2):788–96, 1995.
- J. Béve, G.-Z. Hu, L. C. Myers, D. Balciunas, O. Werngren, K. Hultenby, R. Wibom, H. Ronne, and C. M. Gustafsson. The structural and functional role of Med5 in the yeast Mediator tail module. *J Biol Chem*, 280(50):41366–41372, Dec 2005.
- G. Cai, T. Imasaki, Y. Takagi, and F. J. Asturias. Mediator structural conservation and implications for the regulation mechanism. *Structure*, 17(4):559–567, Apr 2009.
- B. R. Cairns. The logic of chromatin architecture and remodelling at promoters. *Nature*, 461(7261):193–198, Sep 2009.
- E. A. Campbell, L. F. Westblade, and S. A. Darst. Regulation of bacterial RNA polymerase sigma factor activity: a structural perspective. *Curr Opin Microbiol*, 11(2):121–127, Apr 2008.

- G. T. Cantin, J. L. Stevens, and A. J. Berk. Activation domain-mediator interactions promote transcription preinitiation complex assembly on promoter DNA. *Proc Natl Acad Sci U S A*, 100(21):12003–12008, Oct 2003.
- M. Carey, J. Leatherwood, and M. Ptashne. A potent GAL4 derivative activates transcription at a distance in vitro. *Science*, 247(4943):710–712, Feb 1990.
- H. C. Causton, B. Ren, S. S. Koh, C. T. Harbison, E. Kanin, E. G. Jennings, T. I. Lee, H. L. True, E. S. Lander, and R. A. Young. Remodeling of yeast genome expression in response to environmental changes. *Mol Biol Cell*, 12(2):323–37, 2001.
- J. X. Cheng, M. Gandolfi, and M. Ptashne. Activation of the Gal1 gene of yeast by pairs of 'non-classical' activators. *Curr Biol*, 14(18):1675–1679, Sep 2004.
- Y. Chi, M. J. Huddleston, X. Zhang, R. A. Young, R. S. Annan, S. A. Carr, and R. J. Deshaies. Negative regulation of Gcn4 and Msn2 transcription factors by Srb10 cyclin-dependent kinase. *Genes Dev*, 15(9):1078–1092, May 2001.
- C. R. Clapier and B. R. Cairns. The biology of chromatin remodeling complexes. *Annu Rev Biochem*, 78:273–304, 2009.
- A. B. Clark, C. C. Dykstra, and A. Sugino. Isolation, DNA sequence, and regulation of a *Saccharomyces cerevisiae* gene that encodes DNA strand transfer protein alpha. *Mol Cell Biol*, 11(5):2576–82, 1991.
- S. R. Collins, K. M. Miller, N. L. Maas, A. Roguev, J. Fillingham, C. S. Chu, M. Schuldiner, M. Gebbia, J. Recht, M. Shales, H. Ding, H. Xu, J. Han, K. Ingvarsdottir, B. Cheng, B. Andrews, C. Boone, S. L. Berger, P. Hieter, Z. Zhang, G. W. Brown, C. J. Ingles, A. Emili, C. D. Allis, D. P. Toczyski, J. S. Weissman, J. F. Greenblatt, and N. J. Krogan. Functional dissection of protein complexes involved in yeast chromosome biology using a genetic interaction map. *Nature*, 446(7137):806–810, Apr 2007.
- M. P. Cosma, S. Panizza, and K. Nasmyth. Cdk1 triggers association of RNA polymerase to cell cycle promoters only after recruitment of the mediator by SBF. *Mol Cell*, 7(6):1213–1220, Jun 2001.
- P. Cramer. Multisubunit RNA polymerases. *Curr Opin Struct Biol*, 12(1):89–97, Feb 2002.
- P. Cramer, K.-J. Armache, S. Baumli, S. Benkert, F. Brueckner, C. Buchen, G. E. Damsma, S. Dengl, S. R. Geiger, A. J. Jasiak, A. Jawhari, S. Jennebach, T. Kamenski, H. Kettenberger, C.-D. Kuhn, E. Lehmann, K. Leike, J. F. Sydow, and A. Vannini. Structure of eukaryotic RNA polymerases. *Annu Rev Biophys*, 37:337–352, 2008.
- J. A. Davis, Y. Takagi, R. D. Kornberg, and F. A. Asturias. Structure of the yeast RNA polymerase II holoenzyme: Mediator conformation and polymerase interaction. *Mol Cell*, 10(2):409–415, Aug 2002.
- W. L. DeLano. The PyMOL Molecular Graphics System., 2002. URL <http://www.pymol.org/>.
- S. Dengl and P. Cramer. Torpedo nuclease Rat1 is insufficient to terminate RNA polymerase II in vitro. *J Biol Chem*, 284(32):21270–21279, Aug 2009.

- G. Dieci, G. Fiorino, M. Castelnuovo, M. Teichmann, and A. Pagano. The expanding RNA polymerase III transcriptome. *Trends Genet*, 23(12):614–622, Dec 2007.
- R. C. Edgar. MUSCLE: multiple sequence alignment with high accuracy and high throughput. *Nucleic Acids Res*, 32(5):1792–7, 2004.
- S. Egloff and S. Murphy. Cracking the RNA polymerase II CTD code. *Trends Genet*, 24(6):280–288, Jun 2008.
- S. Egloff, D. O’Reilly, R. D. Chapman, A. Taylor, K. Tanzhaus, L. Pitts, D. Eick, and S. Murphy. Serine-7 of the RNA polymerase II CTD is specifically required for snRNA gene expression. *Science*, 318(5857):1777–1779, Dec 2007.
- H. Elmlund, V. Baraznenok, M. Lindahl, C. O. Samuelsen, P. J. B. Koeck, S. Holmberg, H. Hebert, and C. M. Gustafsson. The cyclin-dependent kinase 8 module sterically blocks Mediator interactions with RNA polymerase II. *Proc Natl Acad Sci U S A*, 103(43):15788–15793, Oct 2006.
- P. Emsley and K. Cowtan. Coot: model-building tools for molecular graphics. *Acta Crystallogr D Biol Crystallogr*, 60(Pt 12 Pt 1):2126–2132, Dec 2004.
- C. Esnault, Y. Ghavi-Helm, S. Brun, J. Soutourina, N. V. Berkum, C. Boschiero, F. Holstege, and M. Werner. Mediator-dependent recruitment of TFIID modules in preinitiation complex. *Mol Cell*, 31(3):337–346, Aug 2008.
- X. Espanel and M. Sudol. Yes-associated protein and p53-binding protein-2 interact through their WW and SH3 domains. *J Biol Chem*, 276(17):14514–23, 2001.
- H. Y. Fan and H. L. Klein. Characterization of mutations that suppress the temperature-sensitive growth of the hpr1 delta mutant of *Saccharomyces cerevisiae*. *Genetics*, 137(4):945–956, Aug 1994.
- H. Y. Fan, K. K. Cheng, and H. L. Klein. Mutations in the RNA polymerase II transcription machinery suppress the hyperrecombination mutant hpr1 delta of *Saccharomyces cerevisiae*. *Genetics*, 142(3):749–759, Mar 1996.
- X. Fan, D. M. Chou, and K. Struhl. Activator-specific recruitment of Mediator in vivo. *Nat Struct Mol Biol*, 13(2):117–120, Feb 2006.
- L. Fernandes, C. Rodrigues-Pousada, and K. Struhl. Yap, a novel family of eight bZIP proteins in *Saccharomyces cerevisiae* with distinct biological functions. *Mol Cell Biol*, 17(12):6982–93, 1997.
- J. Fishburn, N. Mohibullah, and S. Hahn. Function of a eukaryotic transcription activator during the transcription cycle. *Mol Cell*, 18(3):369–378, Apr 2005.
- P. M. Flanagan, R. J. Kelleher, M. H. Sayre, H. Tschochner, and R. D. Kornberg. A mediator required for activation of RNA polymerase II transcription in vitro. *Nature*, 350(6317):436–438, Apr 1991.
- J. D. Fondell, H. Ge, and R. G. Roeder. Ligand induction of a transcriptionally active thyroid hormone receptor coactivator complex. *Proc Natl Acad Sci U S A*, 93(16):8329–8333, Aug 1996.

- N. J. Fuda, M. B. Ardehali, and J. T. Lis. Defining mechanisms that regulate RNA polymerase II transcription in vivo. *Nature*, 461(7261):186–192, Sep 2009.
- C. Gao, L. Wang, E. Milgrom, and W.-C. W. Shen. On the mechanism of constitutive Pdr1 activator-mediated PDR5 transcription in *Saccharomyces cerevisiae*: evidence for enhanced recruitment of coactivators and altered nucleosome structures. *J Biol Chem*, 279(41):42677–42686, Oct 2004.
- A. P. Gasch, P. T. Spellman, C. M. Kao, O. Carmel-Harel, M. B. Eisen, G. Storz, D. Botstein, and P. O. Brown. Genomic expression programs in the response of yeast cells to environmental changes. *Mol Biol Cell*, 11(12):4241–57, 2000.
- E. Gasteiger, C. Hoogland, A. Gattiker, S. Duvaud, M. Wilkins, R. Appel, and A. Bairoch. *The Proteomics Protocols Handbook*, chapter Protein Identification and Analysis Tools on the ExPASy Server, pages 571–607. Humana Press, 2005. URL <http://www.expasy.ch/tools/protparam.html>.
- R. C. Gentleman, V. J. Carey, D. M. Bates, B. Bolstad, M. Dettling, S. Dudoit, B. Ellis, L. Gautier, Y. Ge, J. Gentry, K. Hornik, T. Hothorn, W. Huber, S. Iacus, R. Irizarry, F. Leisch, C. Li, M. Maechler, A. J. Rossini, G. Sawitzki, C. Smith, G. Smyth, L. Tierney, J. Y. H. Yang, and J. Zhang. Bioconductor: Open software development for computational biology and bioinformatics. *Genome Biology*, 5:R80, 2004.
- G. Gill and M. Ptashne. Negative effect of the transcriptional activator GAL4. *Nature*, 334(6184):721–724, Aug 1988.
- P. Gouet, E. Courcelle, D. I. Stuart, and F. Metz. ESPript: analysis of multiple sequence alignments in PostScript. *Bioinformatics*, 15(4):305–8, 1999.
- C. K. Govind, S. Yoon, H. Qiu, S. Govind, and A. G. Hinnebusch. Simultaneous recruitment of coactivators by Gcn4p stimulates multiple steps of transcription in vivo. *Mol Cell Biol*, 25(13):5626–5638, Jul 2005.
- I. Grummt. Regulation of mammalian ribosomal gene transcription by RNA polymerase I. *Prog Nucleic Acid Res Mol Biol*, 62:109–154, 1999.
- J.-Y. Gu, J. M. Park, E. J. Song, G. Mizuguchi, J. H. Yoon, J. Kim-Ha, K.-J. Lee, and Y.-J. Kim. Novel Mediator proteins of the small Mediator complex in *Drosophila* SL2 cells. *J Biol Chem*, 277(30):27154–27161, Jul 2002.
- W. Gu, S. Malik, M. Ito, C. X. Yuan, J. D. Fondell, X. Zhang, E. Martinez, J. Qin, and R. G. Roeder. A novel human SRB/MED-containing cofactor complex, SMCC, involved in transcription regulation. *Mol Cell*, 3(1):97–108, Jan 1999.
- B. Guglielmi, N. L. van Berkum, B. Klapholz, T. Bijma, M. Boube, C. Boschiero, H.-M. Bourbon, F. C. P. Holstege, and M. Werner. A high resolution protein interaction map of the yeast Mediator complex. *Nucleic Acids Res*, 32(18):5379–5391, 2004.
- B. Guglielmi, J. Soutourina, C. Esnault, and M. Werner. TFIIS elongation factor and Mediator act in conjunction during transcription initiation in vivo. *Proc Natl Acad Sci U S A*, 104(41):16062–16067, Oct 2007.

- S. Hahn. Structure and mechanism of the RNA polymerase II transcription machinery. *Nat Struct Mol Biol*, 11(5):394–403, May 2004.
- S. Hahn. Structural biology: New beginnings for transcription. *Nature*, 462(7271):292–293, Nov 2009.
- T. Hall. BioEdit software, Nov 2005. URL <http://www.mbio.ncsu.edu/BioEdit/bioedit.html>.
- M. Hallberg, G.-Z. Hu, S. Tronnersjö, Z. Shaikhibrahim, D. Balciunas, S. Björklund, and H. Ronne. Functional and physical interactions within the middle domain of the yeast mediator. *Mol Genet Genomics*, 276(2):197–210, Aug 2006.
- M. Hampsey. A review of phenotypes in *Saccharomyces cerevisiae*. *Yeast*, 13(12):1099–133, 1997.
- S. J. Han, J. S. Lee, J. S. Kang, and Y. J. Kim. Med9/Cse2 and Gal11 modules are required for transcriptional repression of distinct group of genes. *J Biol Chem*, 276(40):37020–37026, Oct 2001.
- A. J. Heck. Native mass spectrometry: a bridge between interactomics and structural biology. *Nat Methods*, 5(11):927–33, 2008.
- C. J. Hengartner, C. M. Thompson, J. Zhang, D. M. Chao, S. M. Liao, A. J. Koleske, S. Okamura, and R. A. Young. Association of an activator with an RNA polymerase II holoenzyme. *Genes Dev*, 9(8):897–910, Apr 1995.
- C. J. Hengartner, V. E. Myer, S. M. Liao, C. J. Wilson, S. S. Koh, and R. A. Young. Temporal regulation of RNA polymerase II by Srb10 and Kin28 cyclin-dependent kinases. *Mol Cell*, 2(1):43–53, Jul 1998.
- J. R. Hesselberth, J. P. Miller, A. Golob, J. E. Stajich, G. A. Michaud, and S. Fields. Comparative analysis of *Saccharomyces cerevisiae* WW domains and their interacting proteins. *Genome Biol*, 7(4):R30, 2006.
- S. Hoepfner, S. Baumli, and P. Cramer. Structure of the mediator subunit cyclin C and its implications for CDK8 function. *J Mol Biol*, 350(5):833–842, Jul 2005.
- L. Holm and J. Park. DaliLite workbench for protein structure comparison. *Bioinformatics*, 16(6):566–7, 2000.
- F. C. Holstege, E. G. Jennings, J. J. Wyrick, T. I. Lee, C. J. Hengartner, M. R. Green, T. R. Golub, E. S. Lander, and R. A. Young. Dissecting the regulatory circuitry of a eukaryotic genome. *Cell*, 95(5):717–728, Nov 1998.
- X. Hu, S. Malik, C. C. Negroiu, K. Hubbard, C. N. Velalar, B. Hampton, D. Grosu, J. Catalano, R. G. Roeder, and A. Gnatt. A Mediator-responsive form of metazoan RNA polymerase II. *Proc Natl Acad Sci U S A*, 103(25):9506–9511, Jun 2006.
- K. L. Husinga and B. F. Pugh. A genome-wide housekeeping role for TFIID and a highly regulated stress-related role for SAGA in *Saccharomyces cerevisiae*. *Mol Cell*, 13(4):573–585, Feb 2004.

- K. L. Huisinga and B. F. Pugh. A TATA binding protein regulatory network that governs transcription complex assembly. *Genome Biol*, 8(4):R46, 2007.
- C. Janke, M. M. Magiera, N. Rathfelder, C. Taxis, S. Reber, H. Maekawa, A. Moreno-Borchart, G. Doenges, E. Schwob, E. Schiebel, and M. Knop. A versatile toolbox for PCR-based tagging of yeast genes: new fluorescent proteins, more markers and promoter substitution cassettes. *Yeast*, 21(11):947–62, 2004.
- I. Jedidi, F. Zhang, H. Qiu, S. J. Stahl, I. Palmer, J. D. Kaufman, P. S. Nadaud, S. Mukherjee, P. T. Wingfield, C. P. Jaroniec, and A. G. Hinnebusch. Activator Gcn4 employs multiple segments of Med15/Gal11, including the KIX domain, to recruit mediator to target genes in vivo. *J Biol Chem*, 285(4):2438–2455, Jan 2010.
- C. J. Jeong, S. H. Yang, Y. Xie, L. Zhang, S. A. Johnston, and T. Kodadek. Evidence that Gal11 protein is a target of the Gal4 activation domain in the mediator. *Biochemistry*, 40(31):9421–9427, Aug 2001.
- Y. W. Jiang and D. J. Stillman. Involvement of the SIN4 global transcriptional regulator in the chromatin structure of *Saccharomyces cerevisiae*. *Mol Cell Biol*, 12(10):4503–4514, Oct 1992.
- Y. W. Jiang, P. Verschambre, H. Erdjument-Bromage, P. Tempst, J. W. Conaway, R. C. Conaway, and R. D. Kornberg. Mammalian mediator of transcriptional regulation and its possible role as an end-point of signal transduction pathways. *Proc Natl Acad Sci U S A*, 95(15):8538–8543, Jul 1998.
- D. T. Jones. Protein secondary structure prediction based on position-specific scoring matrices. *J Mol Biol*, 292(2):195–202, 1999.
- P. W. Jordan, F. Klein, and D. R. F. Leach. Novel Roles for Selected Genes in Meiotic DNA Processing. *PLoS Genet*, 3(12):e222, Dec 2007.
- W. Kabsch. Automatic processing of rotation diffraction data from crystals of initially unknown symmetry and cell constants. *Journal of Applied Crystallography*, 26(6):795–800, Dec 1993.
- J. S. Kang, S. H. Kim, M. S. Hwang, S. J. Han, Y. C. Lee, and Y. J. Kim. The structural and functional organization of the yeast mediator complex. *J Biol Chem*, 276(45):42003–42010, Nov 2001.
- R. J. Kelleher, P. M. Flanagan, and R. D. Kornberg. A novel mediator between activator proteins and the RNA polymerase II transcription apparatus. *Cell*, 61(7):1209–1215, Jun 1990.
- A. Köhler and E. Hurt. Exporting RNA from the nucleus to the cytoplasm. *Nat Rev Mol Cell Biol*, 8(10):761–773, Oct 2007.
- B. Kim, A. I. Nesvizhskii, P. G. Rani, S. Hahn, R. Aebersold, and J. A. Ranish. The transcription elongation factor TFIIS is a component of RNA polymerase II preinitiation complexes. *Proc Natl Acad Sci U S A*, 104(41):16068–16073, Oct 2007.

-
- Y. J. Kim, S. Björklund, Y. Li, M. H. Sayre, and R. D. Kornberg. A multiprotein mediator of transcriptional activation and its interaction with the C-terminal repeat domain of RNA polymerase II. *Cell*, 77(4):599–608, May 1994.
- M. T. Knuesel, K. D. Meyer, A. J. Donner, J. M. Espinosa, and D. J. Taatjes. The human CDK8 subcomplex is a histone kinase that requires Med12 for activity and can function independently of mediator. *Mol Cell Biol*, 29(3):650–661, Feb 2009.
- M. M. Kofler and C. Freund. The GYF domain. *Febs J*, 273(2):245–56, 2006.
- A. J. Koleske and R. A. Young. An RNA polymerase II holoenzyme responsive to activators. *Nature*, 368(6470):466–469, Mar 1994.
- A. J. Koleske, S. Buratowski, M. Nonet, and R. A. Young. A novel transcription factor reveals a functional link between the RNA polymerase II CTD and TFIID. *Cell*, 69(5):883–894, May 1992.
- P. V. Konarev, M. V. Petoukhov, V. V. Volkov, and D. I. Svergun. ATSAS 2.1, a program package for small-angle scattering data analysis. *Journal of Applied Crystallography*, 39(2):277–286, 2006.
- R. D. Kornberg. Eukaryotic transcriptional control. *Trends Cell Biol*, 9(12):M46–M49, Dec 1999.
- D. Kostrewa, M. E. Zeller, K.-J. Armache, M. Seizl, K. Leike, M. Thomm, and P. Cramer. RNA polymerase II-TFIIB structure and mechanism of transcription initiation. *Nature*, 462(7271):323–330, Nov 2009.
- E. Krissinel and K. Henrick. Secondary-structure matching (SSM), a new tool for fast protein structure alignment in three dimensions. *Acta Crystallogr D Biol Crystallogr*, 60(Pt 12 Pt 1):2256–68, 2004.
- N. J. Krogan, M. C. Keogh, N. Datta, C. Sawa, O. W. Ryan, H. Ding, R. A. Haw, J. Pootoolal, A. Tong, V. Canadien, D. P. Richards, X. Wu, A. Emili, T. R. Hughes, S. Buratowski, and J. F. Greenblatt. A Snf2 family ATPase complex required for recruitment of the histone H2A variant Htz1. *Mol Cell*, 12(6):1565–76, 2003.
- L. Kuras, T. Borggreffe, and R. D. Kornberg. Association of the Mediator complex with enhancers of active genes. *Proc Natl Acad Sci U S A*, 100(24):13887–13891, Nov 2003.
- U. K. Laemmli. Cleavage of structural proteins during the assembly of the head of bacteriophage T4. *Nature*, 227(259):680–685, 1970.
- L. Larivière, S. Geiger, S. Hoepfner, S. Röther, K. Strässer, and P. Cramer. Structure and TBP binding of the Mediator head subcomplex Med8-Med18-Med20. *Nat Struct Mol Biol*, 13(10):895–901, Oct 2006.
- L. Larivière, M. Seizl, S. van Wageningen, S. Röther, L. van de Pasch, H. Feldmann, K. Sträßer, S. Hahn, F. C. P. Holstege, and P. Cramer. Structure-system correlation identifies a gene regulatory Mediator submodule. *Genes Dev*, 22(7):872–877, Apr 2008.
- E. Larschan and F. Winston. The *Saccharomyces cerevisiae* Srb8-Srb11 complex functions with the SAGA complex during Gal4-activated transcription. *Mol Cell Biol*, 25(1):114–123,
-

Jan 2005.

- Y. Lee, M. Kim, J. Han, K.-H. Yeom, S. Lee, S. H. Baek, and V. N. Kim. MicroRNA genes are transcribed by RNA polymerase II. *EMBO J*, 23(20):4051–4060, Oct 2004.
- K. Lemieux and L. Gaudreau. Targeting of Swi/Snf to the yeast GAL1 UAS G requires the Mediator, TAF IIs, and RNA polymerase II. *EMBO J*, 23(20):4040–4050, Oct 2004.
- K. Lemieux, M. Laroche, and L. Gaudreau. Variant histone H2A.Z, but not the HMG proteins Nhp6a/b, is essential for the recruitment of Swi/Snf, Mediator, and SAGA to the yeast GAL1 UAS(G). *Biochem Biophys Res Commun*, 369(4):1103–1107, May 2008.
- C. Leroy, L. Cormier, and L. Kuras. Independent recruitment of mediator and SAGA by the activator Met4. *Mol Cell Biol*, 26(8):3149–3163, Apr 2006.
- B. A. Lewis and D. Reinberg. The mediator coactivator complex: functional and physical roles in transcriptional regulation. *J Cell Sci*, 116(Pt 18):3667–3675, Sep 2003.
- B. Li, M. Carey, and J. L. Workman. The role of chromatin during transcription. *Cell*, 128(4):707–719, Feb 2007.
- Y. Li, P. M. Flanagan, H. Tschochner, and R. D. Kornberg. RNA polymerase II initiation factor interactions and transcription start site selection. *Science*, 263(5148):805–807, Feb 1994.
- Y. Li, S. Bjorklund, Y. W. Jiang, Y. J. Kim, W. S. Lane, D. J. Stillman, and R. D. Kornberg. Yeast global transcriptional regulators Sin4 and Rgr1 are components of mediator complex/RNA polymerase II holoenzyme. *Proc Natl Acad Sci U S A*, 92(24):10864–10868, Nov 1995.
- S. M. Liao, J. Zhang, D. A. Jeffery, A. J. Koleske, C. M. Thompson, D. M. Chao, M. Viljoen, H. J. van Vuuren, and R. A. Young. A kinase-cyclin pair in the RNA polymerase II holoenzyme. *Nature*, 374(6518):193–196, Mar 1995.
- T. Linder and C. M. Gustafsson. The Soh1/MED31 protein is an ancient component of *Schizosaccharomyces pombe* and *Saccharomyces cerevisiae* Mediator. *J Biol Chem*, 279(47):49455–49459, Nov 2004.
- T. Linder, X. Zhu, V. Baraznenok, and C. M. Gustafsson. The classical srb4-138 mutant allele causes dissociation of yeast Mediator. *Biochem Biophys Res Commun*, 349(3):948–953, Oct 2006.
- T. Linder, N. N. Rasmussen, C. O. Samuelsen, E. Chatzidaki, V. Baraznenok, J. Beve, P. Henriksen, C. M. Gustafsson, and S. Holmberg. Two conserved modules of *Schizosaccharomyces pombe* Mediator regulate distinct cellular pathways. *Nucleic Acids Res*, 36(8):2489–2504, May 2008.
- Y. Liu, C. Kung, J. Fishburn, A. Z. Ansari, K. M. Shokat, and S. Hahn. Two cyclin-dependent kinases promote RNA polymerase II transcription and formation of the scaffold complex. *Mol Cell Biol*, 24(4):1721–1735, Feb 2004.
- Y. Lorch, J. Beve, C. M. Gustafsson, L. C. Myers, and R. D. Kornberg. Mediator-nucleosome interaction. *Mol Cell*, 6(1):197–201, Jul 2000.

- K. Lorenzen, A. Vannini, P. Cramer, and A. J. Heck. Structural biology of RNA polymerase III: mass spectrometry elucidates subcomplex architecture. *Structure*, 15(10):1237–45, 2007.
- M. J. Macias, S. Wiesner, and M. Sudol. WW and SH3 domains, two different scaffolds to recognize proline-rich ligands. *FEBS Lett*, 513(1):30–7, 2002.
- F. Malagon, A. H. Tong, B. K. Shafer, and J. N. Strathern. Genetic interactions of DST1 in *Saccharomyces cerevisiae* suggest a role of TFIIS in the initiation-elongation transition. *Genetics*, 166(3):1215–1227, Mar 2004.
- T. Max, M. Sogaard, and J. Q. Svejstrup. Hyperphosphorylation of the C-terminal repeat domain of RNA polymerase II facilitates dissociation of its complex with mediator. *J Biol Chem*, 282(19):14113–14120, May 2007.
- A. J. McCoy, R. W. Grosse-Kunstleve, P. D. Adams, M. D. Winn, L. C. Storoni, and R. J. Read. Phaser crystallographic software. *Journal of Applied Crystallography*, 40(4):658–674, 2007.
- A. R. McKay, B. T. Ruotolo, L. L. Ilag, and C. V. Robinson. Mass measurements of increased accuracy resolve heterogeneous populations of intact ribosomes. *J Am Chem Soc*, 128(35):11433–42, 2006.
- A. Meinhart, J. Blobel, and P. Cramer. An extended winged helix domain in general transcription factor E/IIIE alpha. *J Biol Chem*, 278(48):48267–48274, Nov 2003.
- A. Meinhart, T. Kamenski, S. Hoepfner, S. Baumli, and P. Cramer. A structural perspective of CTD function. *Genes Dev*, 19(12):1401–1415, Jun 2005.
- G. Mittler, E. Kremmer, H. T. Timmers, and M. Meisterernst. Novel critical role of a human Mediator complex for basal RNA polymerase II transcription. *EMBO Rep*, 2(9):808–813, Sep 2001.
- F. Müller, M. A. Demény, and L. Tora. New problems in RNA polymerase II transcription initiation: matching the diversity of core promoters with a variety of promoter recognition factors. *J Biol Chem*, 282(20):14685–14689, May 2007.
- N. Mohibullah and S. Hahn. Site-specific cross-linking of TBP in vivo and in vitro reveals a direct functional interaction with the SAGA subunit Spt3. *Genes Dev*, 22(21):2994–3006, Nov 2008.
- Z. Moqtaderi and K. Struhl. Expanding the repertoire of plasmids for PCR-mediated epitope tagging in yeast. *Yeast*, 25(4):287–292, Apr 2008.
- G. N. Murshudov, A. A. Vagin, and E. J. Dodson. Refinement of macromolecular structures by the maximum-likelihood method. *Acta Crystallogr D Biol Crystallogr*, 53(Pt 3):240–255, May 1997.
- L. C. Myers and R. D. Kornberg. Mediator of transcriptional regulation. *Annu Rev Biochem*, 69:729–749, 2000.
- L. C. Myers, C. M. Gustafsson, D. A. Bushnell, M. Lui, H. Erdjument-Bromage, P. Tempst, and R. D. Kornberg. The Med proteins of yeast and their function through the RNA

- polymerase II carboxy-terminal domain. *Genes Dev*, 12(1):45–54, Jan 1998.
- C. Nelson, S. Goto, K. Lund, W. Hung, and I. Sadowski. Srb10/Cdk8 regulates yeast filamentous growth by phosphorylating the transcription factor Ste12. *Nature*, 421(6919):187–190, Jan 2003.
- M. Nishizawa. Negative regulation of transcription by the yeast global transcription factors, Gal11 and Sin4. *Yeast*, 18(12):1099–1110, Sep 2001.
- M. L. Nonet and R. A. Young. Intragenic and extragenic suppressors of mutations in the heptapeptide repeat domain of *Saccharomyces cerevisiae* RNA polymerase II. *Genetics*, 123(4):715–724, Dec 1989.
- A. M. Näär, P. A. Beurang, S. Zhou, S. Abraham, W. Solomon, and R. Tjian. Composite coactivator ARC mediates chromatin-directed transcriptional activation. *Nature*, 398(6730):828–832, Apr 1999.
- A. M. Näär, B. D. Lemon, and R. Tjian. Transcriptional coactivator complexes. *Annu Rev Biochem*, 70:475–501, 2001.
- K. M. Nyswaner, M. A. Checkley, M. Yi, R. M. Stephens, and D. J. Garfinkel. Chromatin-associated genes protect the yeast genome from Ty1 insertional mutagenesis. *Genetics*, 178(1):197–214, Jan 2008.
- M. Oeffinger, K. E. Wei, R. Rogers, J. A. DeGrasse, B. T. Chait, J. D. Aitchison, and M. P. Rout. Comprehensive analysis of diverse ribonucleoprotein complexes. *Nat Methods*, 4(11):951–956, Nov 2007.
- M. Papamichos-Chronakis, R. S. Conlan, N. Gounalaki, T. Copf, and D. Tzamarias. Hrs1/Med3 is a Cyc8-Tup1 corepressor target in the RNA polymerase II holoenzyme. *J Biol Chem*, 275(12):8397–8403, Mar 2000.
- J. M. Park, B. S. Gim, J. M. Kim, J. H. Yoon, H. S. Kim, J. G. Kang, and Y. J. Kim. *Drosophila* Mediator complex is broadly utilized by diverse gene-specific transcription factors at different types of core promoters. *Mol Cell Biol*, 21(7):2312–2323, Apr 2001a.
- J. M. Park, J. Werner, J. M. Kim, J. T. Lis, and Y. J. Kim. Mediator, not holoenzyme, is directly recruited to the heat shock promoter by HSF upon heat shock. *Mol Cell*, 8(1):9–19, Jul 2001b.
- L. A. Pereira, M. P. Klejman, and H. T. M. Timmers. Roles for BTAF1 and Mot1p in dynamics of TATA-binding protein and regulation of RNA polymerase II transcription. *Gene*, 315:1–13, Oct 2003.
- H. P. Phatnani and A. L. Greenleaf. Phosphorylation and functions of the RNA polymerase II CTD. *Genes Dev*, 20(21):2922–2936, Nov 2006.
- S. D. Pringle, K. Giles, J. L. Wildgoose, J. P. Williams, S. E. Slade, K. Thalassinos, R. H. Bateman, M. T. Bowers, and J. H. Scrivens. An investigation of the mobility separation of some peptide and protein ions using a new hybrid quadrupole/travelling wave IMS/oa-ToF instrument. *Int J Mass Spectrom*, 261(1):1–12, 2007.

- N. J. Proudfoot, A. Furger, and M. J. Dye. Integrating mRNA processing with transcription. *Cell*, 108(4):501–512, Feb 2002.
- O. Puig, F. Casparly, G. Rigaut, B. Rutz, E. Bouveret, E. Bragado-Nilsson, M. Wilm, and B. Séraphin. The tandem affinity purification (TAP) method: a general procedure of protein complex purification. *Methods*, 24(3):218–29, 2001.
- H. Qiu, C. Hu, S. Yoon, K. Natarajan, M. J. Swanson, and A. G. Hinnebusch. An array of coactivators is required for optimal recruitment of TATA binding protein and RNA polymerase II by promoter-bound Gcn4p. *Mol Cell Biol*, 24(10):4104–4117, May 2004.
- H. Qiu, C. Hu, F. Zhang, G. J. Hwang, M. J. Swanson, C. Boonchird, and A. G. Hinnebusch. Interdependent recruitment of SAGA and Srb mediator by transcriptional activator Gcn4p. *Mol Cell Biol*, 25(9):3461–3474, May 2005.
- H. Qiu, C. Hu, and A. G. Hinnebusch. Phosphorylation of the Pol II CTD by KIN28 enhances BUR1/BUR2 recruitment and Ser2 CTD phosphorylation near promoters. *Mol Cell*, 33(6):752–762, Mar 2009.
- C. Rachez, B. D. Lemon, Z. Suldan, V. Bromleigh, M. Gamble, A. M. Näär, H. Erdjument-Bromage, P. Tempst, and L. P. Freedman. Ligand-dependent transcription activation by nuclear receptors requires the DRIP complex. *Nature*, 398(6730):824–828, Apr 1999.
- J. A. Ranish and S. Hahn. The yeast general transcription factor TFIIA is composed of two polypeptide subunits. *J Biol Chem*, 266(29):19320–19327, Oct 1991.
- J. A. Ranish, N. Yudkovsky, and S. Hahn. Intermediates in formation and activity of the RNA polymerase II preinitiation complex: holoenzyme recruitment and a postrecruitment role for the TATA box and TFIIB. *Genes Dev*, 13(1):49–63, Jan 1999.
- W. M. Reeves and S. Hahn. Targets of the Gal4 transcription activator in functional transcription complexes. *Mol Cell Biol*, 25(20):9092–9102, Oct 2005.
- G. Rigaut, A. Shevchenko, B. Rutz, M. Wilm, M. Mann, and B. Séraphin. A generic protein purification method for protein complex characterization and proteome exploration. *Nat Biotechnol*, 17(10):1030–1032, Oct 1999.
- B. T. Ruotolo, J. L. Benesch, A. M. Sandercock, S. J. Hyung, and C. V. Robinson. Ion mobility-mass spectrometry analysis of large protein complexes. *Nat Protoc*, 3(7):1139–52, 2008.
- W. Rychlik, W. J. Spencer, and R. E. Rhoads. Optimization of the annealing temperature for DNA amplification in vitro. *Nucleic Acids Res*, 18(21):6409–6412, 1990.
- S. Ryu, S. Zhou, A. G. Ladurner, and R. Tjian. The transcriptional cofactor complex CRSP is required for activity of the enhancer-binding protein Sp1. *Nature*, 397(6718):446–450, Feb 1999.
- A. I. Saeed, V. Sharov, J. White, J. Li, W. Liang, N. Bhagabati, J. Braisted, M. Klapa, T. Currier, M. Thiagarajan, A. Sturn, M. Snuffin, A. Rezantsev, D. Popov, A. Rytsov, E. Kostukovich, I. Borisovsky, Z. Liu, A. Vinsavich, V. Trush, and J. Quackenbush. TM4: a free, open-source system for microarray data management and analysis. *Biotechniques*,

- 34(2):374–8, 2003.
- J. Sambrook and D. Russell. *Molecular cloning: A laboratory Manual*, volume 1-3. Cold Spring Harbor Laboratory, 3rd edition, 2001.
- M. S. Santisteban, T. Kalashnikova, and M. M. Smith. Histone H2A.Z regulates transcription and is partially redundant with nucleosome remodeling complexes. *Cell*, 103(3):411–22, 2000.
- A. Saunders, L. J. Core, and J. T. Lis. Breaking barriers to transcription elongation. *Nat Rev Mol Cell Biol*, 7(8):557–567, Aug 2006.
- M. H. Sayre, H. Tschochner, and R. D. Kornberg. Reconstitution of transcription with five purified initiation factors and RNA polymerase II from *Saccharomyces cerevisiae*. *J Biol Chem*, 267(32):23376–23382, Nov 1992.
- T. Z. Sen, H. Cheng, A. Kloczkowski, and R. L. Jernigan. A Consensus Data Mining secondary structure prediction by combining GOR V and Fragment Database Mining. *Protein Sci*, 15(11):2499–506, 2006.
- M. Sharon and C. V. Robinson. The role of mass spectrometry in structure elucidation of dynamic protein complexes. *Annu Rev Biochem*, 76:167–93, 2007.
- P. A. Sharp. RNA splicing and genes. *JAMA*, 260(20):3035–3041, Nov 1988.
- T. W. Sikorski and S. Buratowski. The basal initiation machinery: beyond the general transcription factors. *Curr Opin Cell Biol*, 21(3):344–351, Jun 2009.
- R. J. Sims, R. Belotserkovskaya, and D. Reinberg. Elongation by RNA polymerase II: the short and long of it. *Genes Dev*, 18(20):2437–2468, Oct 2004.
- H. Singh, A. M. Erkin, S. B. Kremer, H. M. Duttweiler, D. A. Davis, J. Iqbal, R. R. Gross, and D. S. Gross. A functional module of yeast mediator that governs the dynamic range of heat-shock gene expression. *Genetics*, 172(4):2169–2184, Apr 2006.
- G. K. Smyth. Linear models and empirical bayes methods for assessing differential expression in microarray experiments. *Stat Appl Genet Mol Biol*, 3:Article3, 2004.
- J. Soeding, A. Biegert, and A. N. Lupas. The HHpred interactive server for protein homology detection and structure prediction. *Nucleic Acids Res*, 33(Web Server issue):W244–8, 2005.
- H. Spåhr, J. Bève, T. Larsson, J. Bergström, K. A. Karlsson, and C. M. Gustafsson. Purification and characterization of RNA polymerase II holoenzyme from *Schizosaccharomyces pombe*. *J Biol Chem*, 275(2):1351–1356, Jan 2000.
- C. Stark, B. J. Breitkreutz, T. Reguly, L. Boucher, A. Breitkreutz, and M. Tyers. BioGRID: a general repository for interaction datasets. *Nucleic Acids Res*, 34(Database issue):D535–9, 2006.
- P. W. Sternberg, M. J. Stern, I. Clark, and I. Herskowitz. Activation of the yeast HO gene by release from multiple negative controls. *Cell*, 48(4):567–577, Feb 1987.
- J. W. Stiller and B. D. Hall. Evolution of the RNA polymerase II C-terminal domain. *Proc Natl Acad Sci U S A*, 99(9):6091–6096, Apr 2002.

- K. F. Stringer, C. J. Ingles, and J. Greenblatt. Direct and selective binding of an acidic transcriptional activation domain to the TATA-box factor TFIID. *Nature*, 345(6278):783–786, Jun 1990.
- X. Sun, Y. Zhang, H. Cho, P. Rickert, E. Lees, W. Lane, and D. Reinberg. NAT, a human complex containing Srb polypeptides that functions as a negative regulator of activated transcription. *Mol Cell*, 2(2):213–222, Aug 1998.
- J. Q. Svejstrup, W. J. Feaver, J. LaPointe, and R. D. Kornberg. RNA polymerase transcription factor IIIH holoenzyme from yeast. *J Biol Chem*, 269(45):28044–28048, Nov 1994.
- J. Q. Svejstrup, Y. Li, J. Fellows, A. Gnatt, S. Bjorklund, and R. D. Kornberg. Evidence for a mediator cycle at the initiation of transcription. *Proc Natl Acad Sci U S A*, 94(12):6075–6078, Jun 1997.
- M. J. Swanson, H. Qiu, L. Sumibcay, A. Krueger, S. ja Kim, K. Natarajan, S. Yoon, and A. G. Hinnebusch. A multiplicity of coactivators is required by Gen4p at individual promoters in vivo. *Mol Cell Biol*, 23(8):2800–2820, Apr 2003.
- D. J. Taatjes, A. M. Näär, F. Andel, E. Nogales, and R. Tjian. Structure, function, and activator-induced conformations of the CRSP coactivator. *Science*, 295(5557):1058–1062, Feb 2002.
- D. J. Taatjes, T. Schneider-Poetsch, and R. Tjian. Distinct conformational states of nuclear receptor-bound CRSP-Med complexes. *Nat Struct Mol Biol*, 11(7):664–671, Jul 2004.
- Y. Takagi and R. D. Kornberg. Mediator as a general transcription factor. *J Biol Chem*, 281(1):80–89, Jan 2006.
- Y. Takagi, G. Calero, H. Komori, J. A. Brown, A. H. Ehrensberger, A. Hudmon, F. Asturias, and R. D. Kornberg. Head module control of mediator interactions. *Mol Cell*, 23(3):355–364, Aug 2006.
- H. Takahashi, K. Kasahara, and T. Kokubo. *Saccharomyces cerevisiae* Med9 comprises two functionally distinct domains that play different roles in transcriptional regulation. *Genes Cells*, 14(1):53–67, Jan 2009.
- M. C. Teixeira, P. Monteiro, P. Jain, S. Tenreiro, A. R. Fernandes, N. P. Mira, M. Alenquer, A. T. Freitas, A. L. Oliveira, and I. Sa-Correia. The YEASTRACT database: a tool for the analysis of transcription regulatory associations in *Saccharomyces cerevisiae*. *Nucleic Acids Res*, 34(Database issue):D446–51, 2006.
- T. C. Terwilliger. Automated main-chain model building by template matching and iterative fragment extension. *Acta Crystallogr D Biol Crystallogr*, 59(Pt 1):38–44, Jan 2003.
- J. K. Thakur, H. Arthanari, F. Yang, S.-J. Pan, X. Fan, J. Breger, D. P. Frueh, K. Gulshan, D. K. Li, E. Mylonakis, K. Struhl, W. S. Moye-Rowley, B. P. Cormack, G. Wagner, and A. M. Näär. A nuclear receptor-like pathway regulating multidrug resistance in fungi. *Nature*, 452(7187):604–609, Apr 2008.
- M. C. Thomas and C.-M. Chiang. The general transcription machinery and general cofactors. *Crit Rev Biochem Mol Biol*, 41(3):105–178, 2006.

- C. M. Thompson and R. A. Young. General requirement for RNA polymerase II holoenzymes in vivo. *Proc Natl Acad Sci U S A*, 92(10):4587–4590, May 1995.
- C. M. Thompson, A. J. Koleske, D. M. Chao, and R. A. Young. A multisubunit complex associated with the RNA polymerase II CTD and TATA-binding protein in yeast. *Cell*, 73(7):1361–1375, Jul 1993.
- S. J. Triezenberg, R. C. Kingsbury, and S. L. McKnight. Functional dissection of VP16, the trans-activator of herpes simplex virus immediate early gene expression. *Genes Dev*, 2(6):718–729, Jun 1988.
- A. Tóth-Petróczy, C. J. Oldfield, I. Simon, Y. Takagi, A. K. Dunker, V. N. Uversky, and M. Fuxreiter. Malleable machines in transcription regulation: the mediator complex. *PLoS Comput Biol*, 4(12):e1000243, Dec 2008.
- C. Uetrecht, C. Versluis, N. R. Watts, P. T. Wingfield, A. C. Steven, and A. J. Heck. Stability and shape of hepatitis B virus capsids in vacuo. *Angew Chem Int Ed Engl*, 47(33):6247–51, 2008.
- J. van de Peppel, N. Kettelarij, H. van Bakel, T. T. J. P. Kockelkorn, D. van Leenen, and F. C. P. Holstege. Mediator expression profiling epistasis reveals a signal transduction pathway with antagonistic submodules and highly specific downstream targets. *Mol Cell*, 19(4):511–522, Aug 2005.
- B. J. Venters and B. F. Pugh. How eukaryotic genes are transcribed. *Crit Rev Biochem Mol Biol*, 44(2-3):117–141, 2009.
- M. A. Verdecia, M. E. Bowman, K. P. Lu, T. Hunter, and J. P. Noel. Structural basis for phosphoserine-proline recognition by group IV WW domains. *Nat Struct Biol*, 7(8):639–43, 2000.
- V. V. Volkov and D. I. Svergun. Uniqueness of ab initio shape determination in small-angle scattering. *J. Appl. Cryst.*, 36:860–864, 2003.
- A. Wach, A. Brachat, R. Pöhlmann, and P. Philippsen. New heterologous modules for classical or PCR-based gene disruptions in *Saccharomyces cerevisiae*. *Yeast*, 10(13):1793–1808, Dec 1994.
- A. Wach, A. Brachat, C. Alberti-Segui, C. Rebischung, and P. Philippsen. Heterologous HIS3 marker and GFP reporter modules for PCR-targeting in *Saccharomyces cerevisiae*. *Yeast*, 13(11):1065–1075, Sep 1997.
- A. C. Wallace, R. A. Laskowski, and J. M. Thornton. LIGPLOT: a program to generate schematic diagrams of protein-ligand interactions. *Protein Eng*, 8(2):127–34, 1995.
- X. Wu, A. Rossetini, and S. D. Hanes. The ESS1 prolyl isomerase and its suppressor BYE1 interact with RNA pol II to inhibit transcription elongation in *Saccharomyces cerevisiae*. *Genetics*, 165(4):1687–1702, Dec 2003.
- Z. Wu, R. A. Irizarry, R. Gentleman, F. Martinez-Murillo, and F. Spencer. A Model-Based Background Adjustment for Oligonucleotide Expression Arrays. *J Am Stat Assoc*, 99(468):909–917, 2004.

- F. Yang, B. W. Vought, J. S. Satterlee, A. K. Walker, Z.-Y. J. Sun, J. L. Watts, R. DeBeaumont, R. M. Saito, S. G. Hyberts, S. Yang, C. Macol, L. Iyer, R. Tjian, S. van den Heuvel, A. C. Hart, G. Wagner, and A. M. Näär. An ARC/Mediator subunit required for SREBP control of cholesterol and lipid homeostasis. *Nature*, 442(7103):700–704, Aug 2006.
- S. Yoon, H. Qiu, M. J. Swanson, and A. G. Hinnebusch. Recruitment of SWI/SNF by Gcn4p does not require Snf2p or Gcn5p but depends strongly on SWI/SNF integrity, SRB mediator, and SAGA. *Mol Cell Biol*, 23(23):8829–8845, Dec 2003.
- E. T. Young, C. Tachibana, H.-W. E. Chang, K. M. Dombek, E. M. Arms, and R. Biddick. Artificial recruitment of mediator by the DNA-binding domain of Adr1 overcomes glucose repression of ADH2 expression. *Mol Cell Biol*, 28(8):2509–2516, Apr 2008.
- N. Yudkovsky, J. A. Ranish, and S. Hahn. A transcription reinitiation intermediate that is stabilized by activator. *Nature*, 408(6809):225–229, Nov 2000.
- S. J. Zanton and B. F. Pugh. Full and partial genome-wide assembly and disassembly of the yeast transcription machinery in response to heat shock. *Genes Dev*, 20(16):2250–65, 2006.
- F. Zhang, L. Sumibcay, A. G. Hinnebusch, and M. J. Swanson. A triad of subunits from the Gal11/tail domain of Srb mediator is an in vivo target of transcriptional activator Gcn4p. *Mol Cell Biol*, 24(15):6871–6886, Aug 2004.
- Y. Zhang. I-TASSER server for protein 3D structure prediction. *BMC Bioinformatics*, 9:40, 2008.
- Z. Zhang and J. C. Reese. Redundant mechanisms are used by Ssn6-Tup1 in repressing chromosomal gene transcription in *Saccharomyces cerevisiae*. *J Biol Chem*, 279(38):39240–39250, Sep 2004.
- X. Zhu, M. Wirén, I. Sinha, N. N. Rasmussen, T. Linder, S. Holmberg, K. Ekwall, and C. M. Gustafsson. Genome-wide occupancy profile of mediator and the Srb8-11 module reveals interactions with coding regions. *Mol Cell*, 22(2):169–178, Apr 2006.
- J. Zlatanova and A. Thakar. H2A.Z: view from the top. *Structure*, 16(2):166–79, 2008.

Abbreviations

bp base pairs

BSA bovine serum albumine

CTD carboxy-terminal domain

CV column volumes

Da dalton

DMSO dimethyl sulfoxide

DTT 1,4-dithio-D,L-threitol

E. coli *Escherichia coli*

EM electron microscopy

GTF general transcription factor

HEPES N-2-hydroxyethylpiperazine-N'-2-ethane sulfonic acid

IPTG Isopropyl- β -D-thiogalactopyranoside

IM-MS ion mobility mass spectrometry

kDa kilo dalton

LB Luria-Bertani (media)

MCS multiple cloning site

MES (2-(N-morpholino)ethanesulfonic acid)

MOPS 4-morpholinepropanesulfonic acid

MW molecular weight

OD_{Xnm} optical density at a wavelength of X nm

ORF open reading frame

PAGE polyacrylamide gel electrophoresis

PBS phosphate buffered saline

PDB Protein Data Bank

PIC pre-initiation complex

RNA Pol RNA polymerase

rpm rounds per minute

SAGA Spt-Ada-Gcn5 acetylase complex

SAXS Small angle X-ray scattering

S. cerevisiae *Saccharomyces cerevisiae*

S. pombe *Schizosaccharomyces pombe*

SDS sodium dodecylsulfate

SLS static light scattering

SOB Super Optimal Broth (media)

SOC Super Optimal broth with Catabolite repression (media)

Srb Suppressor of RNA Pol B

TAF TBP-associated factor

TCEP tris(2-carboxyethyl)phosphine hydrochloride

TF transcription factor

Tris tris-(hydroxymethyl)-aminomethane

U units

v/v volume per volume

w/v weight per volume

wt wild type

List of Figures

1	The mRNA transcription cycle.	2
2	Transcription initiation.	7
3	Med7N/31 crystals.	36
4	Structure of the Med7N/31 Mediator subcomplex.	38
5	Analysis of the Med7N/31 structure.	39
6	Functional analysis of Med7N/31 <i>in vivo</i> and <i>in vitro</i>	42
7	Gal4-Gal4AH <i>in vitro</i> transcription.	43
8	Transcriptome profiling analysis and phenotypic correlation.	44
9	Analysis of published genetic interactions of Med31 and TFIIS.	49
10	Endogenous Mediator and its middle module.	50
11	Destabilization of the Mediator complex.	51
12	Recombinant Mediator middle module.	52
13	Native mass spectrometry analyses of Mediator middle module.	54
14	Mass spectrometry analyses of Mediator middle modules.	55
15	Yeast complementation assay for <i>MED4</i>	57
16	Limited proteolysis analysis of Mediator middle module.	58
17	Intra-module subunit interactions within the middle module.	60
18	Shape of the middle module.	62
19	Structural overview of the trimeric Med7/21/31 complex architecture.	65

List of Tables

1	Complexes involved in <i>S. cerevisiae</i> RNA Pol II PIC assembly	4
2	Mediator subunits <i>S. cerevisiae</i>	9
3	<i>E. coli</i> strains.	14
4	<i>S. cerevisiae</i> strains.	14
5	<i>E. coli</i> vector list.	16
6	Yeast vector list.	21
7	Media.	22
8	Media additives.	22
9	General buffers, dyes and solutions.	23
10	Crystallization screening of M7N/31 complex.	37
11	Data collection and refinement statistics for Med7N/31.	37
12	Summary of Med7N mutant constructs of the polyproline stretches 1 and 2. .	40
13	GO analysis.	45
14	Analysis of transcriptome profiling.	45
15	Comparative phenotyping of Mediator deletion strains.	47
16	Crystallization screening.	53
17	Mediator middle module interaction assays.	59
18	Static light scattering (SLS) and Small-angle X-ray scattering (SAXS) mea- surements.	61

Curriculum Vitae

Tobias Koschubs

Personal Data

Date of birth: June 5, 1979
Place of birth: Hannover, Germany
Nationality: German
Marital status: married

Education

1986-1999 School education in Seesen,
Abitur equivalent to A-level at Jacobson Gymnasium

1999-2000 Community Service at Youth Center Seesen

2000-2005 Academic studies of biotechnology,
Technical University Carolo Wilhelmina, Braunschweig

2003-2004 University studies abroad in biotechnology,
Lund Institute of Technology, Sweden

2004 Student research project with Prof. Dr. D. Jahn,
Institute for Microbiology, Technical University Braunschweig

2005 Diploma thesis at Sanofi-aventis Pharma, Frankfurt/Main,
with Dr. M.K. Dreyer and Prof. Dr. D. Heinz
Departments Protein Production and Structural Biology

01/2006 Diploma degree in biotechnology

since 01/2006 Doctorate studies at the Gene Center of the
Ludwig-Maximilians-University München
with Prof. Dr. P. Cramer, Department of Biochemistry
Topic: "Structure and functional architecture of the Mediator middle
module from budding yeast"